

# Mechano-regulation of collagen architecture in cardiovascular tissue engineering

**Citation for published version (APA):**

Rubbens, M. P. (2009). *Mechano-regulation of collagen architecture in cardiovascular tissue engineering*. [Phd Thesis 1 (Research TU/e / Graduation TU/e), Biomedical Engineering]. Technische Universiteit Eindhoven. <https://doi.org/10.6100/IR643993>

**DOI:**

[10.6100/IR643993](https://doi.org/10.6100/IR643993)

**Document status and date:**

Published: 01/01/2009

**Document Version:**

Publisher's PDF, also known as Version of Record (includes final page, issue and volume numbers)

**Please check the document version of this publication:**

- A submitted manuscript is the version of the article upon submission and before peer-review. There can be important differences between the submitted version and the official published version of record. People interested in the research are advised to contact the author for the final version of the publication, or visit the DOI to the publisher's website.
- The final author version and the galley proof are versions of the publication after peer review.
- The final published version features the final layout of the paper including the volume, issue and page numbers.

[Link to publication](#)

**General rights**

Copyright and moral rights for the publications made accessible in the public portal are retained by the authors and/or other copyright owners and it is a condition of accessing publications that users recognise and abide by the legal requirements associated with these rights.

- Users may download and print one copy of any publication from the public portal for the purpose of private study or research.
- You may not further distribute the material or use it for any profit-making activity or commercial gain
- You may freely distribute the URL identifying the publication in the public portal.

If the publication is distributed under the terms of Article 25fa of the Dutch Copyright Act, indicated by the "Taverne" license above, please follow below link for the End User Agreement:

[www.tue.nl/taverne](http://www.tue.nl/taverne)

**Take down policy**

If you believe that this document breaches copyright please contact us at:

[openaccess@tue.nl](mailto:openaccess@tue.nl)

providing details and we will investigate your claim.

Mechano-regulation of  
collagen architecture in  
cardiovascular tissue engineering

A catalogue record is available from the Eindhoven University of Technology Library

ISBN: 978-90-386-1931-6

Copyright ©2009 by M.P. Rubbens

All rights reserved. No part of this book may be reproduced, stored in a database or retrieval system, or published, in any form or in any way, electronically, mechanically, by print, photoprint, microfilm or any other means without prior written permission by the author.

Cover design: Anne Seghers

Printed by Universiteitsdrukkerij TU Eindhoven, Eindhoven, The Netherlands.

This research was supported by the Dutch Technology Foundation (STW), applied science division of NWO and the Technology Program of the Dutch Ministry of Economic Affairs.

Financial support by the Netherlands Heart Foundation and the Dutch Society For Matrix Biology for the publication of this thesis are gratefully acknowledged.

# **Mechano-regulation of collagen architecture in cardiovascular tissue engineering**

PROEFSCHRIFT

ter verkrijging van de graad van doctor aan de  
Technische Universiteit Eindhoven, op gezag van de  
rector magnificus, prof.dr.ir. C.J. van Duijn, voor een  
commissie aangewezen door het College voor  
Promoties in het openbaar te verdedigen  
op donderdag 17 september 2009 om 16.00 uur

door

Mirjam Petronella Rubbens

geboren te Spijkenisse



Dit proefschrift is goedgekeurd door de promotor:

prof.dr.ir. F.P.T. Baaijens

Copromotoren:

dr. C.V.C. Bouten

en

dr. A. Driessen-Mol

# Contents

<b>Summary</b>	<b>ix</b>
<b>1 General introduction</b>	<b>1</b>
1.1 Introduction	2
1.2 Cardiovascular tissues in health and disease	2
1.3 Replacement strategies	4
1.3.1 Heart valves	4
1.3.2 Blood vessels	5
1.4 Tissue composition and function	5
1.4.1 Collagen	6
1.4.2 Collagen synthesis and cross-linking	7
1.4.3 Collagen degradation	8
1.4.4 Collagen architecture and remodeling	8
1.5 Cardiovascular tissue engineering	9
1.6 Mechano-regulation of collagen architecture	11
1.7 Mechanical conditioning in cardiovascular tissue engineering	12
1.8 Objective and outline	13
<b>2 Methods to quantify strain-induced collagen architecture in engineered cardiovascular tissues</b>	<b>15</b>
2.1 Introduction	16
2.2 Tissue model	16
2.3 Straining system	17
2.4 Quantification of collagen architecture	20
2.4.1 Collagen amount and cross-links	20
2.4.2 Collagen orientation	21
2.5 Discussion	24
<b>3 Straining mode-dependent collagen remodeling in engineered cardiovascular tissue</b>	<b>27</b>
3.1 Introduction	28
3.2 Materials and methods	29
3.2.1 Cell culture	29
3.2.2 Engineered cardiovascular tissues	30
3.2.3 Tissue culture and mechanical conditioning	30
3.2.4 Quantitative PCR analysis	31
3.2.5 Quantification of matrix composition	32
3.2.6 Medium analysis	32
3.2.7 Statistics	32
3.3 Results	33
3.3.1 Effect of straining mode on gene expression	33

3.3.2	Effect of straining mode on tissue protein content	34
3.3.3	Effect of straining mode on collagen remodeling markers	35
3.4	Discussion	36
<b>4</b>	<b>The role of collagen cross-links in the biomechanical behavior of human native and engineered heart valve tissue</b>	<b>41</b>
4.1	Introduction	42
4.2	Materials and methods	43
4.2.1	Specimen preparation	43
4.2.2	Biomechanical testing and matrix analysis	44
4.2.3	Data analysis	45
4.3	Results	46
4.3.1	Biomechanical properties	46
4.3.2	Collagen content and cross-links	47
4.3.3	Correlation between collagen content, cross-links, and biomechanics	48
4.4	Discussion	49
<b>5</b>	<b>Intermittent strain accelerates the development of tissue properties in engineered heart valve tissue</b>	<b>53</b>
5.1	Introduction	54
5.2	Materials and methods	55
5.2.1	Cell culture	55
5.2.2	Engineered heart valve tissue	55
5.2.3	Tissue culture and mechanical conditioning	56
5.2.4	Tissue morphology and organization	56
5.2.5	Collagen production and cross-link density	57
5.2.6	Mechanical properties	57
5.2.7	Statistics	57
5.3	Results	58
5.3.1	Evaluation of tissue morphology and organization	58
5.3.2	Evaluation of collagen production and cross-link density	62
5.3.3	Evaluation of mechanical properties	62
5.4	Discussion	65
<b>6</b>	<b>Quantification of the temporal evolution of collagen orientation in mechanically conditioned engineered cardiovascular tissues</b>	<b>69</b>
6.1	Introduction	70
6.2	Materials and Methods	71
6.2.1	Tissue culture and mechanical conditioning	71
6.2.2	Visualization of collagen orientation	72
6.2.3	Quantification of collagen orientation	72
6.2.3	Statistics	74
6.3	Results	74
6.3.1	Quantification algorithm	74

6.3.2 Spatial organization of collagen fibers	75
6.3.3 Temporal evolution of collagen fiber orientation	77
6.3.4 Spatio-temporal evolution of collagen fiber orientation	78
6.4 Discussion	79
<b>7 General discussion</b>	<b>83</b>
7.1 Introduction	84
7.2 Summary and discussion of main findings	85
7.3 Critique of methods	90
7.4 Future challenges	92
7.5 Relevance for cardiovascular tissue engineering	96
<b>References</b>	<b>99</b>
<b>Samenvatting</b>	<b>113</b>
<b>Dankwoord</b>	<b>115</b>
<b>Curriculum vitae</b>	<b>117</b>



# Summary

## **Mechano-regulation of collagen architecture in cardiovascular tissue engineering**

Clinically available heart valve replacements consist of non-living materials, lacking the ability to grow with the patient. Therefore, several re-operations are necessary to replace the valve with a larger one. In addition, there is a large need for living blood vessel substitutes that overcome the drawbacks of current vascular prostheses. Cardiovascular tissue engineering focuses on the creation of living heart valves and blood vessels that have the potential to grow and remodel *in vivo*. In brief, cells are acquired from a patient and seeded on a biodegradable material or scaffold. The cell-seeded scaffold is cultured in a bioreactor where mechanical and biochemical stimuli are applied to stimulate tissue development. After several weeks, the scaffold is replaced by tissue produced by the patient's own cells. Ideally, the tissue can be implanted in the patient to replace dysfunctional tissue.

In order to be mechanically functional, such engineered cardiovascular tissues should incorporate load-bearing structures to withstand (changes in) the hemodynamic environment. The mechanical properties of cardiovascular tissues are dictated by a well organized network of collagen fibers. The collagen architecture is influenced by the mechanical environment of the tissue. Hence, mechanical conditioning is considered to be an important regulator to create engineered cardiovascular tissues with defined load-bearing structures and mechanical properties.

The aim of the research presented in this thesis is to elucidate the effects of well-defined mechanical conditioning protocols on the collagen architecture in engineered cardiovascular tissues. In this thesis, three main aspects of the collagen architecture in engineered cardiovascular tissues are quantified: collagen amount, collagen cross-link density, and collagen fiber orientation.

To systematically investigate the effects of mechanical conditioning on collagen architecture, a model system has been employed. The tissues consist of rectangular strips of rapidly degrading polyglycolic acid based scaffolds seeded with human vascular cells. The advantage of the model system is that it reduces the number of required cells and it allows for the application of pre-defined strain regimes to multiple engineered tissues simultaneously. Static conditioning is applied in longitudinal direction by constraining the tissues at their outer ends. In addition, different uniaxial straining protocols, including continuous dynamic strain (4%, 1Hz, for 10 days and 4 weeks) and intermittent dynamic strain (3 hours on/off, 4%, 1Hz, for 2, 3, and 4 weeks) are applied using a modified straining system.

The temporal effects of static and dynamic conditioning on collagen amount and cross-links are assessed up to 10 days of culture from gene and protein measurements. Both conditioning modes upregulate collagen and cross-link expression and protein content with time. Dynamic strain results in lower collagen expression and content, but enhances collagen cross-link expression and density, when compared with static conditioning.

To study the effects of static and dynamic conditioning on the mechanical properties of newly formed tissue, the culture period has been extended to 4 weeks. By that time, the initial scaffold has lost its mechanical integrity and the mechanical properties of the constructs are only determined by the newly formed tissue. Compared to 4 weeks of static conditioning, continuous dynamic strain results in similar collagen contents but higher cross-link densities, which correlate to improved mechanical properties. These findings indicate that, despite a similar collagen amount, the quality and structural integrity of the tissue can be improved by dynamic strain via an increase in collagen cross-link densities.

A novel technique has been used to quantify the orientations of the newly formed collagen fibers, based on 3D vital imaging using two-photon microscopy combined with image analysis. These collagen fiber orientation analyses reveal that mechanical conditioning induces collagen alignment in the constrained and intermittently strained directions. Importantly, intermittent dynamic strain improves and accelerates the alignment of the collagen fibers in the straining direction compared to constraining only. In addition, intermittent dynamic strain results in increased collagen production, cross-link densities, and mechanical properties at faster rates compared to static conditioning, leading to stronger tissues at shorter culture periods.

In conclusion, these studies show that, when compared to constrained tissue culture, continuous dynamic strain does not increase the amount of collagen in the tissue but does enhance cross-link densities and collagen fiber alignment. Intermittent dynamic strain increases and accelerates the production of collagen, cross-links, and collagen fiber alignment. Therefore, intermittent dynamic strain can be used to accelerate the creation of load-bearing tissues with a well organized collagen architecture. This is of considerable importance for cardiovascular tissue engineering, where a functional load-bearing capacity is a prerequisite for in vivo application.

# Chapter 1

## General introduction

Parts of this chapter are based on A. Mol, M.P. Rubbens, M. Stekelenburg, and F.P.T. Baaijens, *Living heart valve and small-diameter artery substitutes - an emerging field for intellectual property development*, *Recent Patents on Biotechnology*, 2(1), 1-9, (2008).



## 1.1 Introduction

Tissue engineering offers promising alternatives for current replacement strategies for heart valves and blood vessels. Using tissue engineering technology, living cardiovascular substitutes can be created that have the potential to grow and remodel in vivo. In order to be mechanically functional, such engineered cardiovascular tissues should incorporate load-bearing structures to withstand (changes in) the hemodynamic environment. In cardiovascular tissues, collagen is the main load-bearing constituent and the mechanical properties of the tissue are associated with the collagen architecture. In this thesis, three main aspects of the collagen architecture are quantified: collagen amount, collagen cross-link density, and collagen fiber orientation. The collagen architecture is strongly influenced by the mechanical environment of the tissue. Hence, mechanical conditioning is considered to be an important regulator to create engineered cardiovascular tissues with defined load-bearing structures and mechanical properties.

The aim of the research presented in this thesis is to elucidate the effects of well-defined mechanical conditioning protocols on collagen architecture in engineered cardiovascular tissues with the ultimate goal to optimize and control collagen architecture and associated mechanical properties.

## 1.2 Cardiovascular tissues in health and disease

The heart is a hollow muscular organ that pumps blood through the vascular system for transport of oxygen and nutrients to the tissue and metabolic waste from the tissue. Returning blood from the body is collected via the vena cava and the right atrium into the right ventricle of the heart (figure 1.1a). Upon contraction of this ventricle, blood is pumped through the pulmonary artery into the lungs (pulmonary circulation). The left ventricle receives oxygenated blood from the lungs through the left atrium and pumps the blood into the aorta (systemic circulation).

To direct the blood flow in one direction, the heart is equipped with four valves which prevent backflow of blood: the tricuspid valve, the mitral valve, the pulmonary valve, and the aortic valve. The tricuspid and mitral valves are situated between the atria and the ventricles. The pulmonary valve is located between the right ventricle and the pulmonary artery, while the aortic valve controls the blood flow from the left ventricle to the aorta.

The heart muscle itself is supplied with oxygen and nutrients by the coronary arteries (figure 1.1b). These arteries originate from three anatomical dilatations in the aorta, called the sinuses. The right coronary artery generally supplies the right ventricle and atrium, while the left coronary artery supplies the intraventricular septum, the left ventricle, and the left atrium. Both arteries course over the heart, branching into segments that penetrate into the tissue, and dividing into capillary networks.

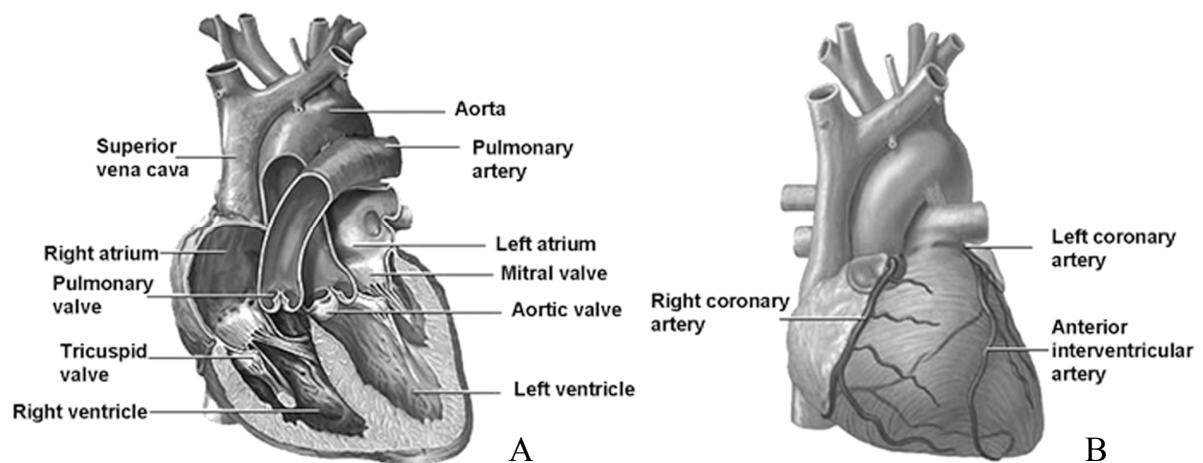


Figure 1.1: A: Schematic overview of the heart and the four heart valves. B: Location of main coronary arteries ([www.urac.org](http://www.urac.org)).

Cardiovascular diseases are, next to cancer, the leading cause of death in the United States (Anderson and Smith, 2005). In 2004, cardiovascular diseases, such as heart valve dysfunction or coronary artery stenosis, accounted for 1 of every 2.8 deaths (Rosamond *et al.*, 2007).

The heart valves can be affected by calcification of the leaflets, endocarditis, rheumatic fever, myxomatous degeneration, or congenital heart diseases, leading to stenosis or insufficiency of the valves. The prevalence of congenital heart disease is 75/1,000 live births, including 6/1,000 live births with moderate and severe forms (Hoffman and Kaplan, 2002). The most frequently affected heart valve associated with congenital heart diseases, such as Tetralogy of Fallot, pulmonary valve stenosis and atresia, is the pulmonary valve. The total prevalence of these 3 congenital heart problems is 6.32 per 10,000 births in Europe (EUROCAT, European Registration Of Congenital Anomalies and Twins, 2005). In adults, and more specifically in people between 26 and 84 years of age, the prevalence of valvular disease is about 1 to 2% (Rosamond *et al.*, 2007) and the aortic valve is most frequently affected. In case of heart valve dysfunction, surgical repair or heart valve replacements are needed to avoid serious cardiac, pulmonary or systemic problems.

Cardiovascular diseases can also cause dysfunctional blood vessels. In coronary artery disease (CAD), the coronary arteries are occluded due to atherosclerotic plaques. Occlusion of these arteries leads to oxygen deprivation of the heart muscle. In 2005, 16 million people were suffering from CAD in the US (Rosamond *et al.*, 2008). Besides this large number of CAD patients, there are 8 million people suffering from peripheral artery disease (PAD) (Rosamond *et al.*, 2008). In this latter condition, narrowing of arteries in the legs leads to cramping pain caused by inadequate supply of blood to the affected muscle and accumulation of lactic acid. When native arteries are occluded or damaged, arterial revascularization needs to be performed.

## 1.3 Replacement strategies

### 1.3.1 Heart valves

Currently used treatments for end-stage valvular disease include the replacement of the native valve. In 2003, 290,000 heart valve replacements were performed worldwide (Rosamond *et al.*, 2007). Due to the ageing population and increase of rheumatic cardiac disease, heart valve disease is increasing rapidly worldwide. Concomitantly, the number of individuals requiring heart valve replacement is predicted to triple to over 850,000 by the year 2050 (Yacoub and Takkenberg, 2005).

Current heart valve replacement strategies include the use of mechanical or bioprosthetic valves. Most of the mechanical valves are fabricated of graphite coated with carbon which renders them very strong and durable. These valves last usually for a life time, but have the disadvantage of being thrombogenic. In order to reduce the risk of thromboembolism, patients with mechanical valves require lifelong anticoagulation therapy, associated with a substantial risk of spontaneous bleeding and embolism (Senthilnathan *et al.*, 1999).

Bioprosthetic valve replacements are either of animal origin (xenografts), such as porcine or bovine pericardial valves, or they can be harvested from human donors (homografts). These valves undergo several chemical processes, including preservative treatment and sterilization to make them suitable for implantation in humans. The major advantage of bioprosthetic valves is that there is no need for anticoagulation therapy. However, they represent non-viable prostheses prone to tissue deterioration and calcification, limiting their durability (Hopkins, 2005). Bearing in mind the extended life span of the general population, the need for re-operation after bioprosthetic valve replacement seems inevitable in the long term (Brown *et al.*, 2008; Hammermeister *et al.*, 2000; Lund and Bland, 2006). Another important aspect of the use of xenografts is the risk of zoonoses, which are human diseases caused by infectious agents from animals. Cryopreserved homografts are substitutes closest to natural valves, not being thrombogenic and with a low risk of infection. However, their use is restrained due to limited availability and high costs.

The overall limitation of the clinically available heart valve replacements is that they consist of non-living structures and are, therefore, not able to grow, repair, and remodel. These necessarily restrict the application of currently available prostheses in pediatric patients. Several re-operations are required to replace the valve with a larger prosthesis, associated with exponentially increased morbidity and mortality (Mayer, 1995). In addition, although current prostheses significantly improve life expectancy, patient longevity after valvular surgery still remains inferior compared to age-matched healthy individuals (Puvimanasinghe *et al.*, 2001). This underlines that the current options for heart valve replacements are suboptimal and, as such, the ideal prosthetic heart valve has yet to be developed.

### 1.3.2 Blood vessels

The major treatment for revascularization in coronary artery disease is bypass grafting. Approximately 427,000 coronary bypass surgeries have been performed in the US in 2004 on more than 249,000 patients to treat coronary artery disease (Rosamond *et al.*, 2008). Autologous small-diameter arteries and veins are commonly used as coronary artery replacements. However, the effectiveness of this treatment is not long term, since only one fifth of the patients are free from ischemic events 15 years postoperatively (Sabik *et al.*, 2006). An estimated 5% of these patients have outlived their native grafts and have no option other than artificial grafts. Synthetic graft replacements, such as expanded polytetra-fluoroethylene (ePTFE) and Dacron®, are successful for grafting medium to large diameter arteries (>5-6 mm), but are not suitable as small-diameter vascular grafts (Canver, 1995). Graft thrombogenicity, poor healing, lack of compliance, and excessive intimal hyperplasia have all been reported using small-diameter synthetic grafts (Bordenave *et al.*, 2005). Arterial grafts are also required in patients with renal failure who depend on dialysis. This procedure requires frequent access to the peripheral circulation, which is usually facilitated by an arteriovenous shunt in the arm. This shunt, however, is subject to repeated cannulation and has a limited lifetime.

To create viable heart valves and blood vessels that offer good alternatives to overcome the limitations of current treatment options, understanding of the native tissue composition and its associated function is crucial.

## 1.4 Tissue composition and function

Connective tissues, such as heart valves and blood vessels, mainly consist of cells and extracellular matrix (ECM). The extracellular matrix is composed of proteoglycans and fibrillar proteins, such as elastin and collagen. Proteoglycans are negatively charged and attract water. This combination of proteoglycans and water protects the tissue against compression and confers a degree of shock absorbance. The collagen fibers provide tensile stiffness and strength to the tissue, whereas the elastin fibers are responsible for resilience of the tissue.

Both native aortic heart valve leaflets and arteries are composed of three layers, each with a distinct matrix composition. The mechanically strongest layer in the leaflet is the lamina fibrosa which is located on the aortic side of the leaflet. In this layer of dense connective tissue, thick parallel collagen fibers run in the circumferential direction from commissure to commissure. The central lamina spongiosa consists of loosely arranged connective tissue with proteoglycans as its main component. The few collagenous fibers in this layer are oriented radially. The ventricularis layer is situated on the ventricular side of the valve leaflet and contains an organized network of elastin fibers. Its function is to restore the collagen fiber geometry to its initial configuration between loading cycles.

The surfaces of the leaflets are covered with endothelial cells that provide a protective, non-thrombogenic layer. The cells present in the leaflets are the valvular interstitial cells. Among the valvular interstitial cells (VICs), different cellular phenotypes are identified including smooth muscle cells, fibroblasts and myofibroblasts. The majority of VICs within heart valve leaflets are the myofibroblasts, due to their dual phenotypic characteristics of both fibroblast and smooth muscle like cells (Messier, Jr. *et al.*, 1994; Taylor *et al.*, 2003).

The three layers in blood vessels are the adventitia, media, and intima located from the outside to the inside of the vessel. The adventitia is a fibrous connective tissue, mainly containing collagen and fibroblasts. Due to the high collagen content, the adventitia provides most of the mechanical stiffness and strength to the vessel. The media contains smooth muscle cells and elastin, important for the visco-elastic behavior of the vessel. The intima, positioned at the lumen, consists of endothelial cells that proactively inhibit thrombosis.

In both heart valves and blood vessels, collagen is specifically organized. Collagen in heart valves resembles a hammock-type orientation, while blood vessels possess helically oriented fibers (figure 1.2). This specific collagen orientation is closely related to the biomechanical behavior of the tissue. In heart valve leaflets for instance, the circumferentially aligned collagen fiber orientation is associated with anisotropic mechanical properties of the leaflets, revealing stronger and stiffer leaflets in the circumferential direction than in the radial direction. In order to understand the functioning of collagen in cardiovascular tissues it is essential to investigate how it is organized by the cells.

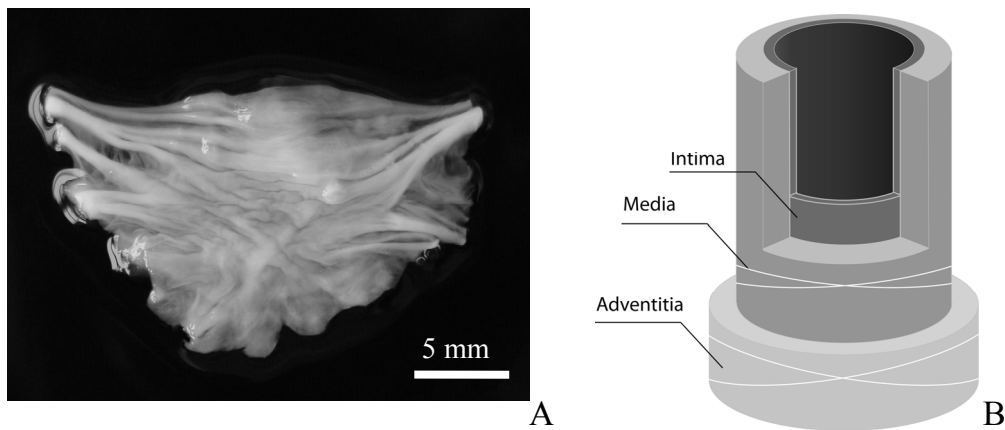


Figure 1.2: Collagen resembles a hammock-type orientation in heart valve leaflets (A) (adapted from Balguid *et al.*, 2007). Blood vessels possess helically oriented fibers, as schematically drawn in the adventitia layer (B).

### 1.4.1 Collagen

Collagens are the major fibrillar and load-bearing components of most connective tissues. Collagen possesses a hierarchical structure (figure 1.3) ranging from fibers down to a triple helix organization. The collagen fibers are composed of fibril bundles.

Fibrils, with a diameter distribution ranging from 10 to 500 nm (Ottani *et al.*, 2001), consist of hundreds of microfibrils. Microfibrils are 4 nm thick assemblies of five collagen triple helices. These triple helices are 1.5 nm in diameter and 300 nm in length (Kadler *et al.*, 1996). The rope-like triple helices are formed by combining three  $\alpha$ -chains, each containing about 1000 amino acids.

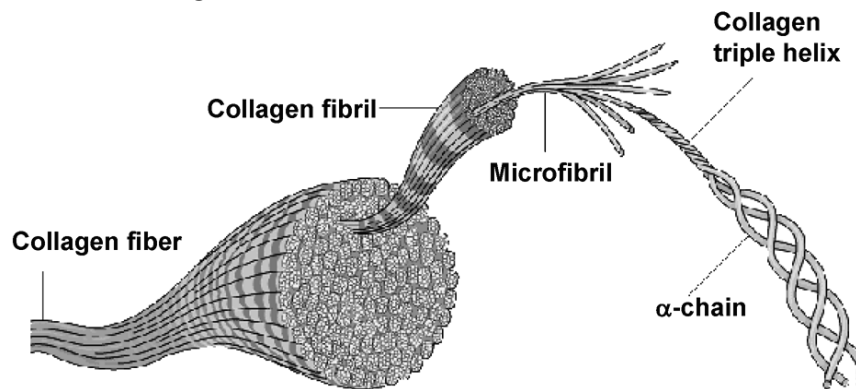


Figure 1.3: The hierarchical structure of collagen from a fiber down to a triple helix organization (adapted from [www.bio.miami.edu](http://www.bio.miami.edu)).

Variations in the amino acid contents of the  $\alpha$ -chains in the triple helices result in structural components with slightly different properties. The type of collagen depends on the composition of these  $\alpha$ -chains. Collagen type I and III are the most abundant types in heart valves and blood vessels. These collagens are classified as fibrous collagens, along with collagen types II, V, and XI.

### 1.4.2 Collagen synthesis and cross-linking

Collagen formation starts in the endoplasmic reticulum of the cell where procollagen triple helices are formed. The procollagen triple helices are transported to the cellular membrane by secretory vesicles and are secreted into the extracellular matrix (figure 1.4a). These procollagen triple helices contain telopeptides, which are important in the formation of cross-links. The triple helices are soluble in the extracellular matrix, but upon cleavage by procollagen C-proteinase and/or procollagen N-proteinase, solubility drops and polymerization of collagen fibrils is initiated.

The collagen fibrils are stabilized by the formation of intermolecular cross-links. Cross-links can be formed via two related routes (figure 1.4b):

- 1) the allysine route, in which a lysine residue within the collagen telopeptide is converted by lysyl oxidase into the aldehyde allysine.

- 2) the hydroxyallysine route, in which a hydroxylysine residue in the telopeptide is converted into the aldehyde hydroxyallysine.

The resulting reactive aldehydes can condense with lysyl or hydroxylysyl residues in the triple helix to form di-, tri-, or tetrafunctional cross-links.

Two chemical forms of mature cross-links have been identified, hydroxylysylpyridinoline (HP) and lysylpyridinoline (LP). HP cross-links are predominant in highly hydroxylated collagens, such as type I collagen in heart valves

and blood vessels. These cross-links are formed by hydroxylation of the telopeptides, where lysine is converted to hydroxylysine, catalyzed by the enzyme lysyl hydroxylase. Following the hydroxyallysine route, HP (derived from 3 hydroxylysyl residues) and LP cross-links (derived from 2 hydroxylysyl and 1 lysyl residue) are formed.

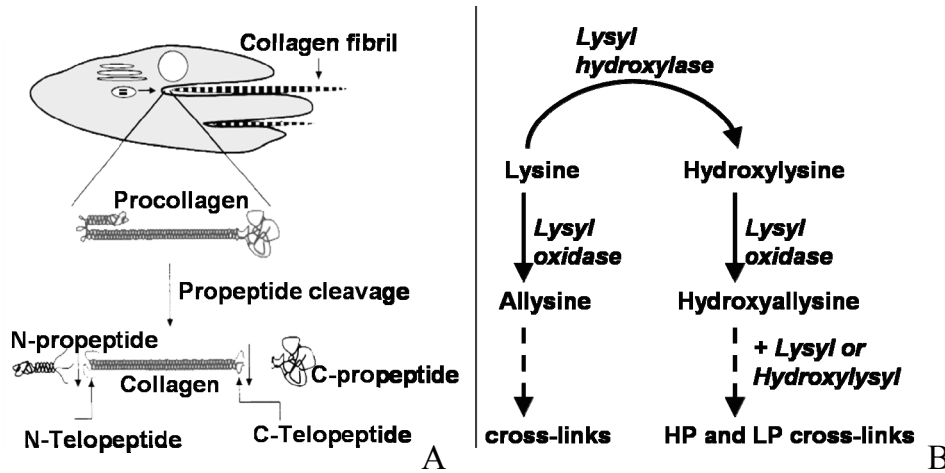


Figure 1.4: A: Fibrillogenesis of collagen, adapted from Kadler et al. (1996). Procollagen triple helices are secreted into the extracellular matrix. Upon cleavage of the propeptides, polymerization of collagen fibrils is initiated. B: Simplified schematic overview of collagen cross-links formation.

### 1.4.3 Collagen degradation

Once formed, collagen fibers are susceptible to degradation by enzymes produced by the cells. The major class of collagen degrading enzymes are the matrix metalloproteinases (MMPs), which is a family of about twenty zinc-dependent endopeptidases. Based on their substrate specificity and primary structure, the family can be subdivided into different groups. The first group, the collagenases (MMP-1, MMP-8 and MMP-13), can cleave fibrillar collagens (e.g., type I, II, and III). Mammalian collagenases cleave the collagen triple helix at 3/4 from the terminal end, generating 3/4 and 1/4 collagen fragments. These fragments unfold their triple helix and fall apart into fragmented single  $\alpha$ -chains, the so-called gelatins. Group 2, the gelatinases (MMP-2 and MMP-9) is well known to degrade such gelatins. Once activated, MMPs are controlled by endogenous inhibitors, the tissue inhibitors of metalloproteinases (TIMPs).

### 1.4.4 Collagen architecture and remodeling

Collagen architecture has been reported to include many aspects, such as collagen amount and type, number and type of cross-links, and orientation, length, and thickness of the collagen fibers. In this thesis, three main aspects of the collagen architecture are quantified: collagen amount, collagen cross-link density, and collagen fiber orientation. Collagen remodeling refers to changes in this architecture.

## 1.5 Cardiovascular tissue engineering

The ideal heart valve and blood vessel replacements are autologous, to prevent an immune response, and living, to allow growth, repair, and remodeling. The emerging field of tissue engineering has tremendous potential in the development of valvular replacements and blood vessel bypasses that possess these characteristics. Tissue engineering was first introduced in 1993 by Langer and Vacanti, who defined it as an interdisciplinary field applying the principles and methods of engineering to the development of biological substitutes that can restore, maintain, or improve tissue function (Langer and Vacanti, 1993). Figure 1.5 shows a schematic overview of an in vitro tissue engineering approach. In this approach, cells are harvested from a patient and subsequently expanded to increase their number. The cells are then seeded onto a scaffold which most often consists of decellularized naturally derived biomaterials, hydrogels, or synthetic scaffolds. To enhance tissue formation, the cell-seeded scaffolds are placed in a bioreactor where biochemical and mechanical stimuli are applied. After several weeks of tissue development and remodeling, a functional tissue can be obtained, which would ideally be implanted back in the patient to replace a dysfunctional tissue.

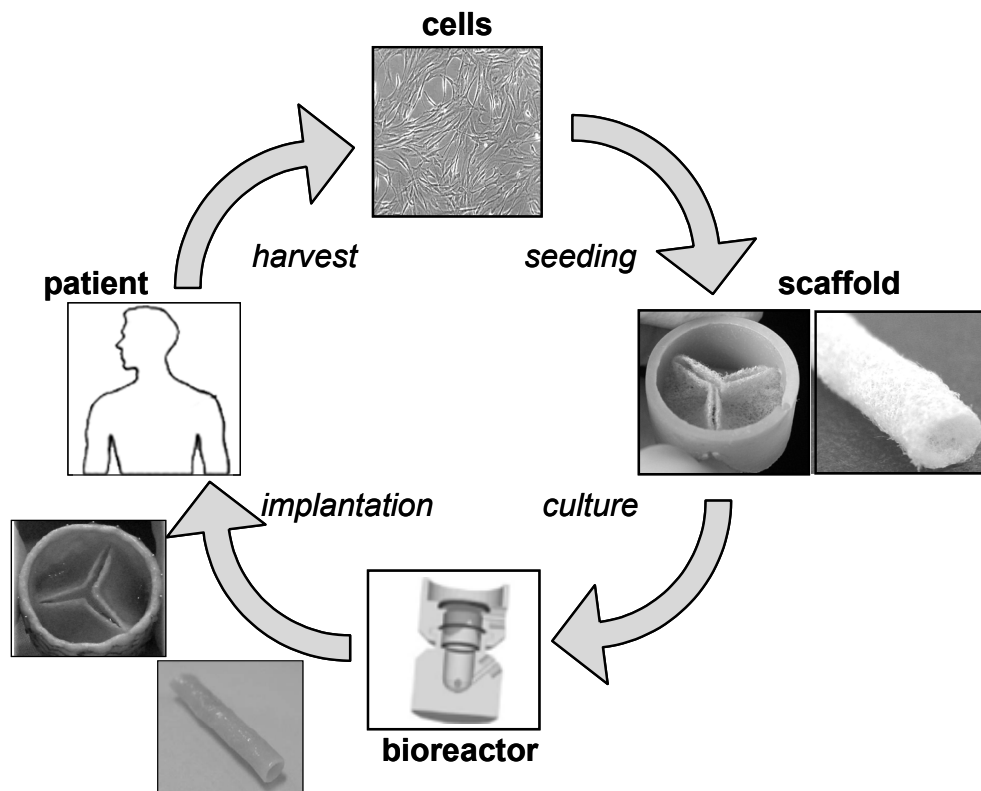


*Figure 1.5: Schematic overview of in vitro tissue engineering of heart valves and blood vessels. Cells, harvested from a patient, are seeded onto a scaffold in the shape of a heart valve or blood vessel. Subsequently, the tissues are cultured in a bioreactor where biochemical and mechanical stimuli are applied. The resulting living, autologous heart valves or blood vessels can be implanted back in the patient.*



Heart valves and blood vessels have been engineered using decellularized xenograft matrices, which were re-populated with cells before implantation. Indeed, implantation of decellularized valves re-populated with autologous vascular cells has shown promising results as a pulmonary valve replacement in sheep (Steinhoff *et al.*, 2000). It should be noted, however, that thickening of the leaflets was apparent, which may indicate structural degeneration. Seeding of decellularized valves and vena cava tissue patches with autologous bone-marrow derived cells, subsequent in vitro culturing and implantation in dogs, has shown partly re-populated and endothelialized tissues after three weeks (Cho *et al.*, 2005; Kim *et al.*, 2006). Despite the fact that decellularized xenografts or allografts seem to be an obvious choice as scaffold for tissue engineering, each has inherent limitations. For example, when the matrices are xenogenic in origin, the risk of zoonoses exists. When using allografts for pediatric patients, the availability of donor valves is still an unsolved problem. Further, remodeling and growth has not yet been demonstrated when using such valves, which is a prerequisite for use in children and young adults.

As an alternative to decellularized matrices, hydrogels consisting of either fibrin (Aper *et al.*, 2007; Cummings *et al.*, 2004; Flanagan *et al.*, 2007; Jockenhoevel *et al.*, 2001) or collagen (Cummings *et al.*, 2004; Seliktar *et al.*, 2000) have been used as scaffolds to create tissue-engineered heart valves and blood vessels. Fibrin-based tissue-engineered small-diameter blood vessels and pulmonary valves have demonstrated good results when implanted in sheep (Flanagan *et al.*, 2009; Liu *et al.*, 2007; Swartz *et al.*, 2005). However, a major concern for fibrin-based tissue-engineered substitutes is the mechanical instability of the tissue, and the potential to rupture in the systemic circulation (Jockenhoevel *et al.*, 2001).

The most promising tissue engineering approach with respect to growth capacity is based on synthetic scaffolds that rapidly degrade within a few weeks. The first successful replacement of a single pulmonary valve leaflet with an in vitro tissue-engineered equivalent based on a synthetic scaffold was demonstrated in young sheep (Shinoka *et al.*, 1995; Shinoka *et al.*, 1996). Full trileaflet valve replacements were subsequently fabricated based on synthetic scaffolds and were shown to be fully remodeled in sheep into native-like tissue structures with adequate functioning up to eight months after implantation (Sodian *et al.*, 2000a; Sutherland *et al.*, 2005). Hoerstrup *et al.* (2000) used mechanical conditioning to create trileaflet heart valves by exposure of the growing tissues to increasing levels of pulsatile flow. This approach has demonstrated potential in animal studies. Vascular patches, based on synthetic polymer scaffolds and seeded with autologous bone marrow-derived cells have demonstrated tissue regeneration after eight weeks of implantation in dogs (Cho *et al.*, 2006). The originally seeded cells were still present in the neo-tissue, indicating their active role in the tissue regeneration process. Similar to heart valves and vascular patches, large blood vessel substitutes (Hoerstrup *et al.*, 2006; Shinoka *et al.*, 1998; Watanabe *et al.*, 2001), as well as small-diameter blood vessels (Niklason *et al.*, 1999), have been tissue-engineered, based on synthetic scaffolds, and have yielded promising results in animal studies. Growth of engineered blood vessels has been demonstrated in a two-year follow-up study in juvenile sheep (Hoerstrup *et al.*, 2006).

The in vitro tissue engineering approach based on synthetic scaffolds has not only shown promising results in animal studies, it could also be translated into the clinical setting. For example, tissue-engineered patches based on a synthetic scaffold seeded with autologous saphenous vein cells have been successfully used for pulmonary artery reconstruction in humans (Matsumura *et al.*, 2003; Shin'oka *et al.*, 2001). However, the clinical feasibility for autologous tissue-engineered heart valves and blood vessels has still to be demonstrated.

## 1.6 Mechano-regulation of collagen architecture

Tissue composition and organization are continuously changing due to growth and environmental stimuli, in particular mechanical stimuli. Cells sense and control their extracellular environment by changing or remodeling their extracellular matrix. Strain is an important modulator as this triggers cells to modulate their environment. Understanding how cells remodel their matrix in response to external forces, such as strain, is crucial to design tissue-engineered substitutes with controlled mechanical properties. Model systems can be used to achieve this understanding in a high-throughput and well-defined environment.

Many devices have been developed to subject individual cells to mechanical strain (Brown, 2000; Lee *et al.*, 1996). The effects on matrix synthesis depended on many factors including the loading regime (magnitude, frequency, straining mode), species, and cell type. The diverse nature of the studies, in terms of strain profiles and cell types, makes direct comparisons very difficult (Berry *et al.*, 2003). In general, dynamic mechanical stimulation of cells seeded on two-dimensional substrates showed upregulation of matrix production (e.g., collagen) (Butt and Bishop, 1997; Ku *et al.*, 2006; O'Callaghan and Williams, 2002) and differences in cell morphology (Wang *et al.*, 2001) and proliferation (Yang *et al.*, 2004).

Cells in two-dimensional culture lack the physiological three-dimensional environment. Therefore, native tissues and cell-seeded collagen gels have often been used to study the effects in a three-dimensional environment. Ex-vivo studies on porcine heart valves (Weston and Yoganathan, 2001; Xing *et al.*, 2004b; Xing *et al.*, 2004a) showed that mechanical stimuli affect matrix synthesis of the cells, depending on the nature of the applied flow, the magnitude of pressure, and pulse frequencies. In the absence of mechanical stimuli, a decrease in tissue properties of porcine valves was observed (Konduri *et al.*, 2005), while cyclic stretching increased collagen content (Balachandran *et al.*, 2006). Mechanical stimulation of cell-seeded collagen gels affected several processes such as matrix production and, in most cases, enhanced the mechanical properties of the constructs (Isenberg and Tranquillo, 2003; Seliktar *et al.*, 2000). These changes in matrix production in response to strain underline the relevance of mechanical conditioning to create functional engineered tissues.

With respect to collagen cross-link formation, the effect of mechanical conditioning is largely unknown, but the relevance of cross-links has been shown for tissue mechanical properties in skin and bone tissue. Research on skin has

demonstrated that with age mechanical strength and stiffness increase in conjunction with an increase in the concentration of the intermolecular collagen cross-links (Avery and Bailey, 2005). Furthermore, in bone tissue, a correlation was found between collagen cross-linking and biomechanical properties (Banse *et al.*, 2002). Although bone is structurally different from cardiovascular tissue, it is proposed that cross-links also enhance the stability and strength of collagen fibrils in cardiovascular tissues.

The effect of mechanical loading conditions on collagen orientation has, for example, been studied in simple geometries of cell-populated collagen gels. It was demonstrated that uniaxial constraints induced anisotropic collagen orientation (Costa *et al.*, 2003; Kostyuk and Brown, 2004), whereas biaxial constraining resulted in isotropic orientations (Thomopoulos *et al.*, 2005).

Studies in these model systems indicate that the collagen architecture is dependent on mechanical cues. It is therefore proposed to use these cues in cardiovascular tissue engineering to induce and control the collagen architecture of engineered tissues.

## **1.7 Mechanical conditioning in cardiovascular tissue engineering**

Although quantitative laws of strain-induced collagen architecture are not available, there is strong evidence that mechanical conditioning enhances tissue properties in engineered cardiovascular tissues. As mentioned earlier, Hoerstrup *et al.* (2000) showed that improved mechanical properties of tissue-engineered heart valves were created by subjecting the tissues to increasing flow and pressure. By contrast, a mechanical conditioning protocol incorporating strain alone has been reported by Mol *et al.* (2005). This protocol, in which the leaflets were mechanically conditioned only in the diastolic phase of the heart, has shown to render tissue-engineered heart valves, capable of withstanding high *in vivo* pressures in the systemic circulation. Also the application of dynamic flexure was shown to improve the mechanical properties of tissue-engineered constructs (Engelmayr, Jr. *et al.*, 2005). In collagen gel-based tissue-engineered heart valves, the application of specific mechanical constraints led to commissural alignment of the collagen fibers (Neidert and Tranquillo, 2006). In a similar manner, mechanical conditioning was shown relevant for enhancing tissue properties of engineered blood vessels (Hoerstrup *et al.*, 2006; Niklason *et al.*, 1999; Stekelenburg *et al.*, 2009).

Although a continuous dynamic strain regime is often applied as it reflects a physiological straining situation for blood vessels and heart valves, this regime might not be optimal to create tissue-engineered substitutes. Indeed, intermittent conditioning has been proposed to disrupt the adaptation response of cells to a continuous stimulus. It has been hypothesized that cells yield a specific upper limit when responding to mechanical load (Chowdhury *et al.*, 2003; Robling *et al.*, 2002). Above this limit, additional loading has no or little effect. Therefore, a delicate balance between periods of mechanical stimulation alternated with periods of recovery seems to be more effective. Indeed in bone, cartilage, and tendon cell studies, an intermittent strain

regime has been demonstrated to be favorable in terms of cell proliferation (Barkhausen *et al.*, 2003; Winter *et al.*, 2003), matrix production (Chowdhury *et al.*, 2003), and mechanical properties (Robling *et al.*, 2002), when compared to a continuous strain regime.

## 1.8 Objective and outline

A main challenge in cardiovascular tissue engineering is to create tissues with optimized and controlled mechanical properties. This can be achieved by controlling tissue architecture, more specifically the collagen architecture, which, in turn, can be regulated via mechanical conditioning (figure 1.6). The goal of this work is to elucidate the effects of well-defined conditioning protocols on collagen architecture (amount, cross-links, orientation) and the changes (remodeling) of this architecture. Understanding these effects will enable optimization of the conditioning regimes for engineered cardiovascular tissues.

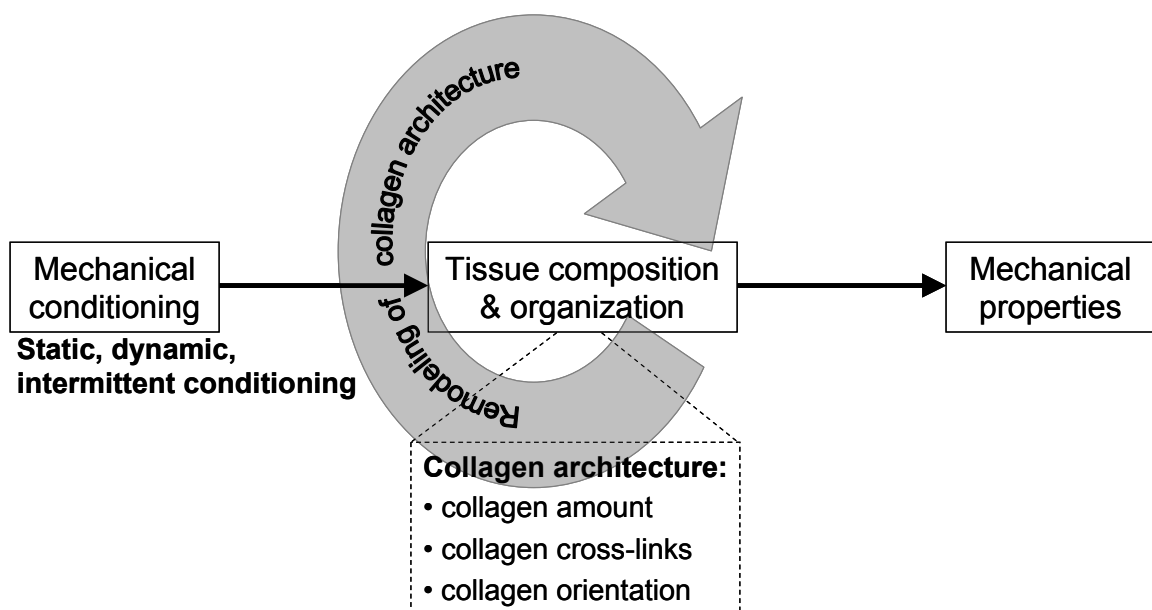


Figure 1.6: A schematic outlining the key objectives of the current work.

Chapter 2 describes the approach and methods to determine the effects of mechanical conditioning on collagen architecture in engineered cardiovascular tissues. These include a tissue model, a straining system, and methods to quantify aspects of the collagen architecture. In chapter 3, the model system is used to study short-term effects (up to 10 days) of static and dynamic conditioning on several aspects of remodeling in engineered tissues. Differences in collagen and cross-link densities are quantified with time at both gene expression and protein levels. In addition, the secretion of collagen synthesis and degradation markers is investigated with time. Long-term effects (4 weeks) of static and dynamic conditioning on collagen amount

and cross-links, and the correlation to mechanical properties of (engineered) heart valve tissues, are examined in chapter 4. Chapter 5 studies the temporal effects of intermittent dynamic strain on tissue properties in engineered cardiovascular tissues. In chapter 6, a new method to quantify collagen orientations is applied to mechanically conditioned engineered cardiovascular tissues. Chapter 7 presents a general discussion based on the findings of the presented studies.

# Chapter 2

## Methods to quantify strain-induced collagen architecture in engineered cardiovascular tissues

Parts of this chapter are based on R.A. Boerboom, M.P. Rubbens, N.J.B. Driessen, C.V.C. Bouten, and F.P.T. Baaijens, *Effect of strain magnitude on the tissue properties of engineered cardiovascular structures*, *Annals of Biomedical Engineering*, 36(2), 244-253, (2008) and F. Daniels, B.M. ter Haar Romeny, M.P. Rubbens, and H.C. van Assen, *Quantification of Collagen Orientation in 3D Engineered Tissue*, in *Proc. Intern. Conf. on Biomedical Engineering BioMed 2006*; Editors: F. Ibrahim, Kuala Lumpur, Malaysia, 344-348, (2006).

## 2.1 Introduction

Similar to native tissues, the mechanical properties of engineered heart valves and blood vessels depend on their structural composition and organization. Collagen is the main load-bearing constituent of these tissues and its architecture is considered in this thesis as the amount of collagen, collagen cross-link density, and the orientation of the collagen fibers. This collagen architecture can be regulated by mechanical conditioning of the growing tissues. This chapter describes the tissue model and straining system which has been developed to study the effects of mechanical conditioning on collagen architecture. In addition, the methods that are used in this thesis to quantify the collagen architecture are illustrated.

## 2.2 Tissue model

To systematically investigate the effects of strain on collagen architecture in engineered tissues, a well-defined model system is required. Based on existing heart valve and blood vessel protocols (Mol *et al.*, 2006; Stekelenburg *et al.*, 2009), rectangular tissue-engineered (TE) strips were made and used as the tissue model for engineered cardiovascular tissues (figure 2.1a). Compared to the more complex geometry of heart valves and blood vessels, these strips are of simple geometry and smaller in size, reducing the required number of cells. In addition, mechanical loading can be applied in a controlled way to multiple strips simultaneously.

To create TE strips, myofibroblast cells were harvested from the saphenous vein from a 44 year old woman. Myofibroblasts have been shown to be a suitable cell source for cardiovascular tissue engineering (Schnell *et al.*, 2001). This cell type is known for its relatively high expression of extracellular matrix (ECM) and its ability to actively remodel the ECM (Merryman *et al.*, 2006). This makes this cell source particularly suitable to study strain-induced effects on collagen architecture and remodeling. After harvesting, the cells were expanded for 7 passages in culture medium consisting of advanced Dulbecco's modified Eagle's medium (DMEM; Gibco, Carlsbad, CA), supplemented with 10% fetal bovine serum (FBS; Greiner Bio One, Monroe, NC), 1% GlutaMax (Gibco, Carlsbad, CA), and 0.1% gentamycin (Biochrom, Terre Haute, IN).

Non-woven polyglycolic acid (PGA) meshes were used as a biodegradable, highly porous synthetic scaffold. The PGA strips (35x5x1 mm) were coated with the thermoplastic poly-4-hydroxybutyrate (P4HB) (Sodian *et al.*, 2000a), which enhances the mechanical integrity of the PGA scaffold by cross-linking of the PGA fibers. The PGA-based scaffold is a rapidly degrading scaffold, which loses its mechanical integrity within several weeks.

To apply controlled dynamic strain to the TE strips, part of the porous PGA-based scaffold was embedded in a thin elastic layer of liquid silicone, to prevent plastic deformation of PGA. By partly pressing the scaffold into uncured silicone (Silastic MDX4-4210; Dow Corning, Midland, MI) a 0.5 mm thick elastic support was created.

After curing, the scaffolds were attached at the outer 5 mm in the longitudinal direction to the flexible membranes of six-well plates (Flexcell Int., McKeesport, PA) using Silastic MDX4-4210 (figure 2.1b). By attaching their outer ends, the tissues were constrained in the longitudinal direction.

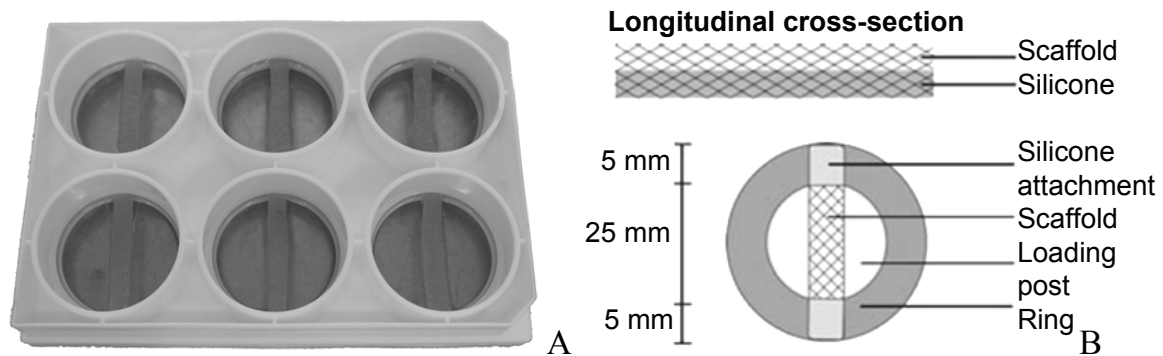


Figure 2.1: A: TE strips consisting of a PGA-P4HB scaffold, seeded with human venous cells using fibrin as a cell carrier. B: Reinforcement of the polyglycolic acid scaffold with an elastic silicone layer. The upper part shows a longitudinal cross-section of the PGA/P4HB scaffold embedded in an elastic silicone layer. The rectangular strips were attached to Bioflex culture wells to the outer 5 mm of these strips (lower part).

The scaffolds were vacuum-dried for 48 hours, followed by exposure to ultraviolet light for 1 hour and were subsequently placed in 70% ethanol for 5 hours to obtain sterility. Prior to cell seeding, tissue culture medium was added to facilitate cell attachment. The scaffolds were seeded with human venous myofibroblasts (passage 7) at a seeding density of  $2 \times 10^6$  cells per  $\text{cm}^2$  using fibrin gel. During the seeding procedure, cells are centrifuged and resuspended in a thrombin solution (10 IU/mL) (Sigma Chemicals, St. Louis, MO), mixed with a fibrinogen solution (10 mg/mL) (Sigma Chemicals), and dripped evenly on the scaffold. The cell–thrombin–fibrinogen solution is absorbed throughout the whole scaffold. Subsequently, polymerization of the fibrin gel starts, serving as a cell carrier during culture (Mol *et al.*, 2005b). The engineered constructs were cultured in tissue culture medium consisting of advanced DMEM (Gibco), supplemented with 10% FBS, 1% GlutaMax, 0.3% gentamycin, and L-ascorbic acid 2-phosphate (0.25 mg/mL; Sigma Chemicals). Medium was changed every 3 days.

## 2.3 Straining system

To investigate the effect of strain on collagen architecture in the TE strips, a straining system has been developed as described by Boerboom *et al.* (2008). The straining system consists of a modified version of a Flexercell FX-4000T (Flexcell Int., McKeesport, PA). This setup allows easy access to straining of cells using a vacuum



controlled deformation of Bioflex six-well plates (Flexcell) over a loading post. The original Flexercell system controls the strain magnitude by the amount of vacuum that was applied. This system was modified in order to apply various strain magnitudes to individual samples simultaneously by controlling the amount of membrane displacement when a vacuum was applied.

Figure 2.2 shows a schematic representation of the modified straining setup. Bioflex plates with flexible silicone membranes were mounted on a loading post. When a vacuum is applied to the flexible membrane of the Bioflex plate, the membrane deforms at the locations where it is not supported by the loading post. In the modified version, polycarbonate rings of varying heights were placed around the original loading posts. When a maximum vacuum is applied in the presence of the polycarbonate rings, the rings limit the deformation of the flexible silicone membrane. By varying the height of these rings the deformation of the membrane can be varied.

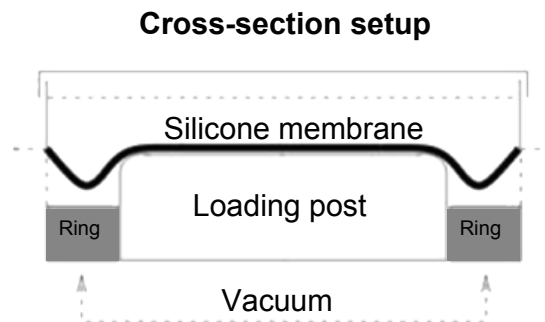


*Figure 2.2: Schematic cross-section of the modified Flexercell system. This schematic shows the polycarbonate rings (gray) placed around the loading post, which limit the deformation of the flexible silicone membrane when a vacuum is applied.*

First, the applied strain fields in this modified setup were validated for the flexible membranes without TE strips using digital image correlation. A random dot pattern was sprayed on the flexible silicone membrane of the Bioflex wells. These membranes were deformed over a round loading post by applying maximum vacuum pressure at a frequency of 1 Hz. During loading, images of the deformed state were recorded at 60 frames per second using a Phantom v5.1 high speed camera (Vision Research Inc., USA). The recorded images were analyzed using Aramis DIC software (Gom mbh., Germany). Strain fields were calibrated for three specific ring heights (8.16, 7.47, and 7.05 mm), corresponding to 4, 8, and 12 % strain, based on theoretical calculations. The strain profiles of the membranes showed homogeneous strain fields (figure 2.3) with resulting average strains (%) of  $3.8 \pm 0.6$ ,  $8.1 \pm 0.7$ , and  $12.5 \pm 0.5$ , respectively.

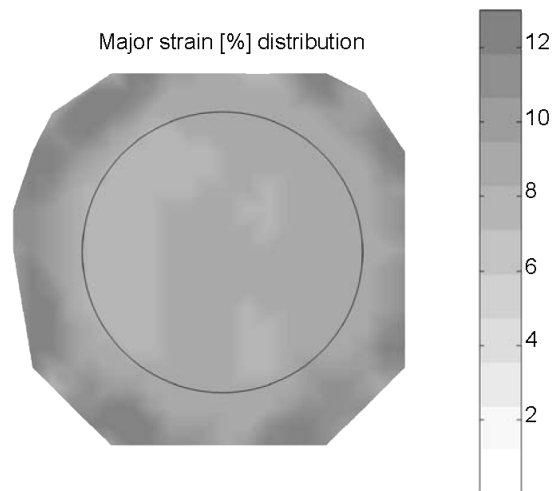


Figure 2.3: Representative two-dimensional strain (%) distribution of the Bioflex flexible membrane with the use of a 7.47 mm ring, corresponding to 8% strain. The strain profiles of the membrane shows a homogeneous strain field with a resulting average strain (%) of  $8.1 \pm 0.7$ . The circle indicates the loading post (Boerboom et al., 2008).

Then, the strain fields were validated at the surface of strained TE strips after 2 weeks of culture (1 week static culture + 1 week dynamic strain at 1 Hz) for two ring heights (8.16 and 7.47 mm), theoretically corresponding to 4 and 8 % strain, respectively. The average strains (%) measured  $4.6 \pm 1.3$  and  $8.0 \pm 2.8$ , respectively. Although the strain fields showed a more inhomogeneous distribution than the strain applied to the membrane without a TE strip, the average measured strains were close to the calculated ones and the major strain direction for both strain conditions was uniaxial in nature (figure 2.4). So, using this straining device, strains can be applied in a controlled manner to study their effects on collagen architecture.

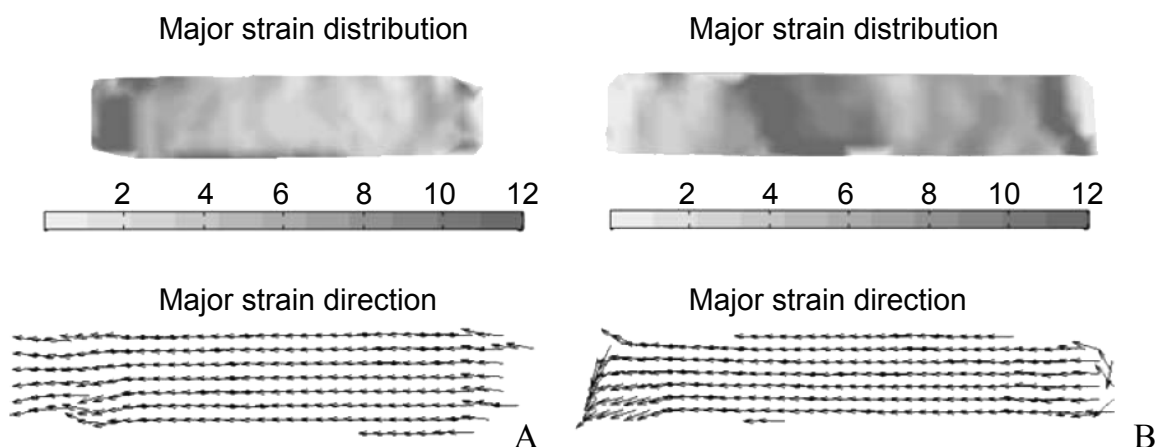


Figure 2.4: Representative two-dimensional tissue strain (%) distributions on the surface of engineered strips, in case of an 8.16 mm ring (A) and a 7.47 mm ring (B). The average strains (%) measured  $4.6 \pm 1.3$  and  $8.0 \pm 2.8$ , respectively. In both cases the strain is uniaxial (Boerboom et al., 2008).

## 2.4 Quantification of collagen architecture

### 2.4.1 Collagen amount and cross-links

Histological stainings, such as Masson Trichrome and Picrosirius Red reveal a qualitative view on the amount and location of collagen formed in engineered tissues. To quantify the effect of mechanical conditioning on collagen and cross-links, measurements on protein and gene expression levels can be performed. In addition, specific collagen synthesis and degradation markers can be measured to quantify the collagen remodeling activity.

#### Protein level

To quantitatively assess the amount of collagen on protein level, the amount of hydroxyproline was measured using reverse-phase high-performance liquid chromatography (HPLC). Hydroxyproline is a major component of the protein collagen and its amount can be converted to the amount of collagen using a conversion factor of 7.4 (Neuman and Logan, 1950) For HPLC, TE strips were lyophilized and subsequently hydrolyzed at 110°C for 22 hours in HCL. Hydroxyproline residues were measured on the acid hydrolysates after derivatization with 9-fluorenylmethyl chloroformate (FMOC) (Bank *et al.*, 1996). The advantage of the reagent FMOC is that it gives rise to a single, stable derivative per amino acid. The resulting derivative is detectable with high sensitivity and FMOC itself does not interfere with the chromatographic separation. The derivatized amino acids were subsequently separated based on their retention time to pass through the HPLC system. The same hydrolyzed samples were used to determine the amount of mature HP cross-links which are the main type of collagen cross-links present in cardiovascular tissues.

#### Gene expression level

In addition to the analysis of collagen and cross-link amount on protein level, quantitative polymer chain reactions (qPCR) were used to determine collagen and cross-link expression on gene expression levels. Accurate and fast qPCR studies reveal gene expression data that could be used to predict strain-induced effects on protein levels. In addition, using qPCR the effects on the expression of different types of collagen were determined. Frozen samples were lysated and RNA was isolated using an RNAeasy extraction kit (Qiagen, Venlo, The Netherlands) according to the manufacturer's instructions. The concentration and purity of the RNA were determined by measuring the absorptions at 260 nm and 280 nm. Subsequently, 500 ng RNA was transcribed into cDNA using random primers. Gene expression of collagen I (COL1A2), collagen III (COL3A1), PLOD-2 (encoding for cross-link enzyme) were analyzed by quantitative PCR using specific forward and backward primers and FAM/TAMRA labeled probes. All data were normalized to glyceraldehyde-3-phosphate dehydrogenase (GAPDH) expression.

### **Collagen synthesis and degradation markers**

The total collagen amount is a result of collagen synthesis and degradation. To discriminate between these processes, specific markers in the culture medium were measured. As described in chapter 1, collagens are synthesized as precursor molecules called procollagens. These contain additional peptide sequences, referred to as “propeptides”, at both the amino-terminal and the carboxy-terminal ends. The function of these propeptides is to facilitate the winding of procollagen molecules into a triple helical conformation within the endoplasmic reticulum. The propeptides are cleaved off from the collagen triple helix molecule during its secretion, after which the triple helix collagens polymerize into extracellular collagen fibrils. Thus, the amount of procollagen type I carboxy-terminal propeptides (PIP) in the medium was used as a measure of the amount of collagen type I molecules synthesized.

The concentration of PIP in the medium was determined using an Enzyme-Linked ImmunoSorbent Assay (ELISA) which is based on a “sandwich” technique. This technique involves several steps. Initially, the coating antibody, specific for the antigen, is bound to the microtiter plate. The first wash step removes unbound antibody and applies a blocking reagent to any surface not bound by the antibody. Next, the medium samples, standards and controls are incubated to allow capture of the antigen by the bound antibody. Subsequently, the unbound antigen is removed, and a labeled antibody, specific for a second site on the target protein, is added. Binding of this antibody forms an antigen “sandwich” with the coating antibody. The label on the second antibody is then detected by substrate addition, and color formation allows detection of the amount of antigen present in medium samples and standards.

ELISA assays were also used to quantify collagen degradation markers. Mature type I collagen is degraded by certain enzymes, such as matrix metalloproteinases (MMPs). Through the action of MMP-1, a carboxy-terminal telopeptide region of type I collagen (ICTP), joined via trivalent cross-links is liberated during the degradation of mature type I. The amount of ICTP in culture medium was measured using ELISA and reflects the amount of collagen molecules degraded.

## **2.4.2 Collagen orientation**

### **Visualization of collagen fibers**

To visualize the collagen fibers in the engineered strips, a fluorescent collagen-specific probe has been developed (Krahn *et al.*, 2006). In short, this development was based on a new approach that takes advantage of the inherent specificity of collagen-binding protein domains present in bacterial adhesion proteins (CNA35). The collagen-binding properties of the protein domain CNA35 are well characterized and this domain can be overexpressed in *Escherichia coli*. To obtain CNA35, a vector coding for the collagen-binding domain A of *Staphylococcus aureus* was transformed into *E. coli* and expression of this collagen-binding domain was induced. Subsequently, CNA35 was fluorescently labeled with Oregon Green (OG-488).

The CNA35-based probe has some important advantages over existing techniques for imaging collagen. Unlike the current label-free microscopic techniques,

the use of fluorescently labeled CNA35 allows visualization of much smaller newly formed fibrils. In addition, the binding of CNA35 to collagen is strong, but not so tight that it becomes irreversible. The latter property is important when such a probe is used to monitor collagen formation in real-time, where a probe should not affect the structural organization of the collagen that is formed. Finally, CNA35 is approximately 5 times smaller than antibodies which is beneficial to tissue penetration.

To image the collagen fibers in TE strips, the tissues were stained with the fluorescently labeled CNA35-OG488 probe (3  $\mu\text{M}$ ). In addition, the cells were labeled with 15  $\mu\text{M}$  Cell Tracker Blue CMAC (CTB; Invitrogen, The Netherlands). CTB and CNA35-OG488 are excitable with two-photon laser scanning microscopy (TPLSM) and exhibit broad spectra at 466 nm and 520 nm, respectively. An inverted Zeiss Axiovert 200 microscope (Carl Zeiss, Germany) coupled to an LSM 510 Meta (Carl Zeiss, Germany) laser scanning microscope was used to visualize cell and collagen organization. A chameleon ultra 140 fs pulsed Ti-Sapphire laser (Coherent, U.S.A) was tuned to 760 nm and two photomultiplier tube (PMT) detectors were defined as 435 – 485 nm for CTB and 500 – 530 nm for CNA-OG488. Two TPLSM images of cells and collagen in engineered tissues after different culture periods using the above mentioned method are shown in figure 2.5.

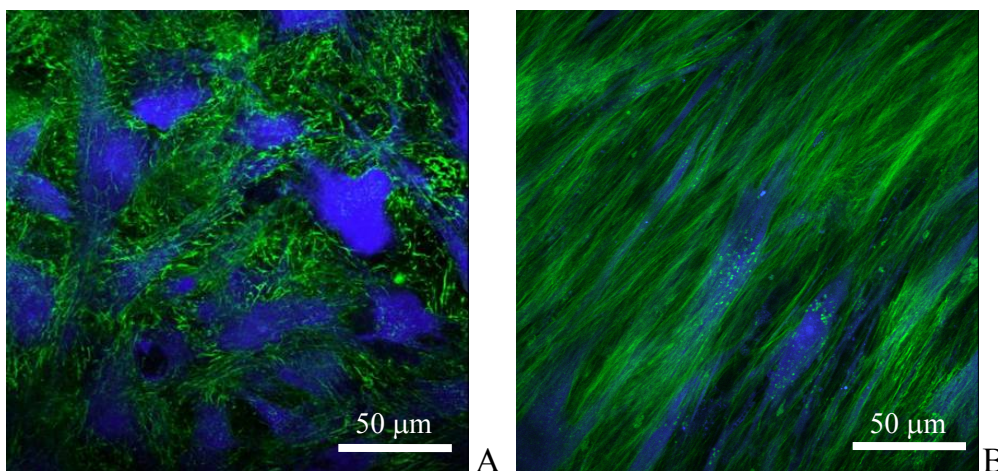


*Figure 2.5: Cells (cell tracker blue) and collagen fibers (CNA35, green) after 5 days (A) and after 4 weeks (B) of culture.*

The advantage of TPLSM is that the region excited by two-photon laser scanning microscopy is more restricted around the focal plane than by confocal laser scanning (CLSM) microscopy. This is due to the fact that the probability of a two-photon event is extremely low and occurs only when the laser light is the most intense, i.e. at the focal point. TPLSM uses longer wavelengths which are inherently less damaging to biological materials and more penetrating than the shorter wavelength used in CLSM. Thus, using the CNA probe in combination with TPLSM, the collagen fibers can be visualized in intact viable samples at different imaging depths.

### Quantification of collagen orientation

To quantify the collagen fiber orientations in the two-photon images, a quantification algorithm was developed (Daniels *et al.*, 2006). First, the images were de-noised by applying coherence-enhancing diffusion (CED) to improve the quality of the structures in the image (Weickert, 1999). Using CED, smoothing occurs along, but not perpendicular, to the preferred orientation of the structures, without destroying the boundaries of the fibers. After applying CED to two-photon images of collagen fibers, the images appear less noisy and the fiber structures are enhanced (figure 2.6).

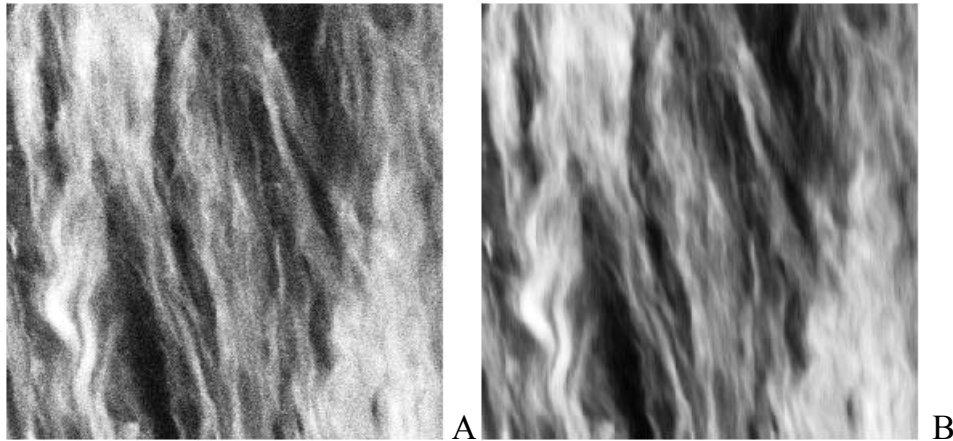


Figure 2.6: Original TPLSM image (A) of collagen fibers in a native heart valve and after application of coherence-enhancing diffusion which enhances the fibers (B).

The local orientations of the collagen fibers were determined by calculating the principal curvature directions. The principal curvatures are the maximum and minimum curvatures on a surface of an object, and the directions in which these occur are the principal curvature directions. At each point on a three dimensional object, three principal curvatures and principal directions ( $\lambda_1$ ,  $\lambda_2$ , and  $\lambda_3$ ) can be defined (figure 2.7a). The general orientation of the object is oriented along the minimal curvature direction.

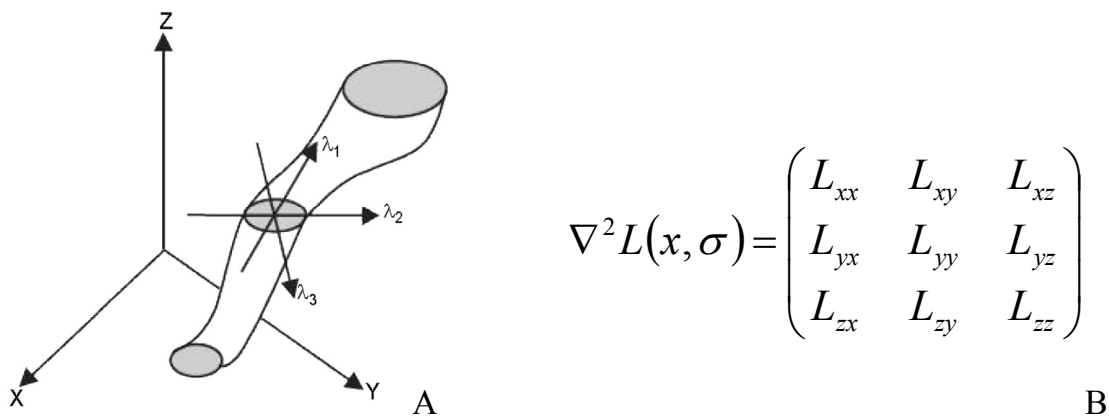


Figure 2.7: The principal curvature directions of a 3D structure (A) correspond to the eigenvectors of the second order Hessian matrix (B).

The principal curvatures can be determined from the Hessian matrix (figure 2.7b), which is a square matrix of second-order partial derivatives (Ter Haar Romeny, 2003) with  $L$  representing the image intensity,  $x$  representing the vector  $(x,y,z)$  and  $\sigma$  as a measure for scale used on the derivation of  $L$ . The eigenvalues and the eigenvectors of the Hessian matrix correspond to the principal curvature magnitudes and directions of the local image structure.

The collagen fibers appear as bright tubular structures in a dark environment. This prior knowledge related to the imaging modality can be used as a consistency check to discard structures with a different polarity. The conditions for an ideal bright tubular structure are:

$$\begin{aligned} |\lambda_1| &\approx 0 \\ |\lambda_1| &\ll |\lambda_2| \\ \lambda_2 &\approx \lambda_3 \end{aligned} \tag{eq. 2.1}$$

with the signs of  $\lambda_2$  and  $\lambda_3$  being negative.

As fibers appear at different widths, the second order derivatives were determined at a scale adaptive to the local width of the fiber. The optimal scale was determined with a contextual confidence measure (Niessen *et al.*, 1997). This confidence measure can be associated with a specific orientation to express the confidence in the principal curvatures and directions. The confidence measure  $C$  is defined as:

$$C(\lambda, \sigma) = \begin{cases} 0 & \text{if } \lambda_2 > 0 \text{ or } \lambda_3 > 0, \\ 1 - e^{-\frac{(\lambda_\Delta)^2}{2c^2}} & \text{otherwise,} \end{cases} \tag{eq. 2.2}$$

with  $\lambda_\Delta^2 = (|\lambda_1| - |\lambda_2|)^2 + (|\lambda_2| - |\lambda_3|)^2 + (|\lambda_3| - |\lambda_1|)^2$ ,  $|\lambda_1| \leq |\lambda_2| \leq |\lambda_3|$ , and  $c$  a predefined threshold.

The confidence measure becomes 0 for regions with no preferred orientation and has a maximum of 1 for regions with a high preference for one orientation. The scale  $\sigma$  for which the confidence measure is optimal, i.e. where  $C$  is closest to 1, is regarded as the optimal scale, and was chosen to analyze the orientation of the collagen fibers with. The quantification method was validated by Daniels *et al.* (2006).

## 2.5 Discussion

To study the effect of mechanical conditioning on collagen architecture, a well-defined three-dimensional model system was developed. Based on cardiovascular tissue engineering protocols, TE strips of simple geometry were created, particular suitable to study the effect of mechanical conditioning. In order to allow stretching of the engineered strips, part of the PGA scaffold was embedded in a thin layer of silicone

to prevent plastic deformation. The presence of the supporting elastic layer resulted in an elastic response on the engineered strips, illustrated by the fact that after two weeks of culture, the initially applied strain was preserved. A limitation of this setup is that tissue formation is constricted to the surface on the TE strips due to reduced supply of nutrients in the presence of the silicone layer.

The described model system and analyses techniques are used in this thesis as valuable tools to determine the effect of different loading protocols on collagen architecture and remodeling. Methods to determine strain-induced collagen amount and cross-links at both gene and protein levels, are applied in chapter 3. The straining system is also used to determine the effect of different straining modes on collagen architecture and associated mechanical properties in chapter 4 and 5. The quantification algorithm for collagen fiber orientations is applied to mechanically conditioned TE samples in chapter 6.





# Chapter 3

## Straining mode-dependent collagen remodeling in engineered cardiovascular tissue

The contents of this chapter are based on M.P. Rubbens, A. Mol, M.H. van Marion, R. Hanemaaijer, R.A. Bank, F.P.T. Baaijens, and C.V.C. Bouten, *Straining mode-dependent collagen remodeling in engineered cardiovascular tissue*, *Tissue Engineering*, 15(4), 841-849, (2009).

### 3.1 Introduction

Cardiovascular diseases are, next to cancer, the leading cause of death in the United States (Anderson and Smith, 2005). In 2004, cardiovascular diseases, such as heart valve dysfunction or coronary artery stenosis, accounted for 1 of every 2.8 deaths (Rosamond *et al.*, 2007). Currently used treatments for end-stage valvular disease include the replacement of the native heart valve by mechanical or biological valves. In case of coronary and peripheral artery diseases, the native, nonfunctional artery needs to be bypassed. Another medical need for vascular grafts exists in patients with renal failure who depend on dialysis. Autologous arteries and veins, as well as synthetic grafts are currently used as vascular grafts. The main drawback of mechanical heart valves and synthetic cardiovascular substitutes is that they are not able to grow, repair, and remodel, which is especially important for pediatric and young adult patients. In addition, biological replacements are highly susceptible to tissue degeneration (Schoen and Levy, 1999) and the progression of cardiovascular diseases (e.g., stenosis and arteriosclerosis), both leading to graft failure (Raja *et al.*, 2004; Sabik *et al.*, 2006). Tissue engineering represents a promising alternative to overcome these limitations by creating living tissue substitutes that are able to grow, repair, and adapt in response to changes in physiological demands.

Mimicking native mechanical behavior represents a major goal in cardiovascular tissue engineering, in particular when facing systemic pressure applications. Similar to native cardiovascular tissues, the mechanical properties of tissue-engineered constructs depend on the composition and quality of the extracellular matrix, which is a net result of matrix remodeling processes in the tissue. The extracellular matrix of tissue-engineered constructs predominantly consists of collagen fibers, embedded in a gel of proteoglycans, including glycosaminoglycans (GAGs). Collagen is the main load-bearing constituent of these tissues, and collagen cross-links and remodeling define their maturity and quality.

To date, tissue engineering of cardiovascular substitutes based on rapidly degrading scaffolds seeded with autologous myofibroblasts has been demonstrated as a promising procedure to produce living heart valve and blood vessel replacements (Hoerstrup *et al.*, 2000; Niklason *et al.*, 1999). In this approach, cells are stimulated to produce de novo extracellular matrix components in vitro. However, engineered tissues often lack sufficient amounts of properly organized matrix components and consequently do not meet in vivo mechanical demands. To optimize tissue quality and hence improve the mechanical properties of engineered tissues, mechanical conditioning strategies are critical (Isenberg and Tranquillo, 2003; Mol *et al.*, 2003; Seliktar *et al.*, 2003).

Various conditioning protocols, such as flow-based and strain-based protocols, have been demonstrated to improve tissue properties. Previous conditioning protocols were often designed to mimic physiological circumstances. For example, using an in vitro pulse duplicator, in which the tissue is exposed to increasing pulsatile flows, tissue-engineered heart valves have been obtained, which were successfully implanted at the pulmonary position in sheep (Hoerstrup *et al.*, 2000). Novel strain-based conditioning protocols combine constrained tissue culture with additional dynamic

conditioning. These conditioning protocols have shown to result in functional tissues that provide the potential for use as aortic valve (Mol *et al.*, 2006) and small artery (Stekelenburg *et al.*, 2009) replacements. However, the biological remodeling mechanisms underlying the strain-induced phenomena remain unclear. Accordingly, the goal of this study is to quantify the effects of strain-induced tissue remodeling, which can subsequently provide an input to mechanical conditioning protocols to fine-tune tissue properties. It is hypothesized that tissue remodeling depends on the mode of straining and thus two modes of straining, either static or dynamic, were quantified on several indices of tissue remodeling over a period of 10 days. Differences in matrix composition (collagen, GAGs, cross-links) were quantified. Collagen and cross-links were measured at both gene expression and protein levels with time. In addition, the secretion of specific collagen remodeling markers was investigated with time: collagen remodeling enzyme matrix metalloproteinase-1 (MMP-1), collagen synthesis marker (procollagen type I carboxy-terminal propeptide, PIP), and collagen degradation marker (carboxy-terminal telopeptide of type I, ICTP).

The effect of strain on matrix production has previously been studied in two-dimensional culture systems (Asanuma *et al.*, 2003; Ku *et al.*, 2006; O'Callaghan and Williams, 2002; Stanley *et al.*, 2000; Yang *et al.*, 1998), lacking a physiological three-dimensional environment. By contrast, strain-stimulated remodeling has only been rarely studied in three-dimensional cell-seeded constructs. In cell-seeded collagen gels, it has been demonstrated that dynamic strain influenced the gene expression of collagen and elastin (Seliktar *et al.*, 2003). However, corresponding levels of protein content were not determined. Studies investigating the effect of dynamic strain on the formation of neo-tissue in cell-seeded rapidly degrading scaffolds do report matrix protein values, but only at the time of sacrifice after several weeks (Boerboom *et al.*, 2008; Mol *et al.*, 2005a). The present study is the first to explore temporal effects of mechanical conditioning on tissue remodeling in a well-defined model system of three-dimensional cardiovascular tissues.

## **3.2 Materials and methods**

### **3.2.1 Cell culture**

Myofibroblasts were acquired from the human vena saphena magna according to the Dutch guidelines for secondary use material and expanded using regular cell culture methods as described previously (Schnell *et al.*, 2001). Culture medium consisted of advanced Dulbecco's modified Eagle's medium (DMEM; Gibco, Carlsbad, CA), supplemented with 10% fetal bovine serum (FBS; Greiner Bio One, Monroe, NC), 1% GlutaMax (Gibco, Carlsbad, CA), and 0.1% gentamycin (Biochrom, Terre Haute, IN).

### 3.2.2 Engineered cardiovascular tissues

Scaffold preparation and cell seeding procedures were performed as described previously (Mol *et al.*, 2005a). Briefly, rectangular strips (35x5x1 mm) of non-woven polyglycolic acid (PGA) meshes (Cellon, Bereldange, Luxembourg) were coated with a thin layer of poly-4-hydroxybutyrate (Hoerstrup *et al.*, 2000) (TEPHA, Cambridge, MA). The PGA scaffold consists of fibers with a diameter of the order of 10–15  $\mu\text{m}$  and pore sizes that are sufficiently large for complete cell penetration within 3 days (Balguid *et al.*, 2008). The bottom surface of the scaffolds was reinforced with a non-toxic elastic silicone layer (Silastic MDX4-4210; Dow Corning, Midland, MI; thickness 0.5 mm), enabling precisely controlled cyclic deformation of the constructs up to several weeks (Boerboom *et al.*, 2008). In the longitudinal direction, the scaffolds were attached at the outer 5 mm to the flexible membranes of six-well plates (Flexcell Int., McKeesport, PA) using Silastic MDX4-4210. By attaching the scaffolds at their outer ends, the tissues were constrained in the longitudinal direction.

The scaffolds were vacuum-dried for 48 hours, followed by exposure to ultraviolet light for 1 hour and were subsequently placed in 70% ethanol for 5 hours to ensure sterility. Prior to cell seeding, tissue culture medium was added to facilitate cell attachment. The scaffolds were seeded with human venous myofibroblasts (passage 7) at a seeding density of  $2 \times 10^6$  cells per  $\text{cm}^2$  using fibrin gel. During the seeding procedure, cells were centrifuged and resuspended in a thrombin solution (10 IU/mL) (Sigma Chemicals, St. Louis, MO), mixed with a fibrinogen solution (10 mg/mL) (Sigma Chemicals), and dripped evenly on the scaffold. The cell–thrombin–fibrinogen solution is absorbed throughout the whole scaffold. Subsequently, polymerization of the fibrin gel starts, serving as a cell carrier during culture (Mol *et al.*, 2005b). The engineered constructs were cultured in tissue culture medium consisting of advanced DMEM (Gibco), supplemented with 10% FBS, 1% GlutaMax, 0.3% gentamycin, and L-ascorbic acid 2-phosphate (0.25 mg/mL; Sigma Chemicals). Medium was changed every 3 days and stored for medium analysis.

### 3.2.3 Tissue culture and mechanical conditioning

As the tissue-engineered strips were attached at their outer ends, static stress was generated by the cells as a response to constraining. After 3 days of culture under static conditions, four samples were sacrificed and used as baseline controls. Then, the engineered tissues were divided into two groups (figure 3.1). One group ( $n = 16$ ) served as static control, whereas the other group ( $n = 16$ ) was subjected to uniaxial dynamic strain (4%, 1 Hz) using a modified version of a Flexercell FX-4000T straining device (Flexcell) (Boerboom *et al.*, 2008). A strain magnitude of 4% was chosen as a suitable strain condition based on previous studies where it was shown that continuous dynamic strain at 8% and above produced reduced tissue properties compared to static conditioning (Boerboom *et al.*, 2008).

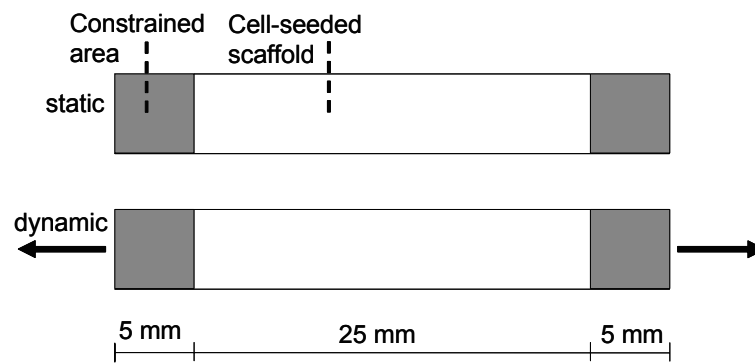


Figure 3.1: Top view of rectangular engineered strips. The strips were longitudinally constrained at the outer 5 mm at both ends using silicone glue. Dynamic strain in longitudinal direction (indicated by arrows) was applied to the samples in the dynamic group.

Static and dynamically conditioned samples ( $n = 4$  for each group per time point) were sacrificed after 3,  $3\frac{1}{3}$  (8 h after start of dynamic conditioning), 4, 6, and 10 days of culture (figure 3.2). The silicon layer was gently removed, and the samples were divided into two; half of the sample was used for quantitative PCR (qPCR) analyses and the other half for tissue content analyses.

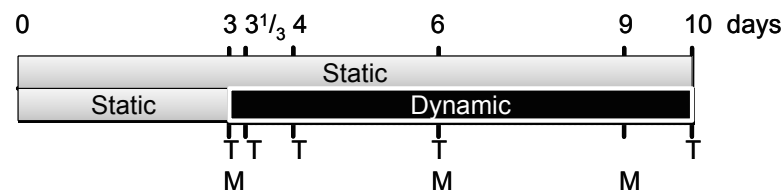


Figure 3.2: Experimental design with schematic overview of time points of analyses. “T” represents tissue analysis after 3,  $3\frac{1}{3}$ , 4, 6, and 10 days, and “M” represents medium analysis after 3, 6, and 9 days of culture ( $n = 4$  per group per time point).

### 3.2.4 Quantitative PCR analysis

RNA isolation and semiquantitative mRNA analysis using real-time competitive PCR (ABI Prism 7700; Applied Biosystems, Nieuwerkerk aan den IJssel, The Netherlands) were performed as described previously (Lindeman *et al.*, 2004; van der Slot *et al.*, 2003). In brief, RNA was isolated using an RNAeasy extraction kit (Qiagen, Venlo, The Netherlands) according to the manufacturer’s instructions. The concentration and purity of the RNA were determined by measuring the absorptions at 260 and 280 nm. Subsequently, 500 ng RNA was transcribed into cDNA using random primers. Gene expression of collagen I (COL1A2), collagen III (COL3A1), PLOD-2 (encoding for cross-link enzyme), and MMP-1 was analyzed by qPCR using specific forward and backward primers and FAM/TAMRA-labeled probes. All data were normalized to glyceraldehyde-3-phosphate dehydrogenase expression (GAPDH).

### 3.2.5 Quantification of matrix composition

Lyophilized samples were digested in papain solution (100 mM phosphate buffer, 5 mM L-cystein, 5 mM ethylenediaminetetraacetic acid, and 125–140 µg papain per mL) at 60°C for 16 hours. The amount of DNA was determined using the Hoechst dye method (Cesarone *et al.*, 1979), and expressed in mg per dry weight (dw). Subsequently, digested tissue samples were hydrolyzed in 6M hydrochloric acid (Merck, Darmstadt, Germany) and used for amino acid analyses. Hydroxyproline (Hyp) residues, as a measure for collagen content, were measured on the acid hydrolysates, using reverse-phase high-performance liquid chromatography after derivatization with 9-fluorenylmethyl chloroformate (Bank *et al.*, 1996). The amount of Hyp was expressed per DNA. The GAG content was determined using a modification of a well established GAG-assay (Farndale *et al.*, 1986). The amount of GAG in the samples was determined from a standard curve and expressed per DNA.

The number of mature collagen hydroxylysylpyridinoline (HP) cross-links, as a measure for tissue maturity, was determined in hydrolyzed samples using high-performance liquid chromatography (Bank *et al.*, 1996; Bank *et al.*, 1997; Robins *et al.*, 1996). The number of HP cross-links was expressed per collagen triple helix (TH).

### 3.2.6 Medium analysis

Concentrations of the remodeling enzyme MMP-1 and markers for collagen synthesis (PIP) and collagen degradation (ICTP) were determined in the culture medium by ELISAs. MMP-1 concentrations were quantified by a nonisotopic immunoassay for human MMP-1 protein (Calbiochem, Merck, Darmstadt, Germany). PIP was measured using a procollagen type I C-Peptide ELISA kit (Takara Bio, Otsu, Shiga, Japan). ICTP was determined using a quantitative enzyme immunoassay designed for in vitro measurement of carboxy-terminal cross-linked telopeptide of human type I collagen (Orion Diagnostica, Espoo, Finland). The ELISAs were performed according to the recommendations from the supplier. The assays were performed on medium samples after 3, 6, and 9 days of culturing (figure 3.2) and corrected for control medium that had been in contact with scaffolds without cells for 3, 6, and 9 days.

### 3.2.7 Statistics

Results are expressed as mean value  $\pm$  standard deviation. Student's t-tests were used to elucidate differences between static and dynamic conditioning at each time point. Dunnett's multiple comparison tests were used to compare values of later time points to the 3-day static baseline control, except for HP cross-links, where values were not detectable at this time point. In this case, values of later time points were compared to the first detectable time point after 4 days of culture. Differences were considered to be significant at a p-value  $< 0.05$ .

### 3.3 Results

#### 3.3.1 Effect of straining mode on gene expression

Human venous myofibroblasts expressed both collagen I and collagen III genes, of which collagen I mRNA was most abundantly expressed. Following 3 days of culture, dynamic strain was applied to the samples in the dynamic group. Both collagen I and III mRNA levels were significantly lower in dynamically strained samples from day 4 onward, when compared to static levels (figure 3.3a,b).

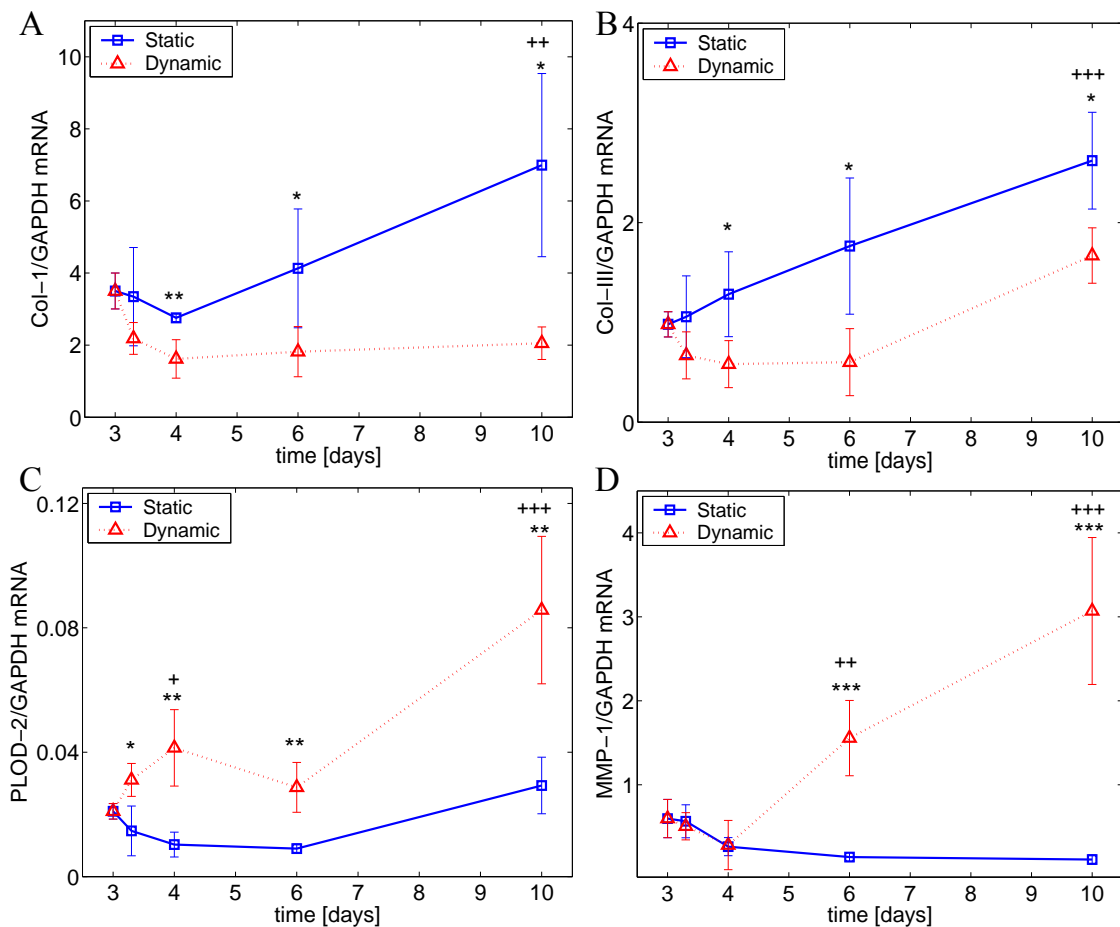


Figure 3.3: Collagen I (A), collagen III (B), PLOD-2 (C), and MMP-1 (D) gene expressions.  $*p < 0.05$ ,  $**p < 0.01$ , and  $***p < 0.001$  represent significant differences between dynamic and static conditioning.  $+p < 0.05$ ,  $++p < 0.01$ , and  $+++p < 0.001$  represent significant differences compared to the static baseline control after 3 days of culture. Dynamic strain resulted in lower collagen gene expressions, but higher PLOD-2 and MMP-1 gene expressions, when compared to static conditioning. In time, static conditioning increased collagen I and III mRNA expressions, while dynamic strain increased PLOD-2 and MMP-1 gene expressions.



In contrast, PLOD-2 mRNA expression was upregulated by dynamic strain, as compared to static conditioning (figure 3.3c). Compared to static conditioning, a significant higher MMP-1 mRNA expression was observed in the dynamically strained group after 6 and 10 days of culture (figure 3.3d). With time, static conditioning increased collagen I and III mRNA expressions, while no temporal variations compared to the 3-day baseline control were found as a consequence of dynamic conditioning. Dynamic strain increased PLOD-2 and MMP-1 mRNA expressions with time, as compared to the static baseline control after 3 days of culture. Static conditioning induced no temporal effects in PLOD-2 and MMP-1 mRNA expressions.

### **3.3.2 Effect of straining mode on tissue protein content**

The effects of static and dynamic conditioning on the amount of DNA, matrix proteins Hyp and GAG per DNA, as well as of HP cross-links per TH are depicted in figure 3.4. There were no significant changes in the amount of DNA per dry weight between static and dynamic conditioning. In addition, no temporal variations were found as compared to the 3-day baseline control (figure 3.4a). The amount of Hyp per DNA increased with time in both groups, although dynamic strain was less favorable for collagen production, as compared to static conditioning (figure 3.4b). On the other hand, GAG production was stimulated by dynamic strain and increased with time (figure 3.4c). In contrast, static conditioning did not show an increasing trend in GAG production with time. HP cross-link densities were not detectable until 4 days of culture. Dynamic strain resulted in significant higher numbers of HP cross-links per TH, as compared to static conditioning (figure 3.4d). With time, cross-link densities increased in both groups.

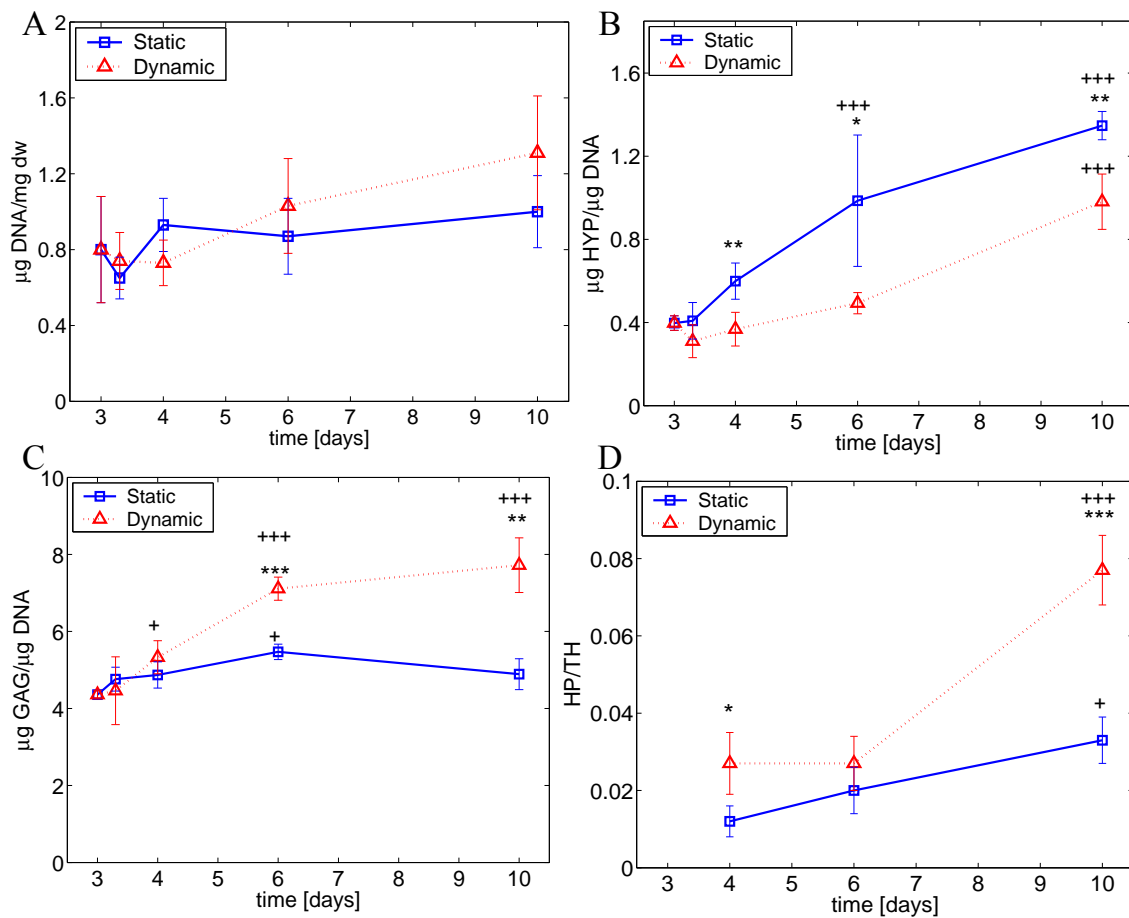


Figure 3.4: Tissue content including DNA (A), Hyp (B), GAGs (C), and HP cross-links (D). \* $p < 0.05$ , \*\* $p < 0.01$ , and \*\*\* $p < 0.001$  represent significant differences between dynamic and static conditioning. + $p < 0.05$  and +++ $p < 0.001$  represent significant differences compared to the static baseline control after 3 days of culture, except for HP cross-links, where values are compared to the first detectable time point. No significant differences in DNA content were found between static and dynamic conditioning. Dynamic strain resulted in lower collagen content, but higher cross-link density and GAG content, as compared to static conditioning. With time, collagen content and HP cross-link density increased in both groups, while GAG content was only increased after 10 days in the dynamically strained samples.

### 3.3.3 Effect of straining mode on collagen remodeling markers

The effects of different straining modes on specific collagen remodeling markers for collagen synthesis (PIP) and degradation (ICTP), and remodeling enzyme MMP-1 are shown in figure 3.5. All three markers of remodeling showed similar effects. PIP, ICTP, and MMP-1 concentrations in culture medium of dynamically strained samples increased with time and were statistically significantly higher compared to static samples. No temporal variations were observed in the concentrations of these markers in the medium of statically conditioned samples over the 9 day culture period.

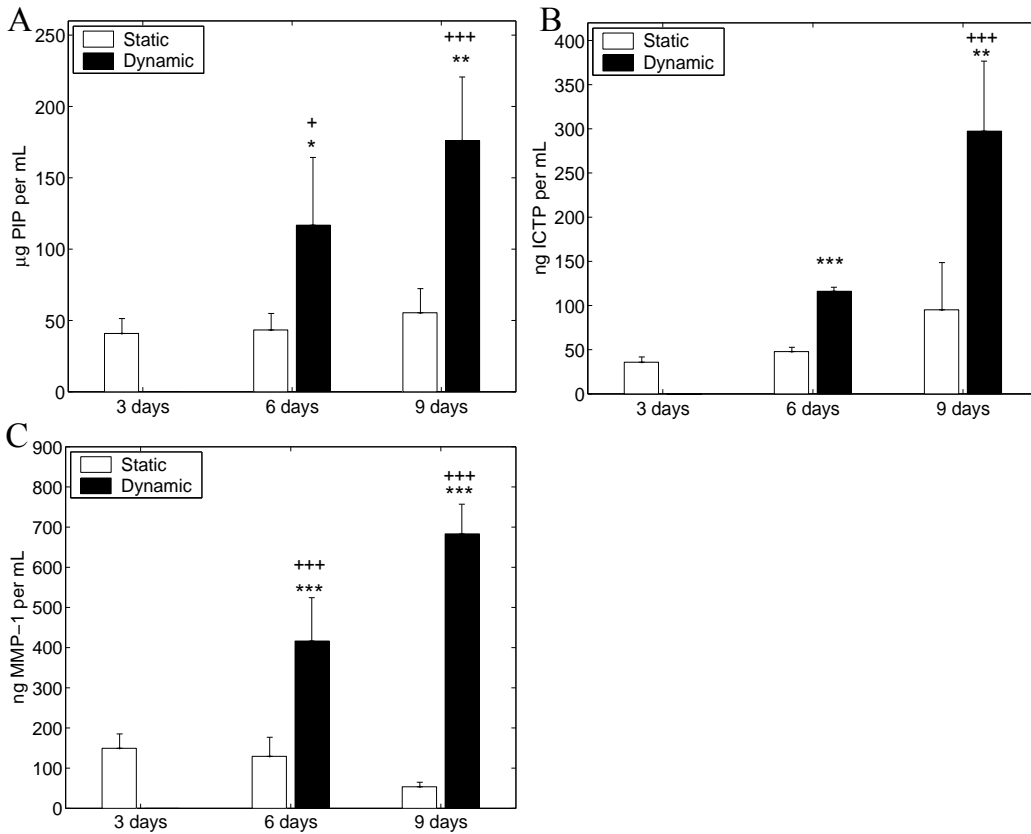


Figure 3.5: Concentrations of PIP (A), ICTP (B), and MMP-1 (C) in culture medium. \* $p < 0.05$ , \*\* $p < 0.01$ , and \*\*\* $p < 0.001$  represent significant differences between dynamic and static conditioning. + $p < 0.05$ , and +++ $p < 0.001$  represent significant differences compared to the static baseline control after 3 days of culture. This static baseline control after 3 days is similar for both conditioning groups. The concentrations of all remodeling markers increased with time for the dynamically strained samples, and were higher compared to statically conditioned samples, where no temporal variations were observed.

### 3.4 Discussion

Similar to native cardiovascular tissues, the mechanical properties of engineered cardiovascular constructs highly depend on the composition and quality of the extracellular matrix. Both the composition and quality are subject to change during tissue remodeling in response to mechanical loading of the tissue. In tissue engineering strategies, this is mimicked by conditioning the tissue with mechanical cues. Strain-based conditioning protocols have been shown to result in functional tissues that provide the potential for use as aortic valve and small artery replacements (Mol *et al.*, 2006; Niklason *et al.*, 1999; Stekelenburg *et al.*, 2009). Nevertheless, the mechanical properties of these engineered tissues still do not meet those of adult native cardiovascular structures due to inefficient remodeling during the *in vitro* culture period. Systematically quantifying the effects of strain on matrix remodeling can

elucidate how conditioning protocols can be optimized to achieve and control tissue properties using mechanical conditioning.

While the majority of studies use two-dimensional systems, in this study a well-defined three-dimensional model system was used to explore temporal strain-induced remodeling responses in engineered cardiovascular tissues. It was hypothesized that these responses are influenced by the mode of straining and thus the effects of two modes of straining, either static or dynamic, were quantified on several indices of tissue remodeling with time. Differences in matrix composition (collagen, GAGs, cross-links) were quantified. In addition, the secretion of specific collagen remodeling markers (MMP-1, PIP, and ICTP) was investigated.

As native heart valves and blood vessels mainly consist of collagen type I and, with smaller amounts of collagen type III, the capacity to produce these types of collagen is crucial for cardiovascular tissue engineering. Both collagens I and collagen III were expressed in the engineered tissues, of which collagen I was most abundantly expressed (figure 3.3a,b). Static conditioning increased collagen I and III expression with time. Apparently, the internal stresses generated due to constraining the tissue are sufficient to stimulate cells to express these collagen types. This emphasizes the relevance of constraining during tissue culture. Additional dynamic strain resulted in lower collagen I and III expressions. This might suggest that dynamic strain might not be required for the production of collagen over the investigated culture period. However, there seems to be an increasing trend in collagen III expression from 6 days onward in the dynamically strained samples. It is probable that cells need some time to produce, remodel, and mature the tissue. Similar to the wound healing process (Stadelmann *et al.*, 1998), during *in vitro* tissue engineering, collagen type III might be formed and deposited at an earlier time point than collagen type I. These early collagen fibers would then be remodeled, leading to a more mature tissue, consisting of mainly type I collagen, which is the predominant type in cardiovascular tissues.

In addition to its content, collagen cross-links play an important role in tissue maturity and are critical in providing mechanical integrity (Balguid *et al.*, 2007). The mature HP cross-links are the main type of collagen cross-links present in cardiovascular tissues. These cross-links are formed following hydroxylation of the telopeptides of collagen. PLOD-2 has been identified as a telopeptide lysyl hydroxylase, the enzyme responsible for this hydroxylation process (van der Slot *et al.*, 2003). In the present study, PLOD-2 mRNA expression levels of dynamically strained constructs increased with time and were higher than for statically conditioned constructs. Thus dynamic strain seems crucial to upregulate PLOD-2 to enhance the formation of HP cross-links.

The effects of strain on gene expression were consistent with those at the level of protein expression: a dynamic strain regime resulted in lower collagen amounts, but enhanced cross-link densities, when compared with static conditioning. This suggests that during continuous dynamic strain, cells switch their metabolic balance from collagen to cross-link synthesis, thus catalyzing a more stable deposition of collagen fibers. This indicates that despite a lower collagen amount, the quality and structural

stability of the neo-tissue might be enhanced by dynamic strain via upregulation of cross-links, enabling well organized collagen fibers.

In contrast to the effect on collagen production, the production of GAGs was enhanced by dynamic strain (figure 3.4c). Most likely, GAG production is upregulated to embed, stabilize, and protect the newly formed matrix components (Grande-Allen *et al.*, 2004; Scott and Parry, 1992; Snowden, 1982). The presence of GAGs will be useful to withstand the in vivo repetitive strains, as GAGs play a role in shock absorbance.

Besides quantification of tissue remodeling on gene expressions and protein levels, specific collagen remodeling markers were investigated. Markers for collagen synthesis (PIP) and degradation (ICTP) were measured to provide insight in the straining mode-dependency of the collagen turnover balance. The formation of collagen from soluble collagen occurs by releasing the procollagen propeptides (PIP). This process seems to be enhanced by a dynamic strain regime. Collagen degradation marker ICTP, which is released after cleavage of collagen by MMPs, was also enhanced by dynamic strain. The balance between synthesis and degradation, and the resulting net collagen content, appeared to be dependent on the straining mode. Thus dynamic strain increased both synthesis and degradation, and hence remodeling, but resulted in lower net collagen levels as compared to static conditioning. In addition, higher MMP-1 mRNA expression and protein levels were found in response to dynamic loading. Changes in remodeling enzymes, such as MMPs, have been reported to play a key role in tissue maintenance, repair, and strain-induced remodeling (MacKenna *et al.*, 2000; Seliktar *et al.*, 2001). The relevance of MMPs in cardiovascular development and remodeling has been confirmed by highly elevated levels of MMP-1 in fetal-developing heart valves compared to very low values in adult valves (Aikawa *et al.*, 2006). These results suggest a direct correlation between MMP-1 levels and remodeling activity. So, in addition to enhanced collagen synthesis and degradation markers, enhanced MMP-1 levels in dynamically strained samples also indicate enhanced remodeling activities due to dynamic conditioning.

It is likely that the strain-enhanced cross-link densities and remodeling activities will eventually lead to a more mature collagen architecture and improved mechanical properties. Other studies based on similar cell-seeded biodegradable scaffolds demonstrated improved mechanical properties after four weeks of culture due to dynamic conditioning, while collagen levels were equal to statically conditioned samples (Boerboom *et al.*, 2008; Mol *et al.*, 2006). The present study now indicates that the improved mechanical properties are most likely due to higher cross-link densities than to the amounts of collagen per se.

To attain native values in engineered cardiovascular constructs, mechanical conditioning protocols need to be optimized and controlled. Where regular autologous tissue engineering protocols take several weeks, the present study has indicated that straining mode-dependent differences are induced and detectable after several days. Interestingly, the effects on the level of gene expression corresponded to protein data. This means that accurate and fast qPCR studies in this well-defined model system can be used as valuable tools to unravel the effects of other strain parameters, such as period, magnitude, and frequency. Moreover, the analysis of specific collagen

remodeling markers in culture medium enables an online non-destructive measurement of collagen remodeling. These methods are helpful towards a well-considered optimization of tissue engineering protocols. For example, current studies in our lab focus on intermittent dynamic strain protocols to combine the favorable effects of collagen production due to static conditioning and of cross-link formation due to dynamic protocols.

This present study mainly focuses on the effect of static and dynamic conditioning on the remodeling of collagen, which represents the main load-bearing part of cardiovascular tissues. Besides collagen, elastin plays a role in the biomechanical behavior of cardiovascular tissues, providing resilience to the tissue. Disturbances in the elastin homeostasis in heart valves and arteries are believed to represent an underlying cause of valve replacement failure (Schoof *et al.*, 2006) and the formation of aneurysms (Anidjar *et al.*, 1990). Therefore, elastin formation has been acknowledged as a “missing link” for a complete biomechanical function of tissue-engineered cardiovascular replacements (Patel *et al.*, 2006). Only few studies have investigated the effect of mechanical conditioning on elastin formation by cardiovascular cells. These studies report that mechanical strain tends to increase elastin synthesis by vascular smooth muscle cells, although the effects are sensitive to both strain magnitude and mode (Isenberg and Tranquillo, 2003; Sutcliffe and Davidson, 1990). Ongoing studies in our lab investigate whether mechanical conditioning alone leads to an adequate elastin network in engineered cardiovascular tissues or whether biochemical cues are additionally needed.

In conclusion, this study demonstrates that collagen remodeling is straining mode-dependent. Static conditioning stimulated collagen gene expression and production with time. Dynamic strain resulted in (1) lower collagen gene expression and protein content, but (2) enhanced collagen cross-link expression and density, and GAG content, and (3) stimulated collagen remodeling, as expressed by enhanced production of specific collagen remodeling markers. This indicates that despite a lower net collagen amount, the quality and structural integrity of the tissue are improved by a dynamic strain regime. These straining mode-dependent remodeling responses provide a balance of collagen production and cross-link formation and thus a mechanism to fine-tune tissue properties. This is of importance for cardiovascular tissue engineering, where insufficient mechanical properties are a main limiting factor for present in vivo application.

### **Acknowledgements**

This research is supported by the Dutch Technology Foundation (STW), Applied Science Division of NWO, and the Technology Program of the Dutch Ministry of Economic Affairs. The authors would like to thank Jessica Snabel and Anita van de Loo for performing the biochemical assays. PCR facilities and materials were kindly provided by TNO Leiden, Department of Tissue Repair.



# Chapter 4

## The role of collagen cross-links in the biomechanical behavior of human native and engineered heart valve tissue

The contents of this chapter are based on A. Balguid, M.P. Rubbens, A. Mol, R.A. Bank, A.J.J.C. Bogers, J.P. van Kats, B.A.J.M. de Mol, F.P.T. Baaijens, and C.V.C. Bouten, *The role of collagen cross-links in biomechanical behavior of human aortic heart valve leaflets – Relevance for tissue engineering*, Tissue Engineering, 13(7), 1501-1511, (2007)



## 4.1 Introduction

Worldwide, approximately 275,000 heart valve replacement surgeries are performed annually as a result of heart valve disease (Rabkin and Schoen, 2002). Although conventional valve replacement therapies offer functional solutions, they are associated with significant risks that limit their success (Grunkemeier and Rahimtoola, 1990; Jamieson, 1993; Schoen and Levy, 1999; Vara *et al.*, 2005). An important shortcoming of prosthetic valves is their inability to grow, adapt, and repair, which is particularly relevant for pediatric patients. This drives the multidisciplinary approach of tissue engineering as a promising technique for heart valve substitutes. In this approach, autologous cells are used to produce living tissues to replace the damaged or diseased native heart valves.

Tissue-engineered (TE) heart valves based on rapidly degrading scaffolds have been successfully implanted in the pulmonary position in sheep, showing function and tissue composition that resembles that of native tissue after 5 months (Hoerstrup *et al.*, 2000). Mol *et al.* (2006) succeeded in the fabrication of human TE valves that were able to withstand physiological systemic pressures up to 4 hours in an *in vitro* setup. The valves showed developing anisotropic properties after 4 weeks of culture in a bioreactor. In view of these developments in the field of human TE heart valves, a comparison between TE and human native valves is necessary as criteria are needed to determine when TE tissue can be considered adequate for future implantations in patients. A detailed understanding of the relationship between matrix architecture and biomechanical function of the native aortic heart valve is therefore crucial to further progress in this field.

In heart valves, like in many tissues, collagens are the main structural proteins and the biomechanical properties depend on the collagen architecture. This collagen architecture includes many aspects such as the collagen amount and type, cross-link densities, collagen fiber morphology and orientation. The collagen fibers of the aortic valve leaflets resemble a hammock-type orientation (figure 4.1a) which allows much higher stiffness in the circumferential direction than in the radial direction of the leaflets, as was demonstrated by biaxial tensile tests on porcine aortic valves (Yacoub *et al.*, 1999). To ensure long-term function, mimicking the native collagen architecture might be essential in heart valve TE, in particular when facing systemic applications. However, how the various aspects of collagen architecture contribute to the biomechanical behavior of heart valves is not fully clear.

Due to the limited availability of fresh material and simulated test environments, biomechanical characterization of human aortic valves has been rarely reported (Clark, 1973; Stradins *et al.*, 2004) and the results have not been correlated to structural properties. Available studies on structure–function relationships have mainly focused on the role of elastin and have been performed on porcine aortic valves (Schoen, 1997; Vesely, 1998). Due to species differences, extrapolation of such results to human valves is problematic. Several studies have been conducted to investigate matrix composition and collagen architecture in healthy and diseased human and animal aortic valves. These incorporate histological examinations of collagen organization (de Lange

*et al.*, 2004; Kunzelman *et al.*, 1993; McDonald *et al.*, 2002; Sauren *et al.*, 1980; Schenke-Layland *et al.*, 2004), quantitative evaluation of the amounts and types of collagen (Bashey *et al.*, 1967; Lis *et al.*, 1987), and quantitative fiber bundle morphology (Doehring *et al.*, 2005). Interestingly, collagen architecture in heart valves has reported to be age-dependent. With growth and maturation, collagen content gradually increases from early to late fetal stages up to a constant level (Aikawa *et al.*, 2006). With aging, decreasing collagen content has been observed in adults (Bashey *et al.*, 1967; McDonald *et al.*, 2002), accompanied by a decrease in the extensibility of the heart valve leaflet (Christie and Barratt-Boyes, 1995). Apart from collagen content, changes in type and/or fibril size have been proposed to influence heart valve biomechanics with age (Christie and Barratt-Boyes, 1995). Indeed research on skin has demonstrated that with age mechanical tissue strength and stiffness increase in association with an increased intermolecular collagen cross-link concentration (Avery and Bailey, 2005). Furthermore, in bone tissue, a correlation was found between collagen cross-linking and biomechanical properties (Banse *et al.*, 2002). Although bone is structurally different from cardiovascular tissue, it is proposed that cross-links would also enhance collagen fibril stability and strength in heart valve tissue. The objective of this study was to investigate the structure–function relationships in human aortic heart valve leaflets, with special emphasis on collagen content and cross-link concentration. Correlations between these structural properties and biomechanical parameters were examined in both native and engineered human leaflet tissue to further optimize tissue engineering of heart valves. Accordingly, dynamic strain protocols were introduced to examine their effects on the enhancement of collagen amount, cross-link density, and mechanical properties.

## 4.2 Materials and methods

### 4.2.1 Specimen preparation

#### Native human valves

Nine healthy human donor aortic valves (6 female, 3 male, mean age  $48.9 \pm 11.4$  years) were obtained from the Rotterdam Heart Valve Bank at the Erasmus University Medical Center, Rotterdam, The Netherlands. The cause of death of the donors did not involve aortic valve disease or other conditions known to precede aortic valve disease. Before donation the donors, or their relatives, consented to experimental use of the cardiovascular tissue after explantation. Upon dissection, the valves were stored at 4°C, and biomechanical experiments were conducted at room temperature within 24 hours.

#### TE constructs

Scaffold preparation, cell culture, and cell seeding procedures were performed as described previously (Boerboom *et al.*, 2008; Mol *et al.*, 2005a). Briefly, rectangular strips (35x5x1 mm) of rapidly degrading non-woven polyglycolic acid meshes (Cellon, Bereldange, Luxembourg) were coated with a thin layer of poly-4-hydroxybutyrate

(TEPHA Inc., Cambridge, MA). The strips were attached to flexible membranes in 6-well plates (Flexcell Int., McKeesport, PA) and seeded with human venous myofibroblasts using fibrin as a cell carrier (Mol *et al.*, 2005b). The cell-seeded scaffolds are referred to as TE constructs. After 5 days of static culture, the TE constructs were divided into two groups and cultured for 3 additional weeks. One group of static constructs (*static*,  $n = 5$ ) was kept constrained at the outer ends and not subjected to additional external strains. The other group (*dynamic*,  $n = 5$ ) was subjected to 4% uniaxial dynamic strain at a physiologically relevant frequency of 1Hz using a Flexercell Fx-4000T straining device (Flexcell Int.).

## 4.2.2 Biomechanical testing and matrix analysis

### Biomechanical testing

To investigate the biomechanical characteristics of the native tissue, each valve was subjected to uniaxial tensile tests in 2 directions (figure 4.2b): strips of 1 valve leaflet in the circumferential direction (each strip was 3 mm wide,  $n = 3-4$  strips per valve) and 3 mm wide strips of another leaflet in the radial direction ( $n = 3-5$  strips per valve). The tensile tests were performed on confined strips, meaning that the ends of the strips were clamped, not allowing translational movement between the layers of the leaflet. The thickness of the leaflet strips was measured using a Digimatic Micrometer (Mitutoyo America Corporation, Aurora, IL). Tensile tests were performed using a custom-built tensile tester, equipped with a 20N load cell. Stress-strain curves were obtained at a strain rate of the initial length per minute ( $l_0/\text{min}$ ) up to failure. From the curves, the ultimate tensile stress (UTS) was determined. The slope of the linear part of the curve represented the modulus of elasticity (further referred to as modulus) of the tissue. Data were averaged per valve leaflet. Anisotropic properties were defined as differences between the moduli in the 2 directions. The biomechanical properties of the TE constructs in the direction of straining were determined from equivalent tensile tests.

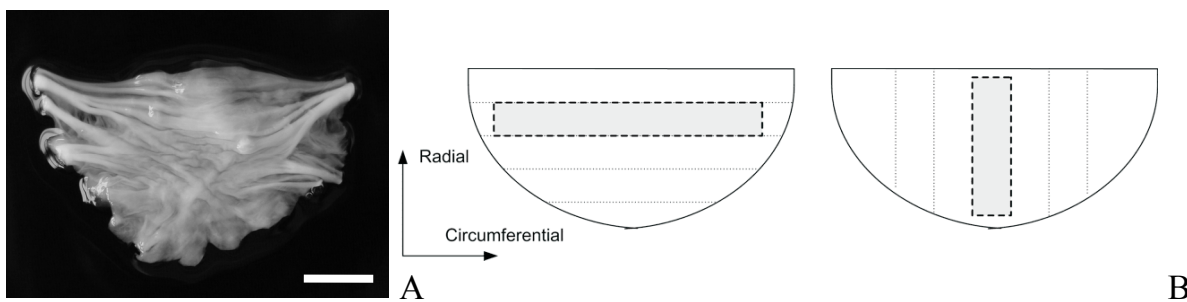


Figure 4.1: (A) Anisotropic matrix structure of an aortic valve leaflet (Balguid *et al.*, 2007). Originating at the commissures, connective tissue bundles run nearly parallel with the free leaflet margin. The white bar represents a scale of 5 mm. (B) Uniaxial tensile tests were performed on tissue strips ( $n = 3-5$ ) from two leaflets in circumferential and radial direction.

### **Matrix analysis: collagen content and cross-links**

After tensile testing, biochemical assays were performed on the valve leaflet tissue strips and TE constructs to evaluate the corresponding tissue matrix composition. The tissues were cut such that each valve leaflet strip yielded 4 to 6 samples, whereas whole TE strips were used for biochemical analyses. Lyophilized tissue samples were hydrolyzed in 6M hydrochloric acid (Merck, Darmstadt, Germany) and used for amino acid and cross-link analyses. Hydroxyproline residues were measured on the acid hydrolysates, using reverse-phase high-performance liquid chromatography after derivatization with 9-fluorenylmethyl chloroformate (Fluka, Buchs, Switzerland) (Bank *et al.*, 1996). Collagen content was expressed as a percentage of the specimens' dry tissue weight. The same hydrolysates were used to measure the number of the mature collagen cross-links hydroxylysylpyridinoline (HP), which is the main type of collagen cross-link present in cardiovascular tissue, using high-performance liquid chromatography as described previously (Bank *et al.*, 1997; Robins *et al.*, 1996). The number of HP cross-links was expressed per collagen triple helix. Data from valve leaflet strips were averaged per valve leaflet.

### **4.2.3 Data analysis**

Descriptive statistics (mean  $\pm$  standard deviation) were performed for collagen content, HP cross-links, and biomechanical properties (modulus and UTS). These parameters were compared between circumferential and radial direction of native leaflet strips, between statically and dynamically conditioned TE constructs, and between native and engineered tissues, using Student t-tests. In native valves, collagen content and cross-link data were correlated to the biomechanical properties using Pearson's correlation analyses. In the two TE groups, correlations between these variables, incorporating interaction effects between variables, were investigated using a general linear model. The correlation coefficient was represented by  $r$ . A  $p$ -value  $< 0.05$  was considered significant. Statistical analysis was performed using SPSS 11.0 software (SPSS Inc., Chicago, IL).

## 4.3 Results

### 4.3.1 Biomechanical properties

In figure 4.2, averaged stress-strain curves are displayed for strips from the native valve leaflets (circumferential and radial direction) and engineered tissues (static and dynamic conditioning).

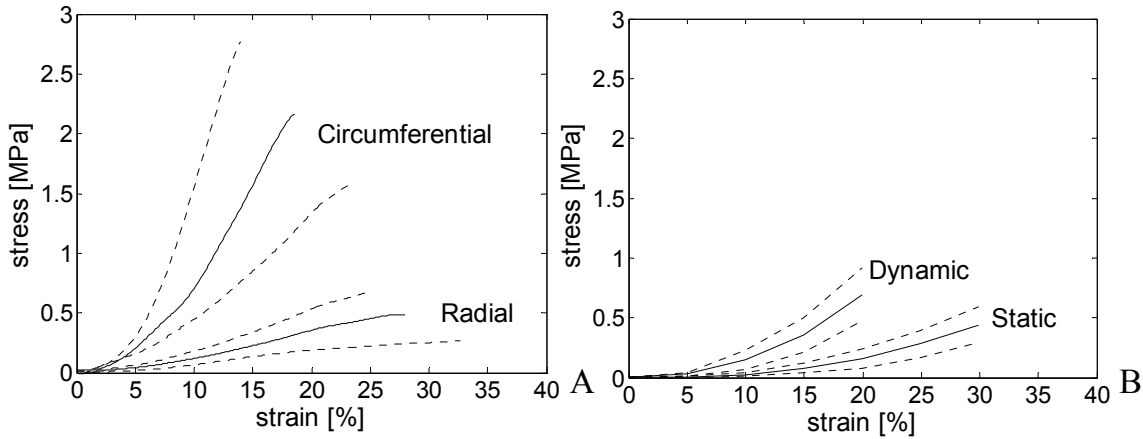


Figure 4.2: Averaged stress–strain curves (solid lines) for human aortic valves in the circumferential and radial directions (A) and for statically and dynamically conditioned engineered tissues (B). The dotted lines represent standard deviations of all measurements.

An overview of the modulus and UTS for native (radial and circumferential direction) and engineered tissues (static and dynamic) is displayed in figure 4.3.

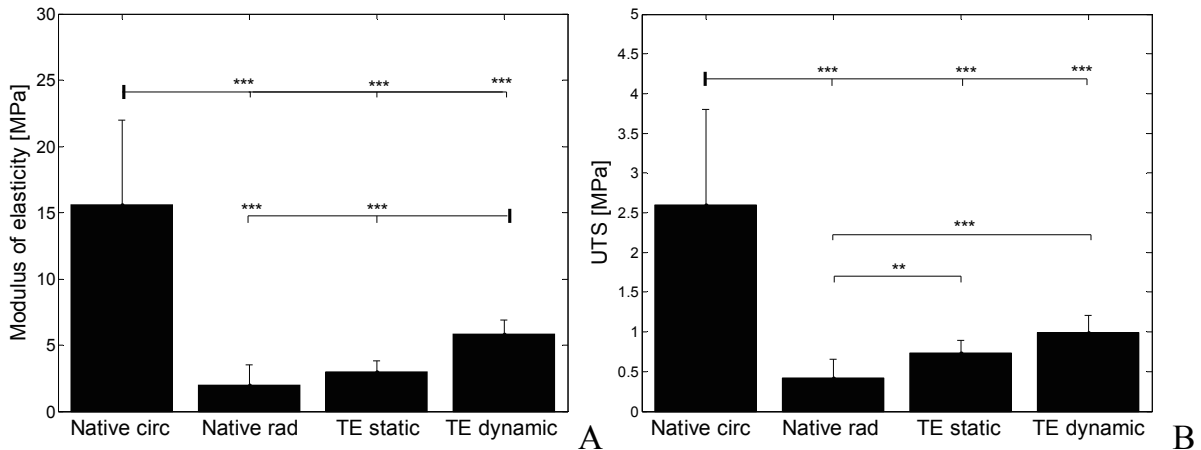


Figure 4.3: Mechanical properties of native human aortic valve leaflets and tissue-engineered (TE) constructs. Modulus (A) and ultimate tensile stress (UTS) (B) of native valve leaflets (circumferential and radial direction) and TE constructs (static and dynamic). In case of multiple comparisons, differences are compared with values below the bold stripe (\*\* $p < 0.01$ ; \*\*\* $p < 0.005$ ).

The modulus and UTS of the native leaflets were higher in the circumferential direction compared to radial direction (modulus:  $15.6 \pm 6.4$  MPa vs  $2.0 \pm 1.5$  MPa, respectively, UTS:  $2.6 \pm 1.2$  MPa vs  $0.42 \pm 0.24$  MPa, respectively). The modulus of dynamically strained constructs ( $5.8 \pm 1.1$  MPa) was higher compared to statically cultured constructs ( $3.0 \pm 0.8$  MPa). No significant changes were found in UTS (static:  $0.73 \pm 0.16$  MPa; dynamic:  $0.99 \pm 0.22$  MPa). The modulus and UTS of statically as well as dynamically cultured constructs were significantly lower, compared to native valve leaflets in circumferential direction. When comparing to native tissue in radial direction, statically cultured constructs had higher UTS and no significantly different modulus. Dynamically cultured constructs showed higher modulus and UTS compared to native tissue in radial direction.

### 4.3.2 Collagen content and cross-links

The amount of collagen per dry weight and the number of HP cross-links per triple helix in the tested human heart valves were  $0.47 \pm 0.09$  mg/mg dry weight and  $0.52 \pm 0.06$ , respectively (figure 4.4). No difference in the amount of collagen per dry tissue weight between statically and dynamically conditioned TE constructs was found (static:  $0.09 \pm 0.01$  mg/mg dry weight; dynamic:  $0.09 \pm 0.01$  mg/mg dry weight). Interestingly, the dynamically strained constructs contained significantly more HP cross-links per triple helix compared to the statically cultured constructs (static:  $0.14 \pm 0.02$ , dynamic:  $0.28 \pm 0.06$ ). Collagen content and cross-link concentration were significantly higher in native tissue compared to TE constructs (static and dynamic).

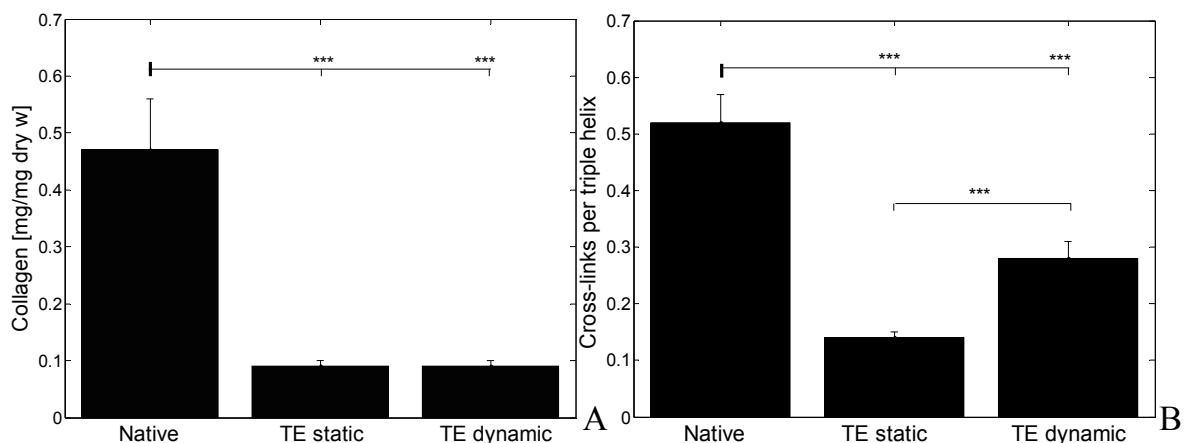


Figure 4.4: Collagen content (A) and cross-links (B) in native human aortic valve leaflets and tissue-engineered (TE) constructs (static and dynamic). In case of multiple comparisons, differences are compared with values below the bold stripe (\*\*\*)  $p < 0.005$ .

### 4.3.3 Correlation between collagen content, cross-links, and biomechanics

#### Native human valves

A significant correlation was found between the modulus and the corresponding values for HP cross-links per collagen triple helix in circumferential direction ( $r = 0.58$ ,  $p < 0.005$ ). No correlation between collagen content and modulus was observed ( $r = 0.05$ ,  $p = 0.80$ ), as shown in figure 4.5. In the radial direction (data not shown), no significant correlations between modulus and HP cross-links per triple helix, or between modulus and collagen content were found ( $r = 0.12$ ,  $p = 0.54$  and  $r = 0.12$ ,  $p = 0.54$ , respectively).

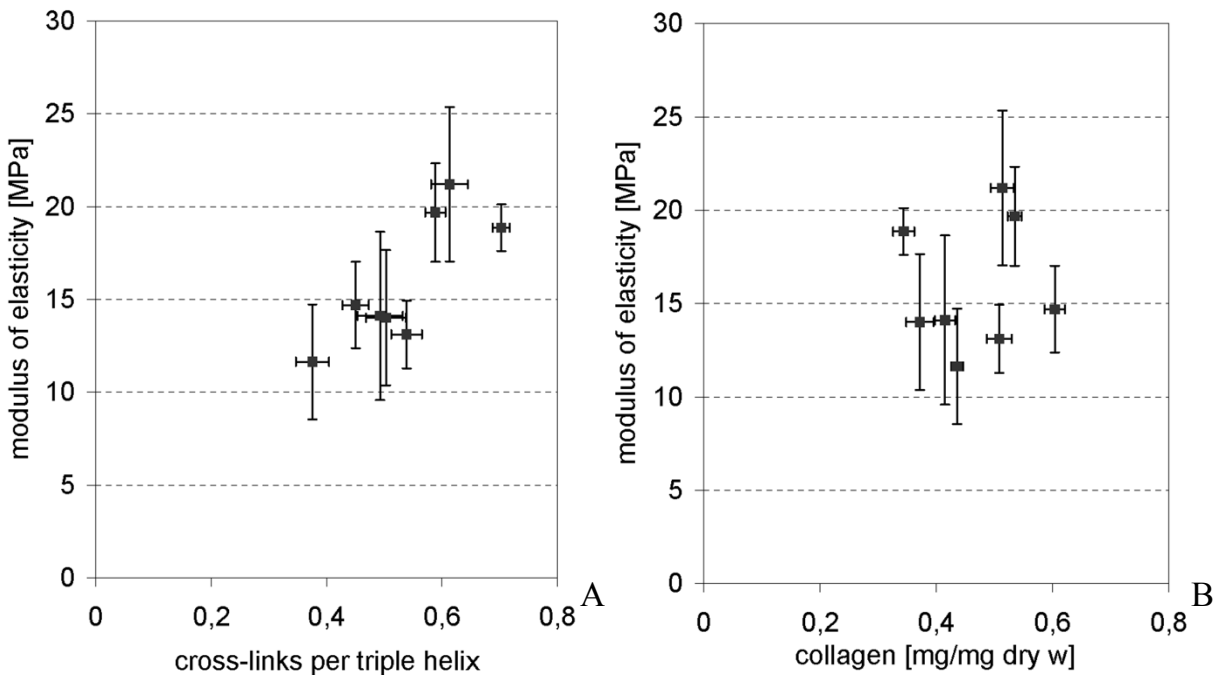


Figure 4.5: Modulus and collagen data in circumferential direction of native valve leaflets. Each marker represents the average ( $\pm$  standard error of the mean) of 1 valve ( $n = 4$  strips). (A) A significant positive linear correlation was present between modulus and cross-links per triple helix ( $r = 0.58$ ,  $p < 0.005$ ). (B) No linear correlation was found between modulus and collagen content ( $r = 0.05$ ,  $p = 0.80$ ).

#### Tissue-engineered constructs

Statistical analysis of the two TE groups showed no significant correlation between the amount of collagen and the modulus ( $r = 0.40$ ,  $p = 0.25$ ) (figure 4.6). However, the number of collagen cross-links per triple helix showed a significant positive linear correlation with the modulus ( $r = 0.89$ ,  $p < 0.005$ ). This correlation was independent of the mode of mechanical conditioning.

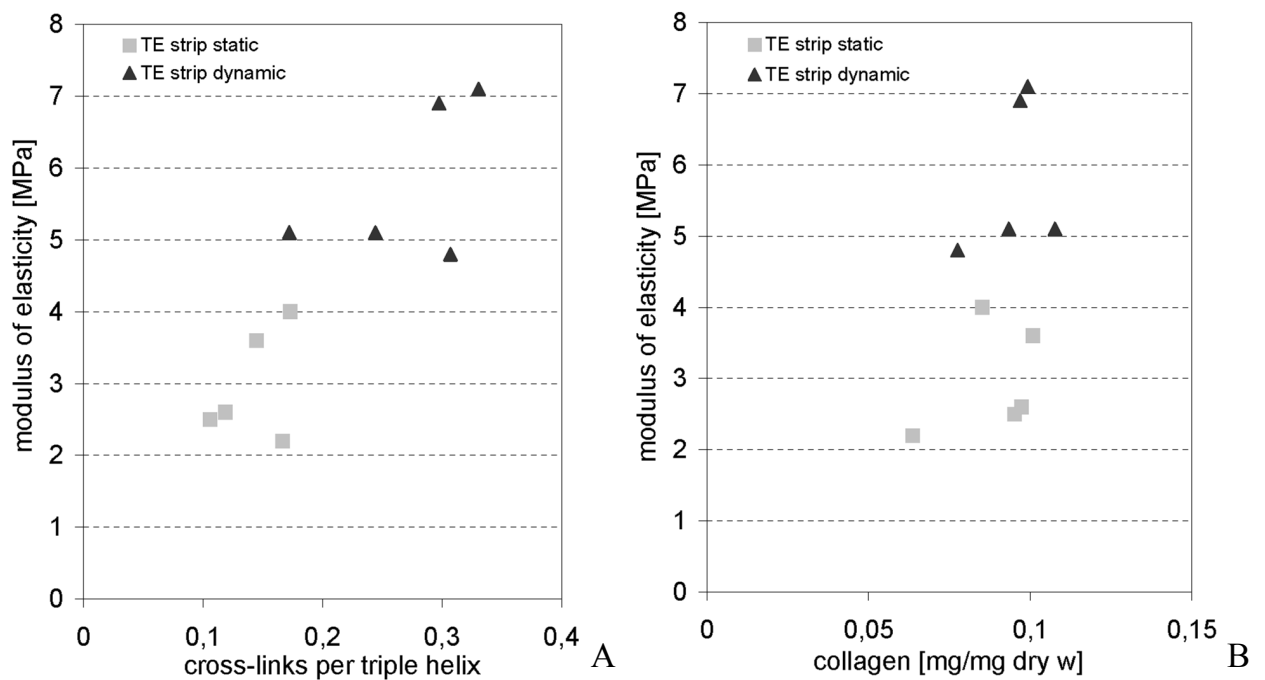


Figure 4.6: Modulus in relation to cross-links per triple helix (A) and collagen content (B) for statically and dynamically conditioned tissue-engineered (TE) constructs. A significant positive linear correlation was observed between modulus and cross-links per triple helix ( $r = 0.89$ ,  $p < 0.005$ ). No linear correlation was found between modulus and collagen content ( $r = 0.40$ ,  $p = 0.25$ ).

## 4.4 Discussion

A thorough insight into the functional structure of native aortic valves related to biomechanics is crucial for progress in the field of heart valve tissue engineering. As a first step, this study investigated the structure-function relationship between collagen content, cross-links, and biomechanical properties in human aortic heart valve leaflets and TE constructs.

Fresh native human valve leaflets were uniaxially tested in two directions, taking account of the natural anisotropy in the leaflets. The valve leaflets were much stiffer and stronger in circumferential direction compared with radial direction, indicating anisotropic mechanical behavior (figure 4.2a). Although uniaxial tensile tests have their limitations and do not reflect the full biaxial mechanical behavior of the valve leaflet, this method does suffice to investigate global differences in mechanical properties in the two perpendicular directions. The biomechanical data were consistent with values published in a recent study (Stradins *et al.*, 2004), and show a high diversity possibly related to the large biological variations in gross fiber architecture observed among the mature heart valve leaflets, due to age and health status of human subjects.



Interestingly, data analysis of the native leaflets showed a significant correlation of collagen cross-linking, but not the amount of collagen, with the tissue stiffness in circumferential direction in native valves (figure 4.5). Similar correlations between mechanical properties and collagen cross-links were reported for bone tissue (Banse *et al.*, 2002), and in scar tissue of collateral ligaments (Frank *et al.*, 1995). Moreover, in patellar tendon the modulus was shown to be related to the amount of insoluble (cross-linked) collagen, but not to the total collagen content (Haut *et al.*, 1992).

The natural anisotropy clearly plays a large role in the biomechanical behavior of the valve leaflets, being more extensible and less stiff in radial compared to circumferential direction. In radial direction, the leaflet strips failed between circumferentially running fibers. In this direction no correlation was observed between the modulus of elasticity and the amount of collagen or cross-links. As the correlation between modulus and cross-links only holds for the circumferential direction, it is likely that collagen cross-links act in conjunction with collagen fiber orientation in providing tissue strength.

The TE experiments show that dynamic strain increased the cross-link density in TE constructs, compared to static conditioning. When data from statically and dynamically conditioned samples were combined, the modulus correlated well with the cross-link density but not with the collagen content. These data confirm the proposed relevance of cross-link stimulation to enhance tissue mechanical properties in engineered tissues (Dahl *et al.*, 2005; Elbjeirami *et al.*, 2003). We hypothesize that in the initial phase of culturing TE constructs, collagen and other extracellular components are produced by the cells to provide biomechanical support at an early stage. In this phase, the amount of collagen increases linearly with the modulus, as observed by Engelmayer *et al.* (2005). After reaching a certain amount of collagen, the tissue matures further and collagen cross-links contribute increasingly to the modulus. Interestingly, this process was enhanced by mechanical stimulation.

The modulus and UTS of dynamically strained constructs were approximately 30% of the leaflet properties in circumferential direction. In addition, cross-link densities as well as collagen content in tissue-engineered constructs were both lower compared to native tissue. An outlook on the tissue engineering pathway towards functional, 'native'-approaching tissue is depicted in figure 4.7. The results in this paper reveal a directive role of collagen cross-links in the biomechanical development of TE constructs towards native tissue.

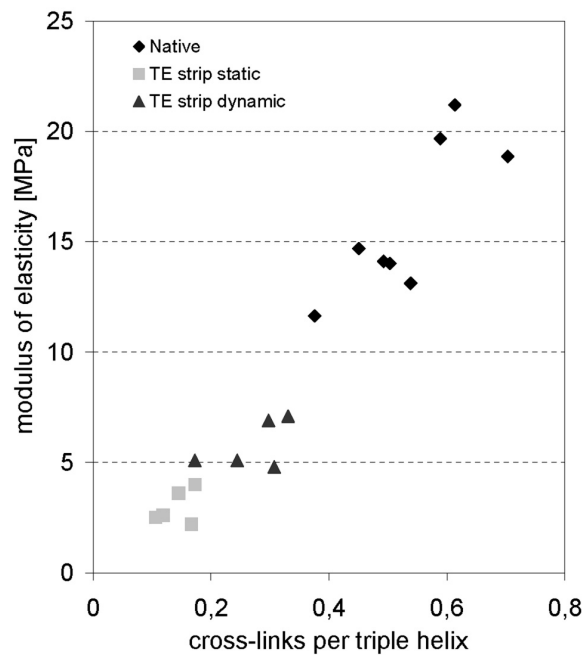


Figure 4.7: Overview of modulus versus cross-links per triple helix for native tissue and TE constructs. A positive linear trend can be observed.

In addition to the use of mechanical stimulation to enhance cross-link densities in TE tissues, biochemical cues can be used to manipulate the formation of enzymatic collagen cross-links. Elbjeirami *et al.* showed that transfection of cells by lysyl oxidase (a collagen cross-link enzyme involved in the formation of enzymatic/natural cross-links) increased the number of cross-links and improved mechanical properties of tissue-engineered constructs (Elbjeirami *et al.*, 2003). Beekman *et al.* inhibited formation of cross-links by beta-aminopropionitrile (an inhibitor of enzymatic cross-links), resulting in less cross-links and decreased tissue stiffness (Beekman *et al.*, 1997).

In conclusion, the data presented here demonstrate the importance of collagen cross-links in determining the biomechanical tissue properties of native heart valve leaflets as well as of tissue-engineered constructs. This correlation emphasizes the necessity to consider the total collagen architecture as a whole, including amount of collagen, cross-link concentration and fiber orientation, as a focus for optimizing structural and mechanical properties in engineered tissues.

### Acknowledgements

This work forms part of the research program of the Dutch Polymer Institute (project 475) and was also supported by the Dutch Technology Foundation (STW), the applied science division of NWO, and the Technology Program of the Dutch Ministry of Economic Affairs. The authors would like to thank Jessica Snabel, TNO Health and Prevention, The Netherlands, for her contribution to this work.



# Chapter 5

## Intermittent strain accelerates the development of tissue properties in engineered heart valve tissue

The contents of this chapter are based on M.P. Rubbens, A. Mol, R.A. Boerboom, R.A. Bank, F.P.T. Baaijens, and C.V.C. Bouten, *Intermittent straining accelerates the development of tissue properties in engineered heart valve tissue*, Tissue Engineering Part A, 15(5), 999-1008, (2009).

## 5.1 Introduction

Approximately 100,000 heart valve replacements to treat end-stage valvular diseases are performed annually in the United States and 285,000 worldwide (Mikos *et al.*, 2006; Rosamond *et al.*, 2007). Existing prostheses for end-stage valvular disease include mechanical or biological valves. Although these substitutes offer long-term efficacy, they have several shortcomings (Mayer, 1995; Schoen and Levy, 1999). For example, mechanical valves require lifelong anticoagulation therapy to reduce the risk of thromboembolism. Biological valves, on the other hand, suffer from calcification and consequent valve failure. The main drawback of these valves is that they do not consist of living material and consequently lack the ability to grow, repair, and remodel, which is of particular importance for pediatric and young adult patients. Tissue engineering represents a promising strategy to overcome this limitation by creating living substitutes that are able to adapt in response to changing physiological demands.

To date, tissue engineering of cardiovascular substitutes based on rapidly degrading biodegradable scaffolds seeded with autologous myofibroblasts has been demonstrated as a promising procedure to create living replacements (Hoerstrup *et al.*, 2000; Niklason *et al.*, 1999). In this approach, cells are stimulated to produce *de novo* extracellular matrix components, including collagen fibers, which are the main load-bearing constituents of cardiovascular tissues. Similar to native tissues, the mechanical properties of engineered tissues depend on the collagen architecture, which is a delicate interplay between the amount of collagen, the number of collagen cross-links, and the orientation of the collagen fibers. Consequently, tissues that do not possess sufficient amounts of functionally organized collagen fibers will not meet *in vivo* mechanical demands. To optimize collagen architecture during tissue culture and hence improve the mechanical properties, *in vitro* mechanical conditioning strategies are crucial (Isenberg and Tranquillo, 2003; Mol *et al.*, 2003; Mol *et al.*, 2006; Neidert and Tranquillo, 2006; Seliktar *et al.*, 2003). For tissue-engineered heart valves, conditioning regimes are often designed to mimic physiological circumstances. Using an *in vitro* pulse duplicator in which the tissues are exposed to increasing gentle pulsatile flows, tissue-engineered heart valves have been obtained that were successfully implanted at the pulmonary position in sheep (Hoerstrup *et al.*, 2000). However, the tensile strength of these valves was insufficient for use in the aortic position, where the mechanical demands are higher (Mol and Hoerstrup, 2004). Development of a novel mechanical conditioning protocol, based on strain, was shown to increase tissue properties of those valves resulting in promising functionality for use as aortic valve replacements (Mol *et al.*, 2006). Nevertheless, due to a lack of adequate tissue model systems, quantitative relationships between mechanical conditioning and resulting tissue structure and mechanical properties have not been fully established yet.

As the development of tissue properties with time is difficult to monitor and predict in complex tissue geometries, such as heart valves, a model system of engineered heart valve tissue is used. This system consists of simple, rectangular-shaped tissue constructs sealed to the elastic membrane of an adapted Flexercell

straining device (Boerboom *et al.*, 2008). In this way, the temporal effects of mechanical conditioning on the evolution of tissue properties can be systematically investigated under strictly controlled conditions

Previous studies in our lab using this model system demonstrate that the application of prolonged continuous dynamic strain (4% and 8%, 1 Hz) to engineered heart valve tissues enhances cross-link densities, but reduces collagen production and even deteriorates the mechanical properties at 8% continuous dynamic strain, when compared to constrained tissue culture (Boerboom *et al.*, 2008). Intermittent loading protocols have been proposed as a method to disrupt the adaptation response of cells to a continuous stimulus. In addition, it has been suggested by Robling *et al.* (2002) and Chowdhury *et al.* (2003) that a certain threshold in the number of loading cycles is needed to obtain a maximum response. After exceeding this threshold in the number of cycles, the effect of additional continuous loading is decreased. When this maximum number of cycles is applied in repeated bursts with sufficient interval time, a more effective stimulation will be achieved. Indeed in bone and cartilage tissue engineering, an intermittent strain protocol has been demonstrated to be favorable in terms of cell proliferation (Winter *et al.*, 2003), matrix production (Chowdhury *et al.*, 2003), and mechanical properties (Robling *et al.*, 2002), when compared to a continuous period of dynamic strain. Similar results have recently been obtained in our lab for human engineered heart valve tissues (Boerboom *et al.*, 2007b), demonstrating the promising nature of intermittent conditioning. In the present study, we focus on temporal variations in these tissue properties, as we hypothesize that the improved tissue properties due to intermittent strain are caused by a more rapid and improved tissue production, maturation, and organization.

## **5.2 Materials and methods**

### **5.2.1 Cell culture**

Myofibroblasts were acquired from the human vena saphena magna according to the Dutch guidelines for secondary use material and expanded using regular cell culture methods, as described previously (Schnell *et al.*, 2001). Culture medium consisted of advanced Dulbecco's modified Eagle's medium (DMEM; Gibco, Carlsbad, CA), supplemented with 10% fetal bovine serum (FBS; Greiner Bio One, Monroe, NC), 1% GlutaMax (Gibco), and 0.1% gentamycin (Biochrom, Terre Haute, IN).

### **5.2.2 Engineered heart valve tissue**

Scaffold preparation and cell seeding procedures were performed as described previously (Mol *et al.*, 2005a). Briefly, rectangular strips (35x5x1 mm) of non-woven polyglycolic acid meshes (PGA; Cellon, Bereldange, Luxembourg) were coated with a thin layer of poly-4-hydroxybutyrate (P4HB; TEPHA Inc., Cambridge, MA). The

bottom surface of the scaffolds was reinforced with a non-toxic elastic silicone layer (Silastic MDX4-4210, thickness 0.5 mm; Dow Corning, Midland, MI), enabling precisely controlled, cyclic deformation of the constructs up to several weeks, as validated previously (Boerboom *et al.*, 2008). In the longitudinal direction, the scaffolds were attached at the outer 5 mm to the flexible membranes of six-well plates (Flexcell Int., McKeesport, PA) using Silastic MDX4-4210. In this way, the tissues were longitudinally constrained. The scaffolds were vacuum-dried for 48 hours, followed by exposure to ultra violet light for 1 hour and were subsequently placed in 70% ethanol for 5 hours to obtain sterility. Prior to cell seeding, tissue culture medium was added to facilitate cell attachment. The scaffolds were seeded with human venous myofibroblasts (passage 7) at a seeding density of 2 million cells per cm<sup>2</sup> using fibrin gel as a cell carrier (Mol *et al.*, 2005b). The engineered constructs (n = 30) were cultured in tissue culture medium consisting of advanced DMEM (Gibco), supplemented with 10% FBS, 1% GlutaMax, 0.3% gentamycin, and L-ascorbic acid 2-phosphate (0.25 mg/mL; Sigma, St. Louis, MO). Medium was changed every 3–4 days.

### 5.2.3 Tissue culture and mechanical conditioning

After 1 week of culture under constrained conditions, the engineered tissues were divided into two groups. One group (n = 15) served as constrained control, whereas the other group (n = 15) was subjected to uniaxial intermittent dynamic strain (4%, 3 hours on/off) at a frequency of 1Hz using a modified version of a Flexercell FX-4000T straining device (Boerboom *et al.*, 2008) (Flexcell Int.). Constrained and intermittently strained samples were sacrificed after 2, 3, and 4 weeks of culture (n = 5 for each group per time point). The silicon layer was gently removed, and the samples were analyzed for tissue morphology and organization, collagen production, cross-link density, and mechanical properties.

### 5.2.4 Tissue morphology and organization

Tissue formation was analyzed qualitatively over time with histology. Representative pieces of constrained and intermittently strained samples were fixed in 4% phosphate-buffered formalin. Subsequently, the pieces were transversely embedded in paraffin, cut in 10 µm sections, and stained with Trichrome Masson to study extracellular matrix formation with light microscopy. Additional sections were stained with Picrosirius red and analyzed under polarized light. The amount and density of birefringent fibers reflect collagen maturity.

To visualize the organization of cells and collagen fibers in the engineered tissues, two-photon microscopy was performed as described previously (Boerboom *et al.*, 2007a). Samples were labeled by 15.0 µM Cell Tracker Blue CMAC (CTB; Invitrogen, Carlsbad, CA) and 3.0 µM CNA35-OG488, which are specific fluorescent markers for cell cytoplasm and collagen, respectively (Krahn *et al.*, 2006). CTB and CNA35-OG488 are excitable with two-photon microscopy and exhibit broad spectra at 466 and 520 nm, respectively. Images were taken using an inverted Zeiss Axiovert 200

microscope (Carl Zeiss, Oberkochen, Germany) coupled to an LSM 510 Meta (Carl Zeiss) laser scanning microscope. A chameleon ultra 140 fs pulsed Ti-Sapphire laser (Coherent, Santa Clara, CA) was tuned to 760 nm, and two photomultiplier tube (PMT) detectors were defined as 435–485 nm for CTB and 500–530 nm for CNA-OG488. Separate images at an imaging depth of 30  $\mu$ m were obtained from each PMT, and combined into single images.

### **5.2.5 Collagen production and cross-link density**

Collagen production was analyzed quantitatively over time with biochemical assays for DNA and hydroxyproline. Lyophilized samples ( $n = 5$  for each group per time point) were digested in papain solution (100 mM phosphate buffer, 5 mM L-cystein, 5 mM ethylenediaminetetraacetic acid (EDTA), and 125–140  $\mu$ g papain per mL) at 60°C for 16 hours. The amount of DNA was determined using the Hoechst dye method (Cesarone *et al.*, 1979), and expressed per mg dry weight. Subsequently, digested tissue samples were hydrolyzed in 6M hydrochloric acid (Merck, Darmstadt, Germany) and used for amino acid analyses. Hydroxyproline residues were measured on the acid hydrolysates, using reverse-phase high-performance liquid chromatography after derivatization with 9-fluorenylmethyl chloroformate (Bank *et al.*, 1996). Collagen production was expressed as the amount of hydroxyproline per DNA.

To quantify the maturity of the tissues, the number of mature collagen hydroxylysylpyridinoline (HP) cross-links, which are the main type of collagen cross-links present in cardiovascular tissue, was determined. HP cross-links were measured in hydrolyzed samples ( $n = 5$  for each group per time point) using high performance liquid chromatography (Bank *et al.*, 1997; Robins *et al.*, 1996). The number of HP cross-links was expressed per collagen triple helix (TH).

### **5.2.6 Mechanical properties**

To determine the mechanical properties, uniaxial tensile tests were performed in longitudinal direction of the engineered constructs ( $n = 5$  for each group per time point) using a tensile stage (Kammrath & Weiss GmbH, Dortmund, Germany) equipped with a 20N load cell. The thickness and width of the tissues were measured using a Pl $\mu$  2300 non-contact optical profiler (Sensofar Tech S.L., Barcelona, Spain), as described previously (Boerboom *et al.*, 2008). The Cauchy stress was defined as the force divided by the deformed cross-sectional area. Stress–strain curves were obtained until rupture at a strain rate of the initial sample length per minute. From the resulting curves the ultimate tensile stress was determined. The slope of the linear part of the curve represented the modulus of the tissue.

### **5.2.7 Statistics**

Results are expressed as mean values  $\pm$  standard deviation. Comparisons between groups were performed by an analysis of variance using Bonferroni post hoc tests



(SPSS Inc., Chicago, IL) to determine significant differences between groups. A level of  $p < 0.05$  was used as level of significance.

## 5.3 Results

### 5.3.1 Evaluation of tissue morphology and organization

Trichrome Masson stainings showed that matrix formation was concentrated at the upper side of the tissues (figure 5.1). It was observed that the dense layer of matrix was thicker in the intermittently strained samples compared to constrained samples and that for both groups the total amount of tissue increased with time.

The Picrosirius red stainings are shown in figure 5.2. Very few birefringent fibers can be identified in the constrained group after 2 weeks of culture (figure 5.2a). Some birefringent fibers were present in this group after 3 and 4 weeks (figure 5.2b,c). By comparison, the amount and density of the birefringent fibers were higher in the intermittently strained samples at all time points (figure 5.2d-f). In addition, it was observed that the amount of red fibers increased with time due to intermittent conditioning (figure 5.2d-f).

Two-photon microscopy was performed to visualize cells and collagen fibers in representative engineered tissues (figure 5.3). Cells and collagen fibers were more randomly distributed in the constrained samples (figure 5.3a-c) when compared to the intermittently strained samples (figure 5.3d-f). From visual inspection, it was concluded that the alignment of the cells and collagen fibers increased with time and was highest in the intermittently strained samples which had been cultured for 4 weeks (figure 5.3f). The observed alignment was in the direction of straining.

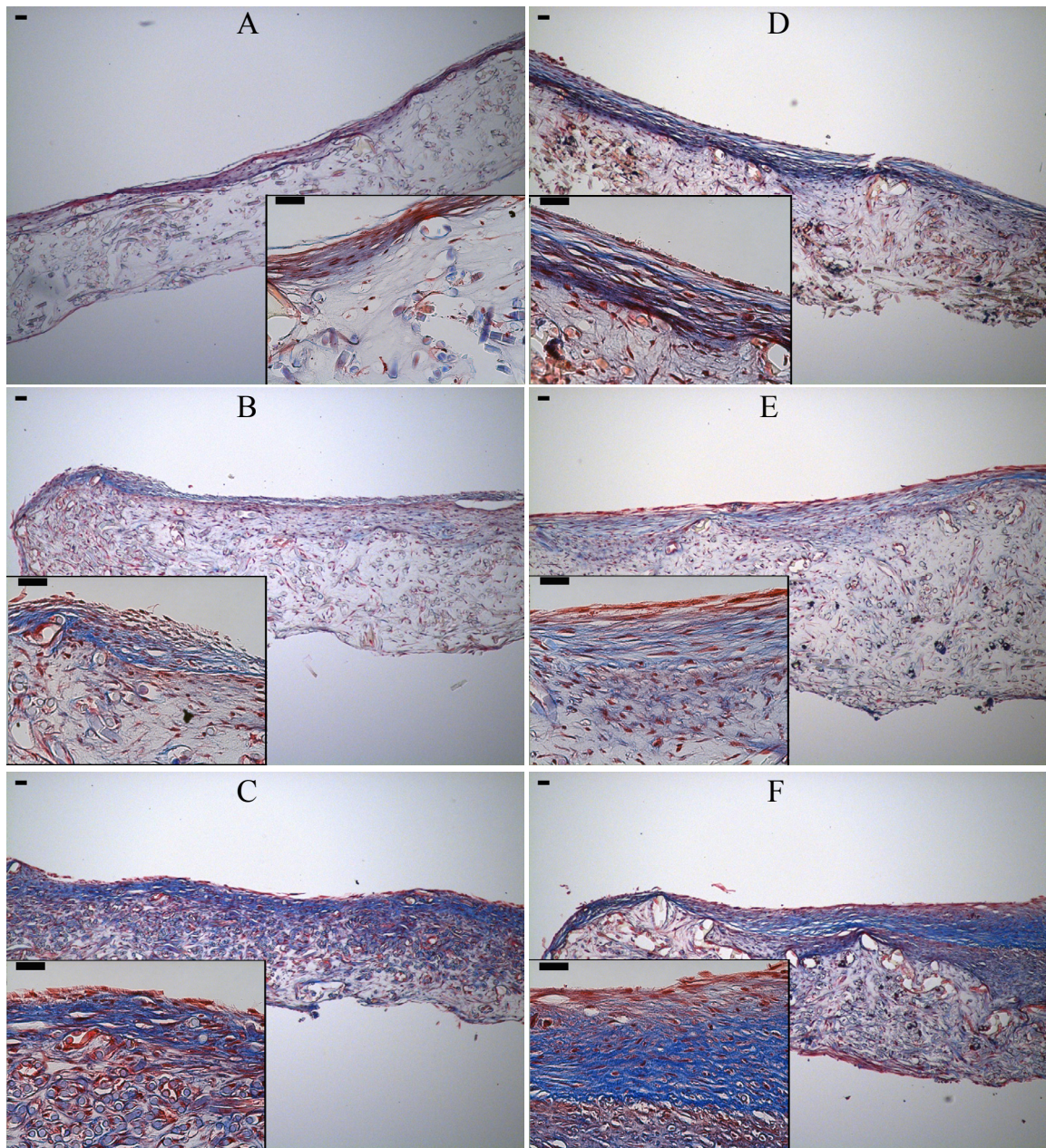


*Figure 5.1: Trichrome Masson stainings of constrained (A–C) and intermittently strained (D–F) samples after 2 (A, D), 3 (B, E), and 4 (C, F) weeks of culture. Collagen is shown in blue, cells are in red, and nuclei are in black. Fragmented scaffold remnants can be identified in light blue. Tissue formation increased with time and was enhanced due to intermittent conditioning. Scale bar represents 50  $\mu\text{m}$ .*



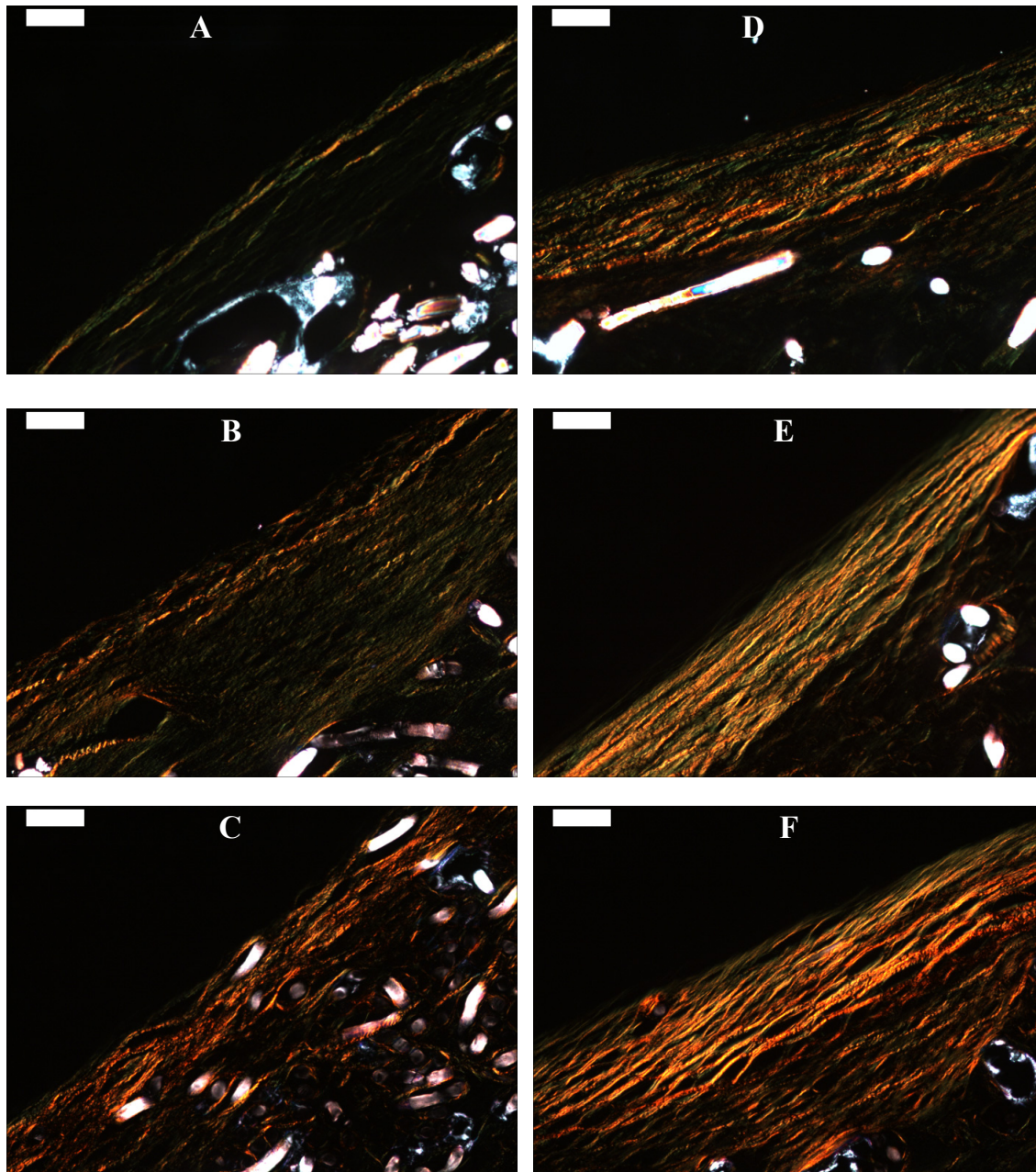


*Figure 5.2: Picrosirius red–stained sections of the upper side of constrained (A–C) and intermittently strained (D–F) samples after 2 (A, D), 3 (B, E), and 4 (C, F) weeks of culture, viewed under polarized light. The amount and density of birefringent fibers increased with time and were higher in intermittently strained samples, suggesting a higher degree of maturation compared to constrained samples. White spots represent remnants of scaffold. Scale bar represents 50  $\mu\text{m}$ .*



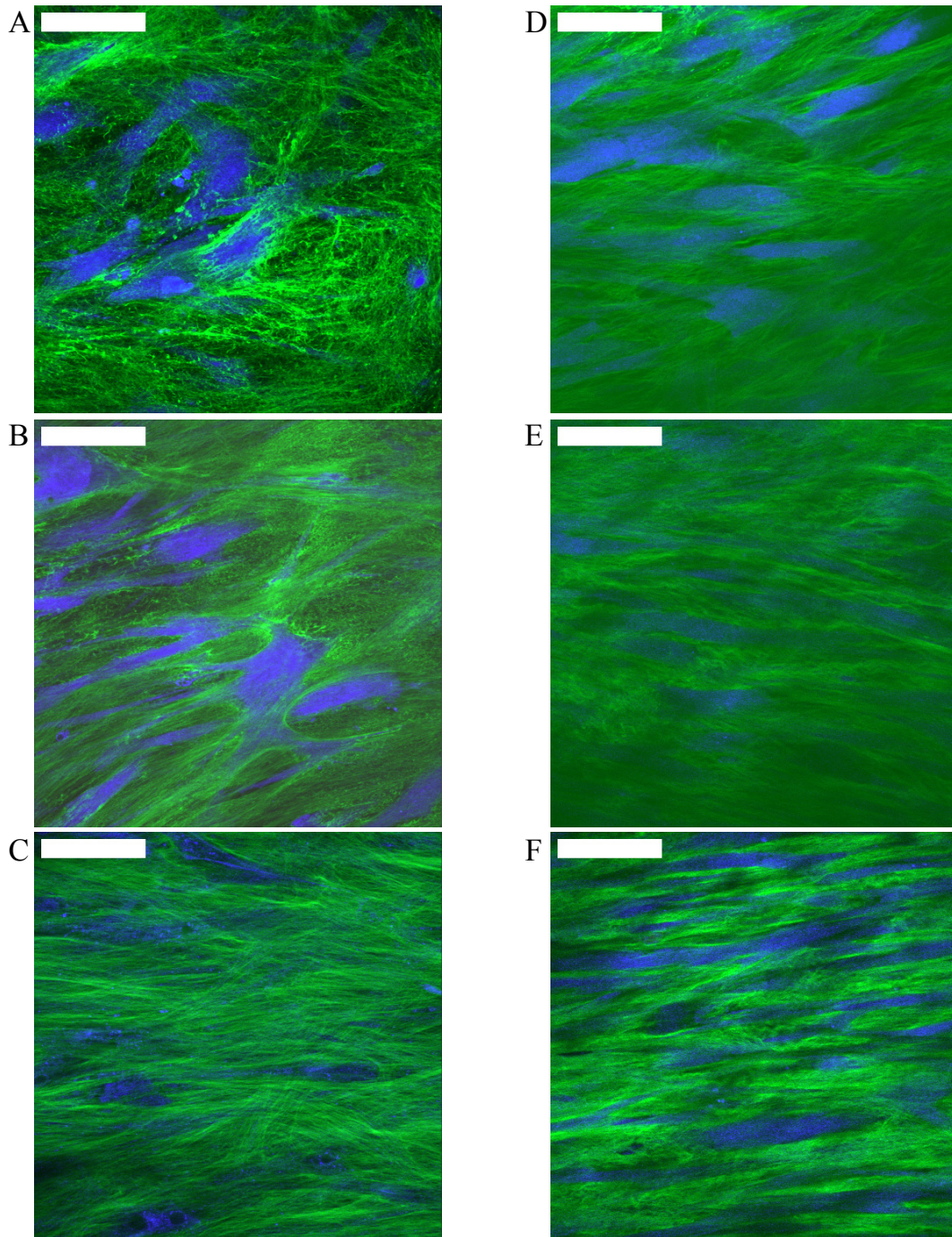


*Figure 5.3: Representative two-photon images of cells (blue) and collagen fibers (green) in constrained (A–C) and intermittently strained (D–F) samples after 2 (A, D), 3 (B, E), and 4 (C, F) weeks of culture. Cells and collagen fibers were randomly distributed in the constrained samples, while in the intermittently strained samples cells and collagen fibers aligned in the strain direction, which was from left to right. The highest degree of alignment was observed in intermittently strained samples after 4 weeks (F). Scale bar represents 50  $\mu\text{m}$ .*

### **5.3.2 Evaluation of collagen production and cross-link density**

The amount of DNA per mg dry weight slightly increased with time for both groups, but no effects of conditioning were observed (figure 5.4a; Table 5.1). By contrast, intermittent strain resulted in a higher collagen production, expressed by higher amounts of hydroxyproline per DNA, compared to constrained controls after 2 and 3 weeks of culture (figure 5.4b; Table 5.1). However, by 4 weeks of culture, both groups had produced similar levels of collagen. The number of HP cross-links per triple helix was higher in the intermittently strained group at all time points. With time HP cross-link density in the intermittently strained group increased, whereas the corresponding concentration of HP cross-links in the constrained samples did not change over time (figure 5.4c; Table 5.1).

### **5.3.3 Evaluation of mechanical properties**

Averaged stress–strain curves for 2-, 3-, and 4-week-old constrained and intermittently strained samples are shown in figure 5.5. After 2 weeks of culture, the tissues of both groups showed linear stress-strain curves, representing scaffold and immature tissue behavior. At later stages, the engineered tissues demonstrated the typical non-linear mechanical behavior representative of soft tissues. The modulus was significantly higher in the intermittently strained group as compared to constrained controls after 2 weeks of culture (Table 5.1). However, after 4 weeks, the moduli of both groups were similar. The ultimate tensile stress increased with time for both groups although values for the intermittently strained samples were significantly higher at all time points (Table 5.1).

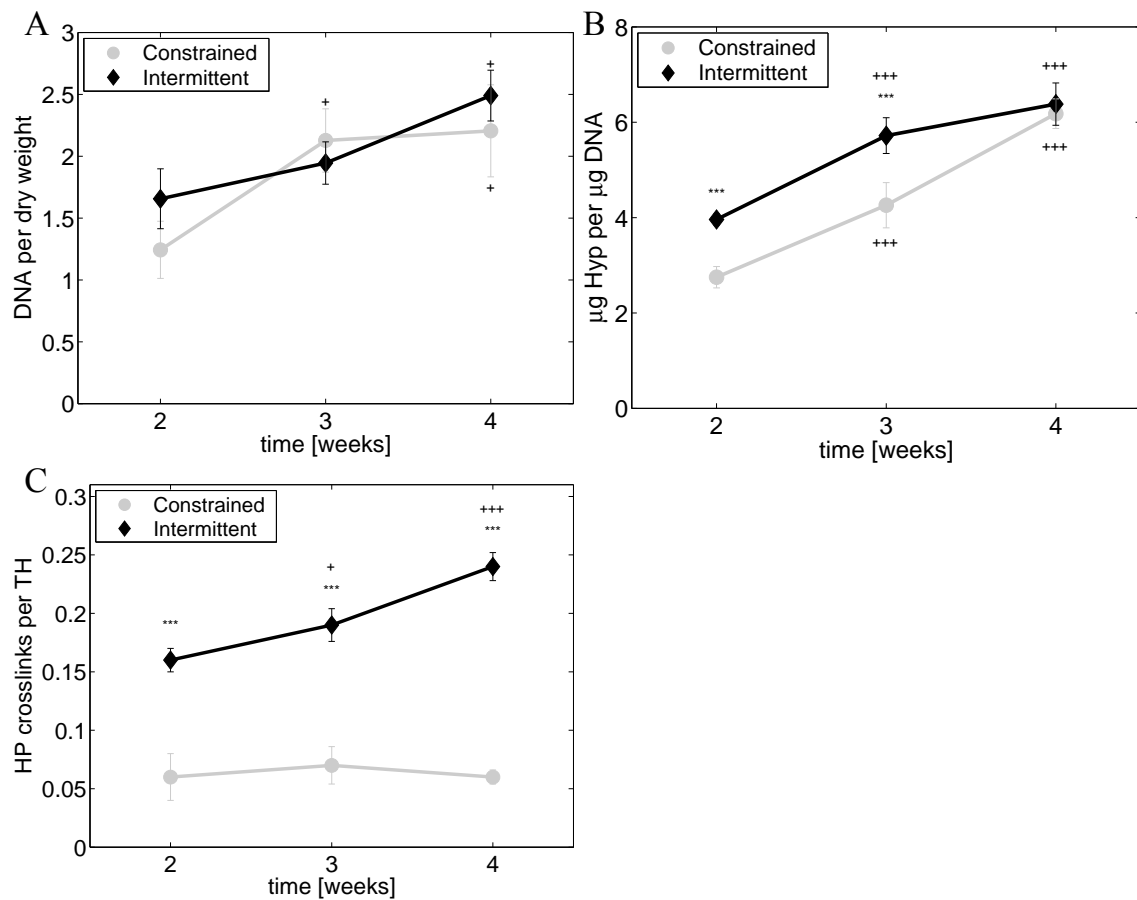


Figure 5.4:  $\mu\text{g DNA per mg dry weight}$  (A), collagen production (B), and concentration of HP cross-links per triple helix (C) for constrained (gray circles) and intermittently strained (black diamonds) samples after 2, 3, and 4 weeks of culture. Significantly different (\*\*\*)  $p < 0.001$  from constrained group. Significantly different (+  $p < 0.05$  and +++  $p < 0.001$ ) from 2 weeks' time point. No differences between the conditioning modes on DNA content were observed. Collagen production in the intermittently strained group was higher after 2 and 3 weeks of culture compared to the constrained samples. After 4 weeks, collagen production was similar in both groups. The number of HP cross-links per triple helix was higher in the intermittently strained group at all time points. With time, HP cross-link concentration increased in the intermittently strained group, while no temporal differences were found in constrained samples.

Table 5.1. Evaluation of tissue properties with time

Tissue properties	Loading condition	Culture method		
		2 weeks	3 weeks	4 weeks
DNA/dry weight	Constrained	1.24 ± 0.23	2.13 ± 0.26 <sup>a</sup>	2.21 ± 0.37 <sup>a</sup>
	Intermittent	1.67 ± 0.24	1.95 ± 0.17	2.49 ± 0.21 <sup>a</sup>
Hyp/DNA (μg/μg)	Constrained	2.75 ± 0.22	4.26 ± 0.48 <sup>b</sup>	6.18 ± 0.3 <sup>b</sup>
	Intermittent	3.96 ± 0.11 <sup>c</sup>	5.72 ± 0.38 <sup>b,c</sup>	6.38 ± 0.44 <sup>b</sup>
HP per triple helix	Constrained	0.06 ± 0.02	0.07 ± 0.02	0.06 ± 0.01
	Intermittent	0.16 ± 0.01 <sup>c</sup>	0.19 ± 0.01 <sup>a,c</sup>	0.24 ± 0.01 <sup>b,c</sup>
Modulus (MPa)	Constrained	0.61 ± 0.07	1.09 ± 0.29	2.69 ± 1.08 <sup>b</sup>
	Intermittent	2.55 ± 0.36 <sup>c</sup>	1.83 ± 1.15	2.88 ± 0.95
UTS (MPa)	Constrained	0.18 ± 0.01	0.24 ± 0.04	0.49 ± 0.15 <sup>b</sup>
	Intermittent	0.47 ± 0.07 <sup>c</sup>	0.54 ± 0.12 <sup>c</sup>	0.76 ± 0.08 <sup>b,c</sup>

Significantly different (<sup>a</sup> $p < 0.05$  and <sup>b</sup> $p < 0.001$ ) from 2-week time point. Significantly different (<sup>c</sup> $p < 0.001$ ) from constrained group. Hyp: hydroxyproline; UTS: ultimate tensile stress.

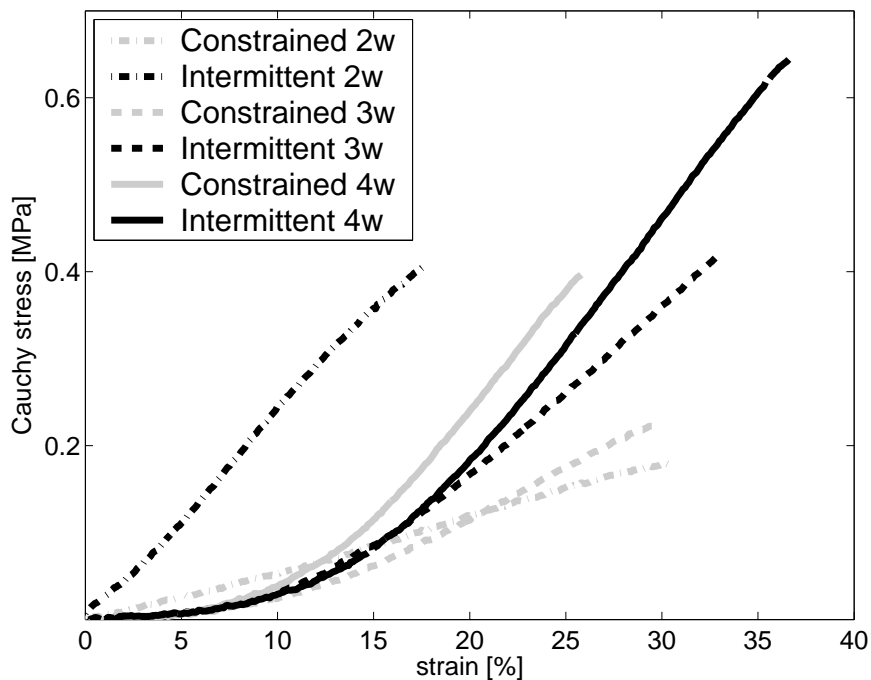


Figure 5.5: Averaged stress–strain curves until break for constrained (gray) and intermittently strained (black) samples after 2, 3, and 4 weeks (w) of culture. After 2 weeks, the mechanical behavior of constrained and intermittently strained samples was linear. Non-linear tissue-like behavior developed with time.

## 5.4 Discussion

Mechanical conditioning has proven to be a successful strategy in heart valve tissue engineering to improve tissue architecture and mechanical properties. Strain-based conditioning was demonstrated to render tissue-engineered heart valves with promising tissue properties. However, quantitative laws for the effect of mechanical conditioning have not been fully established. To obtain a thorough insight into the evolution of tissue properties in response to mechanical loading, a well-defined model system for cardiovascular structures, such as tissue-engineered heart valves, is required. In this study, rectangular strips of a biodegradable PGA scaffold seeded with human saphenous vein cells were mechanically conditioned using a Flexercell straining device. As PGA does not show elastic material behavior (Kim and Mooney, 2000; Webb *et al.*, 2004), part of the porous PGA scaffold was embedded in a thin layer of liquid silicone. This enabled engineered tissues to be dynamically conditioned to a strain amplitude of 4% for up to several weeks (Boerboom *et al.*, 2008).

Native tissue strains have been reported to amount up to 12% in circumferential direction during diastole (Thubrikar *et al.*, 1980). It is questionable whether a stimulus with this physiological strain magnitude is the optimal conditioning strategy for engineering valves. In fact, previous application of dynamic strains with strain magnitudes of 8% and 12% to the engineered constructs resulted in decreased tissue properties (Boerboom *et al.*, 2008). Compared to regular conditioning protocols, including constrained and continuous cyclic loading, intermittent strain has been demonstrated to be a promising strategy to improve tissue properties. Here, we investigated the temporal effects of intermittent strain on tissue properties in human engineered heart valve tissue. Samples were sacrificed after 2, 3, and 4 weeks of conditioning and subsequently analyzed for matrix morphology and organization, collagen production, cross-link density, and mechanical properties.

Intermittent strain resulted in increased matrix formation when compared to constraining, as shown qualitatively by histology (figures 5.1). These findings were confirmed by quantitative assays that showed improved collagen production in the intermittently strained group after 2 and 3 weeks of culture. Thereafter, collagen production stabilized in the intermittently strained samples, while it was still increasing in the constrained samples (figure 5.4b). A potential mechanism to explain the higher collagen production in the intermittently strained samples is a change in phenotype of myofibroblasts toward a more synthetic type as a consequence of mechanical loading and unloading. It is well known that vascular cells differentiate from a quiescent fibroblast phenotype into a more active phenotype, with increased proliferative and matrix synthesis activity, in response to mechanical conditioning (Rabkin-Aikawa *et al.*, 2004; Stegemann and Nerem, 2003).

After reaching stable levels of collagen production in the intermittently strained samples, the concentration of HP cross-links increased. Interestingly, intermittent strain accelerated the maturation process of these tissues, as evidenced from an increase in cross-link density. Apparently, cells in the intermittently strained group shifted from collagen synthesis to cross-link formation after reaching a stable collagen turnover. By



contrast, collagen production did not attain stable levels in the constrained samples after 3 weeks, and cells kept increasing collagen production and did not alter cross-link formation. These results indicate a lower level of maturation in the constrained samples, when compared to the intermittently strained samples.

The observed differences in maturation, expressed by differences in HP cross-link concentrations between the constrained and intermittently strained samples, were confirmed by Picrosirius red staining (figure 5.2). Polarization microscopy revealed more red birefringent fibers in the intermittently strained group, which amount increased with time. A higher amount of red fibers has been reported to be related to larger collagen diameters, improved alignment, more tightly packed collagen molecules (Dayan *et al.*, 1989; Rabau and Dayan, 1994), as well as fibers of increasing age (Pickering and Boughner, 1991), which are all measures for improved maturation. Thus, in addition to higher cross-link concentrations in intermittently strained samples, higher amounts of birefringent fibers indicate enhanced maturation of these constructs, as compared to constrained samples.

The amount of collagen and the concentration of HP cross-links play an important role in the biomechanical behavior of soft tissues (Balguid *et al.*, 2007; Banse *et al.*, 2002; Elbjeirami *et al.*, 2003). In the present study, the strain-induced increase in HP cross-link density was reflected in the modulus after 2 weeks of culture and in the ultimate tensile stress at all time points. Corresponding to an increasing amount of tissue with time, the mechanical behavior shifted from linear to non-linear, representing immature tissue behavior after 2 weeks and more mature tissue-like behavior thereafter (figure 5.5). This non-linear behavior is typical for biological, cardiovascular tissues. Intermittent strain did not further increase this non-linearity, but stimulated collagen organization as expressed by a better alignment of the collagen fibers in the direction of straining, as shown with a specific viable collagen probe and two-photon microscopy (figure 5.3). This sophisticated technique can provide valuable input for the quantification of the effect of strain on collagen orientation and alignment as a function of tissue depth, which is the subject of future studies. It is likely that alignment of collagen fibers results in anisotropic properties. However, the dimensions of the strips were not suitable to perform tensile tests in two directions. Local indentation tests represent a promising alternative to characterize the anisotropic mechanical behavior of these engineered tissues (Cox *et al.*, 2006).

Although an intermittent strain regime resulted in increasing and near-native levels of cross-link densities, mechanical properties and collagen synthesis stabilized at levels still below adult native values, as previously reported (Balguid *et al.*, 2007). To increase collagen production *in vitro*, current studies investigate whether optimization of the intermittent strain regime e.g., shorter straining periods, may lead to further improvement of collagen levels or that other cues, such as biochemical stimuli should also be applied.

In conclusion, the data presented here demonstrate the beneficial effects of intermittent dynamic conditioning over constrained loading on the development of tissue properties in human engineered tissues. Intermittent strain accelerated tissue formation and maturation, expressed by a higher collagen production and HP cross-link

concentration, respectively. In addition, tissue organization and mechanical properties were enhanced by intermittent strain. These results are important for heart valve tissue engineering to create strong tissue-engineered heart valves in shorter culture times.

**Acknowledgements**

The authors thank Anita van de Loo and Jessica Snabel for performing the biochemical assays. This research was supported by the Dutch Technology Foundation (STW), Applied Science Division of NWO, and the Technology Program of the Dutch Ministry of Economic Affairs.



# Chapter 6

## Quantification of the temporal evolution of collagen orientation in mechanically conditioned engineered cardiovascular tissues

The contents of this chapter are based on M.P. Rubbens, A. Mol, R.A. Boerboom, M.M.J. Koppert, H.C. van Assen, B.M. TerHaar Romeny, F.P.T. Baaijens, and C.V.C. Bouten, *Quantification of the temporal evolution of collagen orientation in mechanically conditioned engineered cardiovascular tissues*, *Annals of biomedical engineering*, 37(7), 1263-1272, (2009).

## 6.1 Introduction

Load-bearing soft tissues have a well structured extracellular matrix, organized to perform their specialized functions. This extracellular matrix (ECM) is synthesized and organized by the cells under the (guiding) influence of external stimuli, such as tissue loading directions. It is composed of a network of fibrous proteins, predominantly collagen and elastin, embedded in a gel of proteoglycans, glycoproteins, and water. Collagen serves as the main load-bearing component of the matrix, whereas the elastin fibers give the tissue its resilience. Load-bearing tissues in general exhibit anisotropic, non-linear visco-elastic behavior, which is strongly dictated by the extracellular matrix organization, in particular the collagen fiber organization. In native heart valve leaflets, for example, collagen fibers are oriented primarily in the circumferential direction, resulting in stiffer tissue in circumferential compared with the radial direction. Likewise, other cardiovascular tissues, such as blood vessels and pericardium, display similar complex (biaxial) mechanical properties, related to the particular collagen organization within these tissues.

Mimicking the native structural organization and hence biomechanical tissue behavior, provides a major goal in cardiovascular tissue engineering, in particular when creating tissues with high biomechanical demands, such as blood vessels or heart valves for systemic, high pressure applications. In its most investigated paradigm, cardiovascular substitutes are engineered *in vitro* by using rapidly degrading scaffolds, seeded with autologous myofibroblasts (Hoerstrup *et al.*, 2000; Niklason *et al.*, 1999). The so-obtained constructs were cultured in bioreactors under conditions that favor the production of *de novo* extracellular matrix components by the cells, including collagen fibers. However, these engineered tissues often lack sufficient amounts of properly organized matrix components and consequently do not meet the *in vivo* mechanical demands. To optimize the collagen architecture and hence enhance the mechanical properties of engineered tissues, mechanical conditioning strategies are crucial (Isenberg and Tranquillo, 2003; Mol *et al.*, 2003; Seliktar *et al.*, 2003). Mol *et al.*, for example, demonstrated that enhanced (anisotropic) mechanical properties can be obtained in tissue-engineered heart valves by conditioning with dynamic strain (Mol *et al.*, 2006). These results may be attributed to an upregulation of remodeling enzymes (Asanuma *et al.*, 2003; Seliktar *et al.*, 2001), growth factors (Butt and Bishop, 1997), and matrix production (Bishop and Lindahl, 1999; Engelmayer *et al.*, 2006; O'Callaghan and Williams, 2002), but also to an improved collagen organization due to mechanical loading. Nevertheless, quantitative relationships between mechanical conditioning and resulting tissue structure and mechanical properties have not been fully established yet, due, in part, to a lack of adequate tissue model systems and measurement techniques.

The effect of different mechanical loading conditions on the collagen orientation in engineered tissues has been studied using elastic scattering spectroscopy (Kostyuk and Brown, 2004), microscopic elliptical polarimetry (Tower and Tranquillo, 2001a), and small light scattering (Engelmayer *et al.*, 2006). In simple geometries of cell-populated collagen gels, it was demonstrated that uniaxial constraints induced anisotropic collagen orientation (Costa *et al.*, 2003; Kostyuk and Brown, 2004), whereas biaxial

constraining resulted in an isotropic orientation (Thomopoulos *et al.*, 2005). Comparable results were found by Cox *et al.* (2008) in engineered cardiovascular tissues based on cell-seeded biodegradable scaffolds. In collagen-based tissue-engineered heart valves, the application of specific mechanical constraints led to commissural alignment of the collagen fibers (Neidert and Tranquillo, 2006). However, the measurement techniques used in these studies only monitor global collagen orientation, and do not provide three-dimensional spatial information throughout the sample. Although the importance of a detailed description of collagen fiber orientation in the mechanics of load-bearing structures is widely recognized, 3D collagen fiber orientations have not yet been examined in response to mechanical loading in engineered tissues.

In this study a novel method for the quantification of collagen orientation, consisting of a combination of vital two-photon imaging and mathematical algorithms, is applied to engineered tissues to study the effects of mechanical conditioning on the temporal evolution of collagen orientation as a function of tissue depth. Cell-seeded biodegradable rectangular scaffolds were constrained or intermittently strained in the longitudinal direction. Intermittent strain regimes were demonstrated to be favorable in terms of cell proliferation (Barkhausen *et al.*, 2003; Winter *et al.*, 2003), matrix production (Chowdhury *et al.*, 2003), collagen cross-link density (Boerboom *et al.*, 2007b), and mechanical properties (Robling *et al.*, 2002), when compared to continuous strain protocols. In addition, intermittent strain was shown to yield stronger tissues in shorter culture periods in engineered heart valve tissue (Rubbens *et al.*, 2009b). We hypothesize that the improved mechanical properties of the engineered tissues, when exposed to intermittent loading during culture, is also attributed to an improved and accelerated (anisotropic) collagen organization. Therefore, the present study extends the analyses of these engineered tissues by quantifying the collagen orientations after 2, 3, and 4 weeks of constrained and intermittent conditioning.

## 6.2 Materials and Methods

### 6.2.1 Tissue culture and mechanical conditioning

The methods of scaffold preparation, cell culture, seeding, and mechanical conditioning have been described previously (Rubbens *et al.*, 2009c). To review briefly, human saphenous vein myofibroblasts (p7) were seeded using fibrin as a cell carrier onto rectangular strips (35x5x1 mm) of non-woven polyglycolic acid scaffolds, coated with a thin layer of poly-4-hydroxybutyrate. In the longitudinal direction, the scaffolds were attached at their outer 5 mm to the flexible membranes of 6-well plates (Flexcell Int., USA). After 1 week of culture under these constrained conditions, the engineered tissues were divided into two groups (figure 6.1). One group (n = 6) served as constrained control, whereas the other group (n = 6) was subjected to uniaxial intermittent dynamic strain (4%, 3 hours on/off, 1 Hz) using a modified version of a Flexercell FX-4000T straining device (Flexcell Int., USA) (Boerboom *et al.*, 2008).

After 2, 3, and 4 weeks of culture the collagen orientation was visualized and quantified.

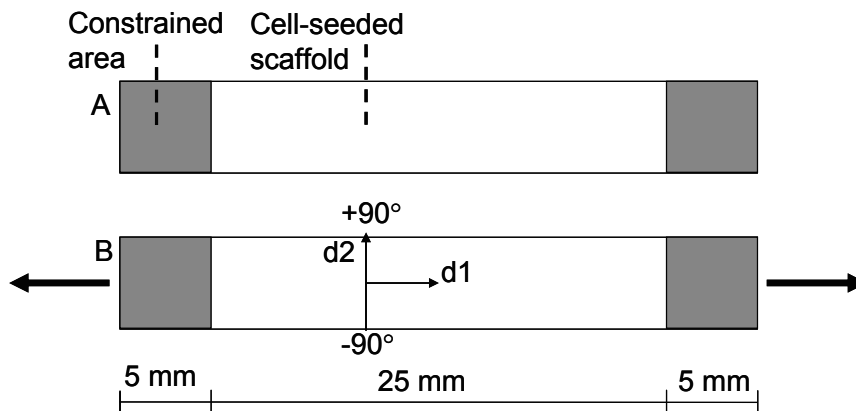


Figure 6.1: Top view of rectangular engineered constructs. The strips were longitudinally constrained at the outer 5 mm at both ends using silicone glue. Samples were either constrained (A) or intermittently dynamically loaded (B) in longitudinal direction ( $d1$ ). Direction  $d2$  represents the direction perpendicular to the long axis. Positive ( $+90^\circ$ ) and negative ( $-90^\circ$ ) directions of  $d2$  are indicated.

### 6.2.2 Visualization of collagen orientation

To visualize the collagen fiber orientation, samples were labeled by 15  $\mu\text{M}$  Cell Tracker Blue CMAC (CTB; Invitrogen, The Netherlands) and 3  $\mu\text{M}$  CNA35-OG488 as specific vital fluorescent markers for cell cytoplasm and collagen, respectively (Krahn *et al.*, 2006). CTB and CNA35-OG488 are excitable with two-photon microscopy and exhibit broad spectra at 466 nm and 520 nm, respectively. An inverted Zeiss Axiovert 200 microscope (Carl Zeiss, Germany) coupled to an LSM 510 Meta (Carl Zeiss, Germany) laser scanning microscope was used to visualize cell and collagen organization. A chameleon ultra 140 fs pulsed Ti-Sapphire laser (Coherent, U.S.A) was tuned to 760 nm and two photomultiplier tube (PMT) detectors were defined as 435 – 485 nm for CTB and 500 – 530 nm for CNA-OG488. Two samples per group were scanned at three different locations: 1) the center point of the tissue, 2) 5 mm left to the center point, and 3) 5 mm right to the center point. At each location a stack of image slices was obtained. The thickness of one image slice was 1  $\mu\text{m}$  and the maximum thickness of the stack was 100  $\mu\text{m}$ . Separate images were obtained from each PMT and combined into single images.

### 6.2.3 Quantification of collagen orientation

The collagen fiber orientations were determined by analyzing the individual images of each image stack as described by Daniels *et al.* (2006). To review briefly, coherence-enhancing diffusion (CED) was applied for de-noising to improve the quality of structures in the image without destroying the boundaries of the fibers (Weickert,

1999). Using CED, smoothing occurs along, but not perpendicular, to the preferred orientation of the structures in the image. Subsequently, the local orientations of all collagen fibers were determined by calculating the principal curvature directions from the eigenvectors of the Hessian matrix (second order structure) (Ter Haar Romeny, 2003). As fibers appear at different widths, the second order derivatives were determined at a scale adaptive to the local width of the fiber. The optimal scale was determined with a contextual confidence measure (Niessen *et al.*, 1997). At each location a stack of (in-plane) orientation histograms was obtained, representing the statistical distribution of local orientations in each image. To calculate the mean fiber angle and the dispersity of the distributions, circular statistics were required due to the periodicity of the fiber distributions (Karlou *et al.*, 1998; Thomopoulos *et al.*, 2005; Zar, 1999). Circular statistics handle periodic data by representing each angle as a unit vector oriented at that angle. To calculate the mean angle, the individual unit vectors are decomposed into vector components on which statistical operations, such as averaging, are permitted (figure 6.2). Histograms of collagen orientations were obtained from each two-photon image, and of each the mean vector was calculated, representing a mean angle  $\alpha$  and a mean vector length  $r$ . The mean vector length represents a measure of the dispersity of the fiber orientations. A vector length of 1 indicates no variation in fiber orientations (i.e., all fibers perfectly aligned) while a vector length of 0 indicates a random distribution of fiber orientations. Mean angles and vector lengths as a function of tissue depth were obtained per image location. To generalize the results, the vector components at each depth were averaged over all the samples per loading condition per time point. Subsequently, averaged mean angles and vector lengths per loading condition per time point were obtained. It should be noted that when the dispersity of the collagen orientation distribution is large, the distribution becomes essentially random. This diminishes the meaning of the value of the mean angle. Hence, for clarity, orientation angles were not reported when mean vector lengths ( $r$ ) were consistently lower than 0.2.



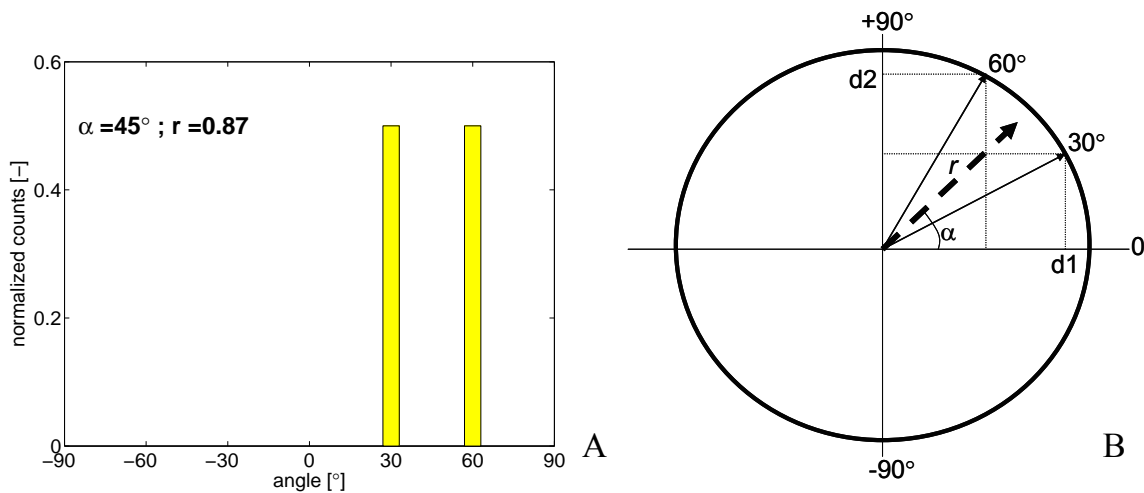


Figure 6.2: Example of circular statistics. A circular distribution is represented in a histogram (a) and depicted as unit vectors with corresponding angles of 30 and 60 degrees in a unit circle (b). The mean vector (dashed line) is calculated by averaging the decomposed sine and cosine vector components of the individual vectors.  $\alpha$  represents the mean angle and  $r$  the length of the mean vector. A vector length of 1 indicates no variation in fiber orientations, while a vector length of 0 indicates a random orientation of fiber orientations.

### 6.2.3 Statistics

Statistics were performed, where appropriate, to determine the effect of mechanical loading on the alignment of the collagen fibers, as described previously (Thomopoulos *et al.*, 2005). To review briefly, alignment in the longitudinal (d1) direction was tested for significance at each imaging depth in each set of samples per time point and loading condition by performing one-sample t-tests against a reference value of 0 on the cosine components of the mean vectors. A p-value lower than 0.05 was considered statistically significant.

## 6.3 Results

### 6.3.1 Quantification algorithm

A representative example of the application of the orientation algorithm is shown in figure 6.3. For each two-photon image of cells and collagen fibers (figure 6.3a), coherence-enhancing diffusion is applied, to enhance the collagen fiber structures (figure 6.3b). Next, the principle curvature directions are calculated per pixel (figure 6.3c). Subsequently, the orientation analysis program generates a histogram of the orientations (figure 6.3d), from which the mean angle and vector length are calculated using circular statistics.

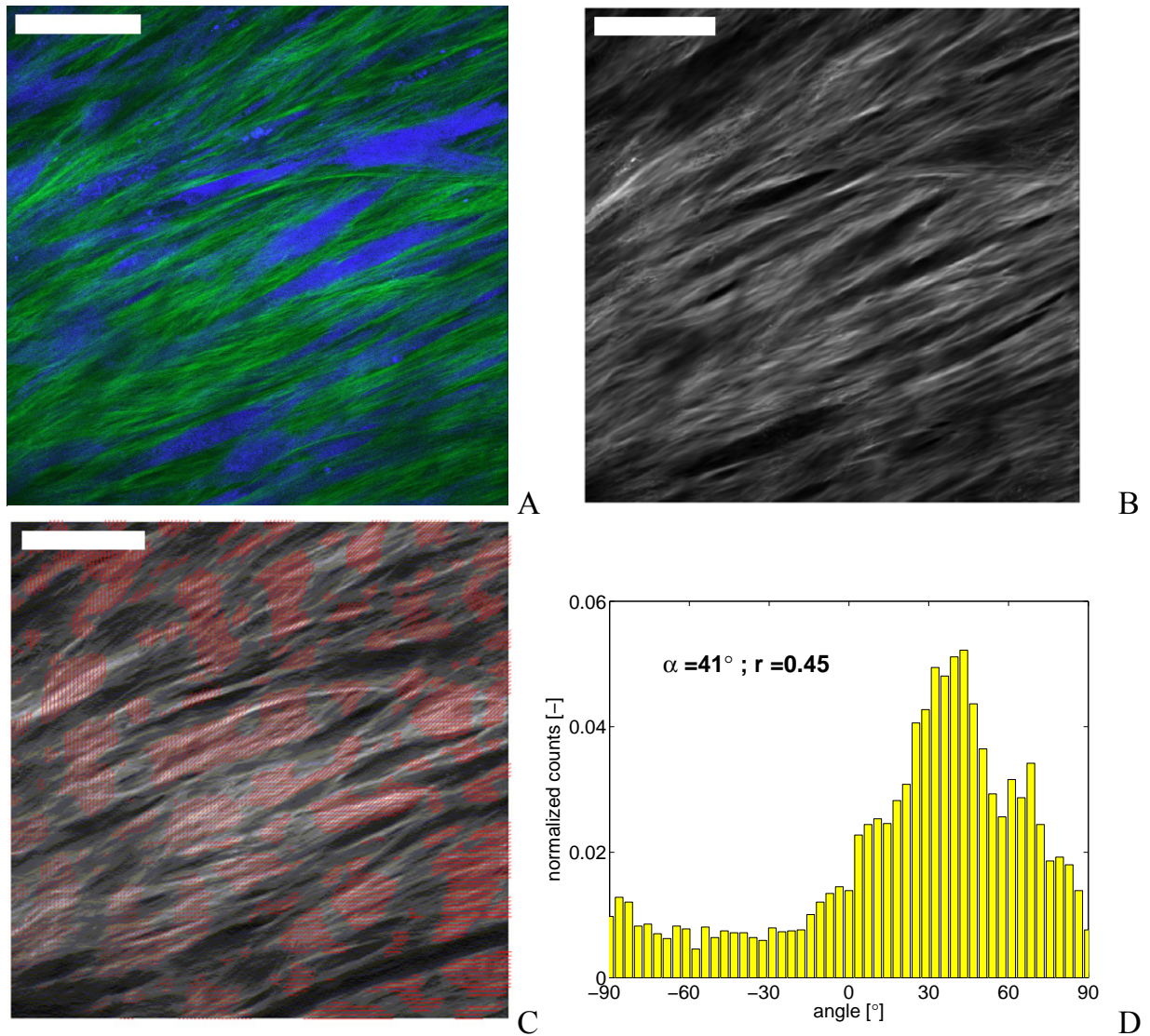


Figure 6.3: Different steps of the orientation analysis. On the two-photon image (A) coherence-enhancing diffusion is applied (B). Using the Hessian matrix the principal curvature directions are calculated (C) which results in a histogram of orientations (D). Scale bars represent 50  $\mu\text{m}$ .

### 6.3.2 Spatial organization of collagen fibers

Representative images of constrained and intermittently strained samples at 15  $\mu\text{m}$  and 50  $\mu\text{m}$  depth after 2 weeks of culture are depicted in figure 6.4. Collagen fibers were more randomly distributed in the constrained samples (figure 6.4a,b), when compared with the intermittently strained samples (figure 6.4c,d), as is depicted in the corresponding histograms. No preferred orientations were found in the constrained samples ( $r = 0.13$  at 15  $\mu\text{m}$  and  $r = 0.03$  at 50  $\mu\text{m}$ ), whereas intermittent loading resulted in fiber distributions with more distinct fiber orientations ( $r = 0.42$  at 15  $\mu\text{m}$  and  $r = 0.37$  at 50  $\mu\text{m}$ ).

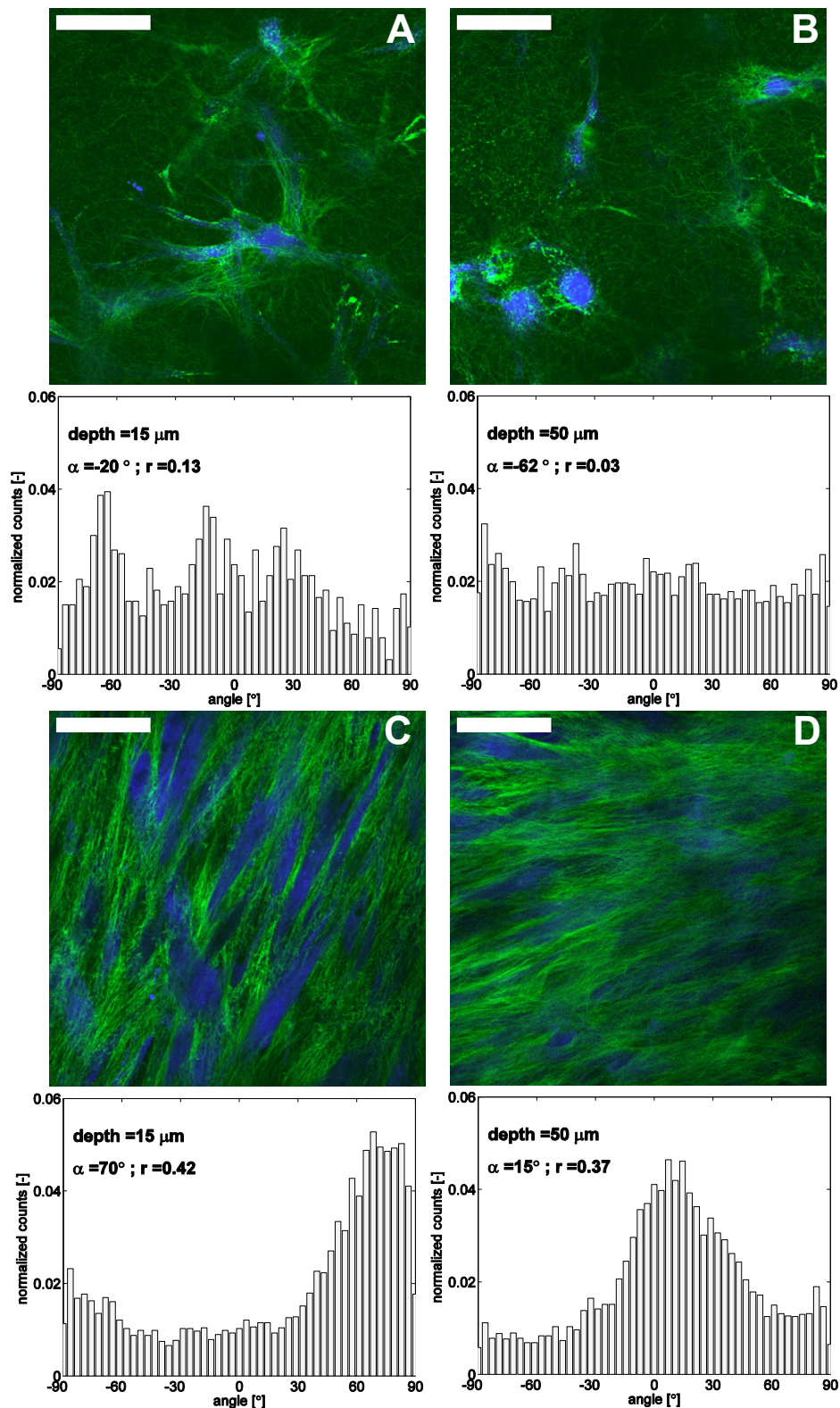


Figure 6.4: Representative two-photon images of cells (blue) and collagen (green) in constrained (A,B) and intermittently strained (C,D) samples after 2 weeks at a depth of 15  $\mu\text{m}$  (A,C) and 50  $\mu\text{m}$  (B,D) with corresponding histograms of collagen orientations. Straining direction was from left to right. Scale bars represent 50  $\mu\text{m}$ .

The angles and vector lengths as a function of depth of the same samples are shown in figure 6.5. No alignment was observed in the constrained samples (figure 6.5a), except for the first few slices. On the contrary, higher values of the vector length were found throughout the imaging stack of the intermittently strained samples (figure 6.5b), indicating a higher degree of alignment. Interestingly, the orientation of the collagen fibers in the intermittently strained samples shifted from an almost perpendicular orientation at the surface to an orientation into the direction of straining approximately 50  $\mu\text{m}$  deep into the tissue.

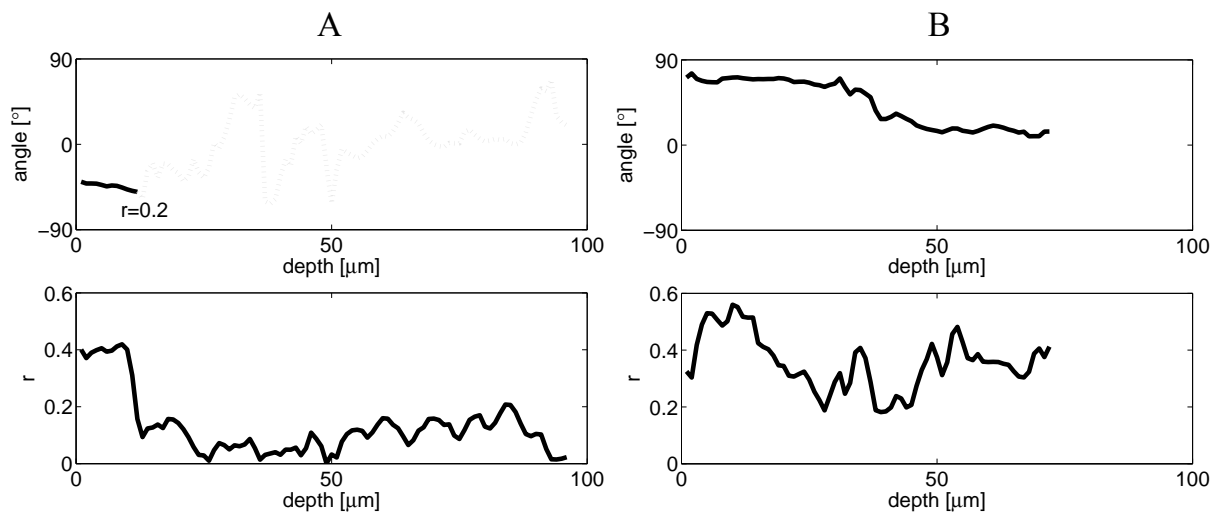


Figure 6.5: Orientation angles and vector lengths as a function of the imaging depth for constrained (A) and intermittently strained (B) samples after 2 weeks of culture. These figures correspond to the samples of which 2 images are depicted in figure 6.4. Note that the meaning of the mean angle diminishes for low mean vector lengths. Therefore, the mean angle of the constrained sample is not shown when the mean vector length is consistently lower than 0.2 (indicated by  $r = 0.2$ ).

### 6.3.3 Temporal evolution of collagen fiber orientation

Figure 6.6 shows representative pictures of constrained and intermittently strained samples at an imaging depth of 50  $\mu\text{m}$  after 2, 3, and 4 weeks of culture. Cells and collagen fibers were randomly distributed in the constrained samples after 2 (figure 6.6a) and 3 (figure 6.6b) weeks of culture. After 4 weeks, some alignment of the collagen fibers in the constrained direction was observed (figure 6.6c). However, for the intermittently strained samples, both collagen and cellular alignment was evident after 2 weeks of culture (figure 6.6d), which were maintained after 3 (figure 6.6e) and 4 weeks of culture (figure 6.6f).



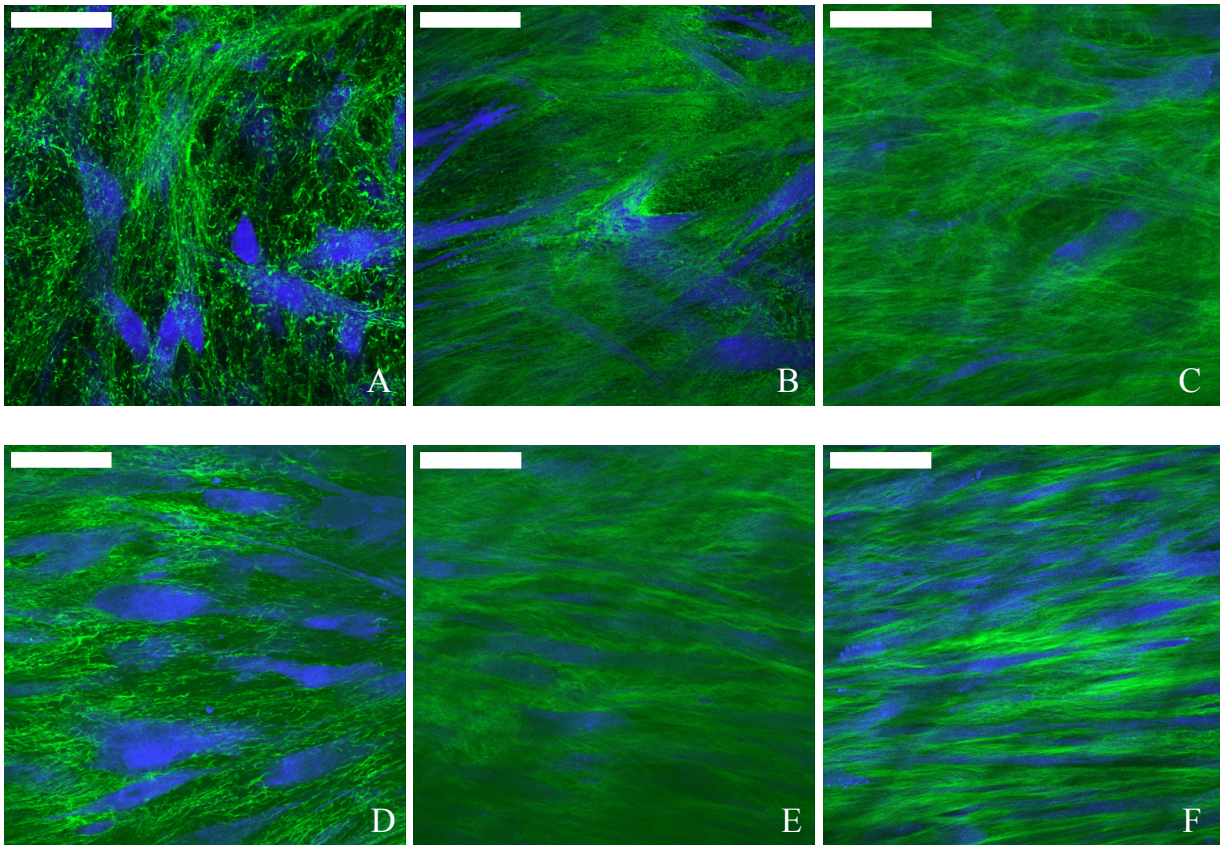


Figure 6.6: Representative two-photon images of cells (blue) and collagen fibers (green) in constrained (A-C) and intermittently strained (D-F) samples at an imaging depth of  $50\ \mu\text{m}$  after 2 (A,D), 3 (B,E), and 4 (C,F) weeks of culture. Straining direction was from left to right. Alignment of cells and collagen fibers developed in time and was enhanced by intermittent strain. Scale bars represent  $50\ \mu\text{m}$ .

### 6.3.4 Spatio-temporal evolution of collagen fiber orientation

The quantified collagen fiber orientations were averaged using circular statistics for all imaging depths per loading condition per time point. The profiles of the resulting orientation angles and vector lengths (as a measure of dispersity) as a function of the imaging depth are depicted in figure 6.7. With the exception of the first few slices, low values for the vector length ( $<0.2$ ) were found in the constrained samples after 2 and 3 weeks of culture, indicating a random orientation of the collagen fibers (figure 6.7a). Interestingly, after 4 weeks, the vector lengths became higher ( $>0.2$ ) and a change in orientation from 70 degrees at the surface to an orientation along the longitudinal sample direction (d1) in deeper tissue layers was found. Significant alignment ( $p < 0.05$ ) in the d1 direction was found at imaging depths ranging from 35 to  $40\ \mu\text{m}$ . The orientation angles were found to adopt similar profiles in the intermittently strained samples for all time points (figure 6.7b). Here, the orientation of the collagen fibers shifted from an oblique orientation (70 to 80 degrees) at the surface to a parallel orientation along d1 at  $50\ \mu\text{m}$  deeper into the samples. The lowest dispersities were

found in the intermittently loaded samples after 4 weeks of culture. Significant alignment ( $p < 0.05$ ) in the direction of straining was found at an imaging depth of 30  $\mu\text{m}$  and deeper.

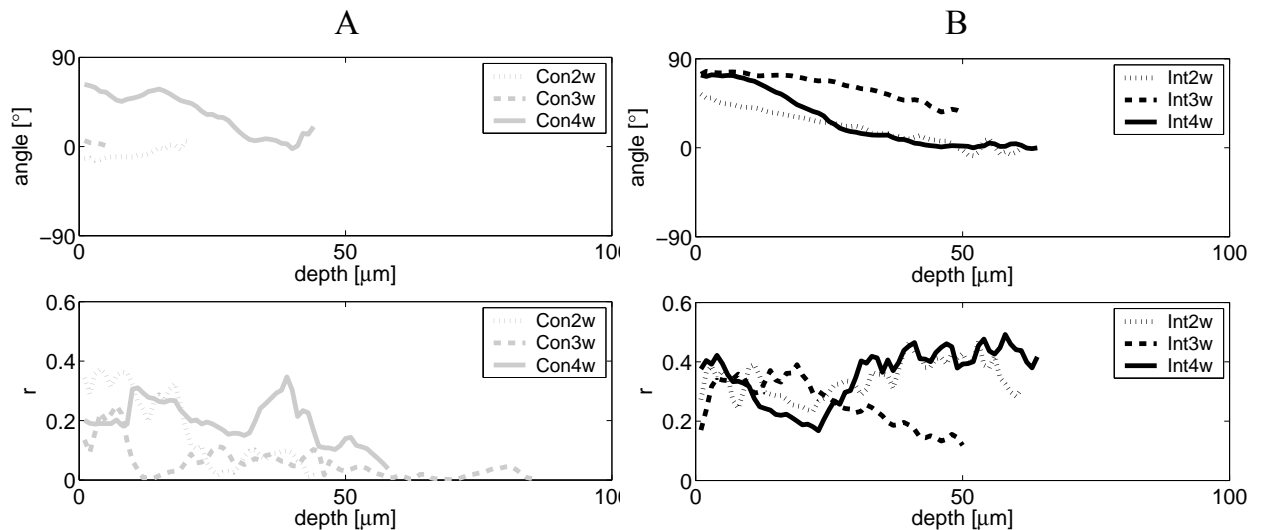


Figure 6.7: Orientation angle ( $\alpha$ ) and vector lengths ( $r$ ) as a function of the penetration depth into the tissue for constrained (A) and intermittently loaded (B) samples after 2, 3, and 4 weeks (w) of culture. For clarity, orientation angles at low mean vector lengths ( $< 0.2$ ) are not shown. In the constrained samples, alignment of the fibers and a shift in orientation were obtained after 4 weeks of culture. Similar results were found in the intermittently strained samples at all time points.

## 6.4 Discussion

Mimicking native biomechanical behavior is a major challenge for tissue engineering cardiovascular substitutes. The anisotropic mechanical behavior of these load-bearing tissues depends on the tissue architecture and, in particular, on its collagen fiber organization. To optimize collagen orientation and alignment, and hence improve the mechanical properties of engineered tissues, in vitro mechanical conditioning strategies are crucial. Although the importance of collagen orientation in the determination of anisotropic mechanical properties has been widely recognized, the effect of mechanical conditioning on the temporal development of 3D collagen fiber orientation has not yet been quantified in engineered tissues. In this study a new method to quantify collagen orientation was used to investigate the temporal and spatial effects of intermittent dynamic strain on the collagen orientation in engineered cardiovascular tissues.

The collagen fibers were stained with a vital collagen-specific probe and visualized with two-photon laser scanning microscopy to obtain detailed images of the collagen structure as a function of depth within the tissue. Due to the penetration depth of the laser, this technique is limited to the top 100  $\mu\text{m}$  of the tissue. Two-photon microscopy

produces large three-dimensional datasets. Due to the size, and the complexity of the collagen network an automated method for the observation and extraction of quantitative orientation information provides a faster, more objective and more accurate way to analyze the data compared to analysis by hand. Wu *et al.* (Wu *et al.*, 2003a; Wu *et al.*, 2003b) previously designed an automated analysis algorithm to extract quantitative structural information of collagen in bovine collagen gels. Collagen fibers were visualized using confocal laser scanning microscopy and the orientation, length, and diameter of individual fibers were quantified. In contrast to those datasets, the two-photon images generated in the present study contain complex collagen networks, making it unfeasible to extract and analyze single fibers. Therefore, similar to other studies (Elbischger *et al.*, 2004; Karlon *et al.*, 1998; Karlon *et al.*, 1999), the orientation analysis was based on the spatial context of the images using methods from differential geometry, based on an Eigen-analysis of the second order Hessian matrix. The principal curvatures, calculated at multiple scales, are used in adaptive de-noising of datasets and proved to be robust measures for the local fiber shape and orientation (Ter Haar Romeny, 2003).

Subsequently, this collagen fiber quantification method was used to study the effect of intermittent dynamic strain on temporal variations in collagen orientation in engineered cardiovascular tissues. It has been demonstrated that factors, such as tissue compaction, contact guidance, and aspect ratio of the scaffold may influence collagen orientation (Costa *et al.*, 2003; Engelmayer *et al.*, 2006; Neidert and Tranquillo, 2006; Sawhney and Howard, 2002). Since these factors were assumed to be identical in both strained and constrained samples in the present study, their interference with the effect of mechanical conditioning is considered to be minimized.

In the constrained samples, a random organization of cells and collagen fibers was observed after 2 and 3 weeks of culture. However, after 4 weeks, constraining led to alignment of the collagen fibers in the constrained direction (figure 6.6c). This can be explained by the generation of internal stresses in this direction due to tissue compaction (Neidert and Tranquillo, 2006). Interestingly, in the intermittent dynamically strained samples, collagen alignment was already present after 2 weeks of culture and continued to improve up to 4 weeks (figure 6.6d-f, 6.7b). By this time, the lowest fiber dispersities were observed, indicating a highly aligned collagen structure. Significant alignment ( $p < 0.05$ ) in the straining direction was found at an imaging depth of 30  $\mu\text{m}$  and deeper.

It is likely that the improved alignment of collagen will result in enhanced anisotropy with regards to the mechanical properties of the tissue. In a parallel experiment with similar culture and conditioning regimes, it was shown that the mechanical properties in the straining direction (d1) of intermittently strained samples were indeed higher when compared to constrained samples (Rubbens *et al.*, 2009b). Scaffolds of different geometries would be required to study the effect of uniaxial strain regimes on the mechanical properties in different directions. Furthermore, with the use of square or circular scaffold geometries, the developed quantification method could examine the influence of biaxial loading protocols that closely resemble the in vivo environment of cardiovascular tissues.

In addition to the assessment of temporal development, collagen orientation was quantified as a function of depth into the tissue. Analyses revealed a shift from a perpendicular or an oblique orientation at the surface to an orientation in the direction of straining deeper into the tissue. The orientation of the cells was observed to change in a similar way. This co-alignment of cells and collagen fiber orientations corresponds to previous findings (Glass-Brudzinski *et al.*, 2002; Wang *et al.*, 2003). Interestingly, the oblique or perpendicular orientation of the cells in the superficial layer of our tissue-engineered constructs corresponds well to that observed for monolayers of strained cells (Dartsch and Hammerle, 1986; Hamilton *et al.*, 2004; Iba and Sumpio, 1991; Neidlinger-Wilke *et al.*, 2001), where cells align perpendicular to the applied strains. We therefore assume that the superficial cells in our 3D tissues behave like a monolayer or cell coverage on top of the construct. Similar to monolayers, relatively low amounts of collagen are present in this superficial layer, which might explain the comparable orientation results. By contrast, cells entrapped in three-dimensional environments are known to align to the strain direction (Eastwood *et al.*, 1998; Grenier *et al.*, 2005; Seliktar *et al.*, 2000). This corresponds to the orientation of cells below the surface layer, where a three-dimensional collagen network collagen is present. Regarding the collagen fibers that we were not able to analyze, namely below a depth of 100  $\mu\text{m}$ , we hypothesize that the collagen fibers are mainly aligned in the constrained and dynamically strained direction.

In conclusion, a novel method to quantify collagen orientations was applied to examine the effect of intermittent strain over time in engineered cardiovascular tissues. Intermittent loading resulted in improved collagen alignment in the direction of straining in shorter culture periods, compared to constrained loading. Both the method and the results are important to create and monitor load-bearing tissue-engineered substitutes with an organized (anisotropic) collagen network.

### **Acknowledgements**

The authors wish to thank Florie Daniels for developing the orientation analysis software. This research is supported by the Dutch Technology Foundation (STW), applied science division of NWO and the Technology Program of the Dutch Ministry of Economic Affairs (efb. 6233).





# Chapter 7

General discussion

## 7.1 Introduction

Cardiovascular diseases are, next to cancer, the leading cause of death in the United States (Anderson and Smith, 2005). In 2004, cardiovascular diseases, such as heart valve dysfunction or coronary artery stenosis, accounted for 1 of every 2.8 deaths (Rosamond *et al.*, 2007). Currently used treatments for end-stage valvular disease include the replacement of the native heart valve by mechanical or biological valves. In 2003, 290,000 heart valve replacements were performed worldwide (Rosamond *et al.*, 2007). Due to the ageing population and increase of rheumatic cardiac disease, the incidence of heart valve disease is increasing rapidly worldwide. Concomitantly, the number of individuals requiring heart valve replacement is predicted to triple to over 850,000 by the year 2050 (Yacoub and Takkenberg, 2005). In case of coronary artery diseases, the native, non-functional artery needs to be bypassed. Approximately 427,000 coronary bypass surgeries were performed in the US in 2004 on more than 249,000 patients (Rosamond *et al.*, 2008). Saphenous vein grafts are commonly used for these procedures, although they have a limited lifespan (Raja *et al.*, 2004), demonstrated by a patency of 57% after 10 years (Sabik, III *et al.*, 2005). Vascular grafts are increasingly in demand for patients who need follow-up surgery and do not have sufficient native graft material. The same is true for arteriovenous shunt material for vascular access in dialysis patients.

The main limitation of currently used heart valve and large blood vessel replacements is that they are not able to grow, repair, and remodel, which is especially important for pediatric and young adult patients. Tissue engineering represents a promising alternative to overcome this limitation by creating living tissue substitutes that are able to grow, repair, and adapt in response to changing physiological demands.

In the most investigated *in vitro* tissue engineering paradigm, cells are harvested from a patient and subsequently expanded to increase their number. The cells are then seeded onto a biodegradable synthetic scaffold. To enhance tissue formation by the cells, the cell-seeded scaffolds are placed in a bioreactor where biochemical and mechanical stimuli are applied. With this approach, tissue-engineered heart valves and blood vessels have been created with promising functionality (Hoerstrup *et al.*, 2000; Mol *et al.*, 2005a; Niklason *et al.*, 1999; Stekelenburg *et al.*, 2009)

A main challenge in cardiovascular tissue engineering is to create tissues with a well organized tissue structure. As collagen is the main load-bearing constituent of these tissues, this can be achieved by regulating the collagen architecture (amount, cross-links, and orientation) using mechanical conditioning. Quantitative relationships between mechanical conditioning, collagen architecture, and mechanical properties have not been fully established yet. Therefore, the goal of this work was to elucidate the effects of well-defined mechanical conditioning protocols on collagen architecture. This may ultimately result in specified conditioning regimes for engineered tissues with controlled collagen architecture and mechanical properties.

## 7.2 Summary and discussion of main findings

Table 7.1 shows a general overview of the effects of the applied mechanical conditioning protocols on collagen architecture (collagen amount, cross-links, orientation) and mechanical properties (modulus and ultimate tensile stress (UTS)). In chapter 3, temporal effects of different straining modes, either static (constrained) or dynamic, on collagen amount and cross-links on both gene and protein levels were examined. Compared to constraining, a dynamic strain regime resulted in lower collagen expression and production, but enhanced collagen cross-link expression and density. To determine the mechanical properties of newly formed tissue, the tissues were cultured for 4 weeks (chapter 4). By that time, the initial scaffold has lost its mechanical integrity and the mechanical properties of the constructs were determined by the newly formed tissue. Compared to static conditioning, dynamic conditioning resulted in higher cross-link densities, which correlated to improved mechanical properties of the dynamically strained samples.

Table 7.1: Effect of conditioning on collagen architecture and mechanical properties

Chapter	Loading condition (time)	Collagen content	Cross -links	Orientation	Modulus	UTS
3	Continuous dynamic vs static (up to 10 days)	–	++			
4	Continuous dynamic vs static (4 weeks)	n.c.	++		++	+
5 & 6	Intermittent dynamic vs static (2 weeks)	+	++	+++	+++	++
5 & 6	Intermittent dynamic vs static (3 weeks)	+	++	++	n.c.	++
5 & 6	Intermittent dynamic vs static (4 weeks)	n.c.	+++	+	n.c.	++

*Table 7.1: Summary of the effects of different loading protocols on collagen architecture and mechanical properties. The influence of each loading condition is indicated with – (decrease) or with +, ++, and +++ (increase) with respect to the statically conditioned (constrained) samples. n.c. indicates no change with respect to static conditioning. UTS refers to ultimate tensile stress.*

Intermittent dynamic strain resulted in increased collagen production, cross-link densities, collagen organization, and mechanical properties at faster rates, leading to stronger tissues at shorter culture periods, as compared to static conditioning (chapter 5). Collagen fiber orientation analyses revealed that mechanical conditioning induced collagen alignment in the constrained and intermittent dynamically straining directions (chapter 6). Importantly, intermittent dynamic strain improved and accelerated the alignment of the collagen fibers in the straining direction compared to constraining only.

### **Intermittent dynamic strain can enhance collagen production**

Constraining the tissues generates internal stresses by contraction of the cells. These internal stresses were shown to be sufficient to stimulate the myofibroblast cells to produce collagen. This emphasizes the relevance of constraining during tissue culture, as was also demonstrated by Neidert and Tranquillo (2006). Our studies showed that dynamic strain on top of constraining enhanced both collagen synthesis markers as well as degradation markers, compared to static conditioning up to 10 days (chapter 3). This indicates that the remodeling activity of the cells was enhanced by dynamic strain. The higher concentration of the synthesis marker in the medium was not reflected by a higher collagen gene expression. In contrast, collagen expression was lower in the dynamically compared to the statically conditioned samples. Continuous dynamic strain also resulted in a lower net collagen amount on protein level compared to static conditioning. This might be explained by the phenomenon that cells yield a certain upper limit for responding to mechanical load. Above this limit, the effect of additional loading is decreased. To increase the efficacy of mechanical stimulation, an intermittent dynamic strain regime was proposed. Compared to constraining, intermittent dynamic strain indeed enhanced collagen amounts after 2 and 3 weeks. Thus, a delicate balance between periods of mechanical stimulation alternated with periods of recovery is relevant to enhance collagen production.

Dynamic strain has been reported to enhance collagen production in short-term studies (Kolpakov *et al.*, 1995; Ku *et al.*, 2006). However, for prolonged straining of engineered tissues such an increase was not always reported (Boerboom *et al.*, 2008; Isenberg and Tranquillo, 2003; Mol *et al.*, 2006). This corresponds to the present findings where no differences were found in collagen amount between static and continuous dynamic conditioning (figure 4.4a), and between static and dynamic intermittent conditioning after 4 weeks of culture (figure 5.4b).

### **Dynamic strain is required to increase collagen cross-link formation**

Using constraining only, the number of cross-links did not significantly increase during culture. To enhance cross-link formation, a dynamic strain component was required. Apparently, this component does not need to be applied continuously. Intermittent dynamic strain demonstrated to be sufficient to enhance cross-link formation. The increased cross-link concentration due to dynamic strain may suggest that cells improve the intrinsic mechanical properties of collagen. The mature HP cross-links are formed following hydroxylation of the telopeptides of collagen. PLOD-2 has

been identified as a telopeptide lysyl hydroxylase, the enzyme responsible for this hydroxylation process (van der Slot *et al.*, 2003). Chapter 3 showed that PLOD-2 mRNA expression levels of dynamically strained constructs increased with time and were higher than for statically conditioned constructs (figure 3.3.c). This suggests that an upregulation of PLOD-2 by dynamic strain contributes to an increase in the formation of cross-links.

### **Intermittent dynamic strain accelerates collagen alignment**

In the constrained samples, a random orientation of cells and collagen fibers was observed after 2 and 3 weeks of culture. However, after 4 weeks, alignment of the collagen fibers was in the constrained direction. This can be explained by the generation of internal stresses in this direction due to tissue compaction (Neidert and Tranquillo, 2006). By contrast, in the intermittent dynamically strained samples, collagen alignment was already present after 2 weeks of culture and continued to improve up to 4 weeks. By this time, the lowest fiber dispersities were seen, indicating a highly aligned collagen structure (figure 6.7b). Thus, intermittent dynamic loading can be used to accelerate and improve anisotropic collagen organization in engineered tissues.

Collagen orientation analyses revealed a transfer from a perpendicular or an oblique orientation at the surface to an orientation in the direction of straining deeper into the tissue. The orientation of the cells was observed to change in a similar way. This co-alignment of cells and collagen fibers corresponds to previous findings, where it was demonstrated that collagen orientation was reflected by cell orientation (Glass-Brudzinski *et al.*, 2002; Wang *et al.*, 2003). Interestingly, the oblique or perpendicular orientation of the cells in the superficial layer of our tissue-engineered constructs corresponds well to the that observed for monolayers of strained cells, where cells align perpendicular to the applied strain (Dartsch and Hammerle, 1986; Hamilton *et al.*, 2004; Iba and Sumpio, 1991; Neidlinger-Wilke *et al.*, 2001). We therefore assume that the superficial cells in our 3D tissues behave like a monolayer or cell coverage on top of the construct. Similar to monolayers, relatively low amounts of collagen are present in this superficial layer, which might explain the comparable orientation results. By contrast, cells entrapped in three-dimensional environments are known to align to the straining direction (Eastwood *et al.*, 1998; Grenier *et al.*, 2005; Nieponice *et al.*, 2007; Seliktar *et al.*, 2000). This corresponds to the orientation of cells below the surface layer, where a three-dimensional collagen network is present. Regarding the collagen fibers that we were not able to analyze, namely below a depth of 100  $\mu\text{m}$ , it is hypothesized that the collagen fibers are mainly aligned in the constrained or dynamically strained direction.

### **Collagen cross-links are important for tissue mechanical properties**

The moduli of the engineered tissues were enhanced by continuous dynamic conditioning compared to static conditioning after 4 weeks of culture (figure 4.3). This result is consistent with previously published data showing that dynamic loading of tissue-engineered constructs resulted in higher modulus and strength values (Mol *et al.*,

2003). It was suggested that this was due to enhanced tissue organization, based on qualitative observations by histology. As mentioned earlier, our experiments showed that dynamic strain increased the cross-link density. This increase in cross-links was reflected in an increase in modulus, which confirms the proposed relevance of cross-link stimulation to enhance tissue mechanical properties in engineered tissues (Dahl *et al.*, 2005; Elbjeirami *et al.*, 2003).

In the intermittent dynamically strained samples, the increase in HP cross-link density was reflected in the modulus after 2 weeks of culture and in the ultimate tensile stress at all time points (table 5.1). As cross-links were still higher in the intermittently strained samples after 4 weeks of culture, it could be predicted that these samples would show a higher modulus compared to the statically conditioned tissues. However, no differences in modulus between the two groups were found. It is unclear what the cause of this discrepancy is. Clearly, collagen cross-links do not exclusively determine the modulus of the tissue, requiring analyses of multifactorial influences.

### Evolution of tissue properties with time

Based on the studies on the temporal effects of strain, a schematic of the proposed evolution of DNA, collagen, and cross-links with time is presented in figure 7.1.

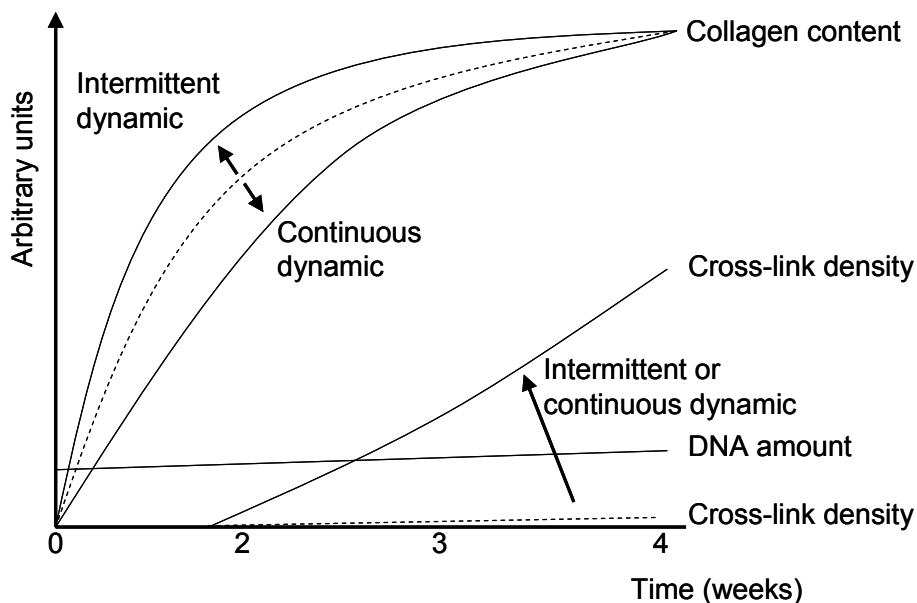


Figure 7.1: Temporal evolution of DNA, collagen, and cross-links in statically (dashed line) and dynamically (straight line) conditioned tissues. DNA was not influenced by dynamic strain. In contrast, the temporal evolution of collagen amount and cross-links was dependent on the mode of conditioning.

The amount of DNA marginally increased with time in the engineered samples and was not influenced by dynamic strain. In literature, the effects of dynamic strain on the amount of DNA are not consistent among studies. Increased amounts were reported (Jeong *et al.*, 2005; Mol *et al.*, 2003; Sodian *et al.*, 1999; Sodian *et al.*, 2000b; Stegemann and Nerem, 2003), as well as no differences (Engelmayr, Jr. *et al.*, 2005;

Hoerstrup *et al.*, 2002a; Isenberg and Tranquillo, 2003), and decreased amounts (Hoerstrup *et al.*, 2002b). The phenotype of the cells may influence the reported results. Vascular cells are known to be able to differentiate from a quiescent phenotype into a more active myofibroblast phenotype (Rabkin-Aikawa *et al.*, 2004), with increased proliferative and/or matrix synthesis activity in response to mechanical stimulation. With time, static and dynamic conditioning increased matrix production, as reflected by an increase in collagen amount. The rate of this increase depends on the mode of conditioning. Continuous dynamic strain both increased collagen synthesis and degradation with a net lower collagen amount compared to static conditioning (chapter 3). By contrast, intermittent dynamic strain enhanced the amount of collagen compared to the constrained state (chapter 5). These effects seem to be temporal in nature. After 4 weeks of culture the amount of collagen stabilized and was similar in the (intermittent) dynamically conditioned samples compared to the statically conditioned tissues. This indicates that a certain maximum amount of collagen can be achieved *in vitro* using the current protocols. This amount can be reached more rapidly using intermittent dynamic strain.

The amount of cross-links in the static samples did not increase with time. The formation of cross-links was enhanced by (intermittent) dynamic strain and increased with time, although an equilibrium number has not been reached by 4 weeks of culture. It is hypothesized that hereafter the tissue matures further by increasing cross-link densities.

Regarding the relative contribution of collagen amount and cross-links to the mechanical properties, we hypothesize that in the initial phase of tissue culturing, collagen and other extracellular matrix components are produced by cells to provide biomechanical support at an early stage. In this phase, the amount of collagen increases linearly with the modulus, as shown by Engelmayer *et al.* (2005). Thereafter, the tissue matures further and collagen cross-links contribute increasingly to the modulus.

Corresponding to an increasing collagen content with time, the mechanical response changes from a linear to a non-linear form, representing immature tissue behavior after 2 weeks and more mature tissue-like behavior thereafter. This non-linear behavior is typical for mature cardiovascular tissues. An intermittent strain regime did not further increase this non-linearity, but stimulated collagen organization as expressed by an improved alignment of the collagen fibers in the direction of the applied strain. It is likely that this alignment of collagen fibers results in anisotropic properties. However, the dimensions of the strips did not allow tensile testing in more than one direction. Local indentation tests represent a promising alternative to characterize the anisotropic mechanical behavior of these engineered tissues (Cox *et al.*, 2006).



## 7.3 Critique of methods

### Tissue model and straining system

To thoroughly investigate the effects of strain on collagen architecture, a well-defined model system was required. Based on existing heart valve and blood vessel tissue engineering protocols, rectangular tissue-engineered strips were made and used as tissue model for engineered cardiovascular tissues. Compared to the more complex geometry of heart valves and blood vessels, these strips are of simple geometry and smaller in size, reducing the required number of cells per experiment. In these simple geometries strain can be applied in a controlled way to study its effects on collagen architecture and remodeling.

The tissue model consisted of venous myofibroblasts, seeded with fibrin onto a biodegradable scaffold of polyglycolic acid (PGA) coated with P4HB. Seeding and culture protocols were similar to the protocols that rendered tissue-engineered heart valves and blood vessels with promising mechanical functionality. PGA has widely been used as scaffold material for cardiovascular tissue engineering, as it is a porous rapidly degrading scaffold. As PGA does not show elastic material behavior, the bottom part of the porous PGA scaffold was embedded in a thin layer of liquid silicone. This allowed the application of dynamic strain on these engineered tissues up to several weeks. A limitation of this approach is that the silicon layer restricts the diffusion of nutrients and oxygen to one side of the tissue. The use of thinner scaffolds would reduce this problem.

By constraining the tissue, compaction of the tissue by the cells is prevented and internal stresses are generated. This might favor tissue formation and remodeling. The use of the silicon layer resulted in a complex constrained reference condition. The bottom of the tissue was embedded in a silicon layer and not able to compact freely in lateral direction. This could influence the orientation of the collagen fibers in the lower part of the tissue. Extending our experimental models with numerical models should elucidate the effects of constraining on a number of factors including tissue stress/strain, compaction, and collagen fiber orientation.

To apply dynamic strains to the engineered tissues, a Flexercell straining system was used. By controlling the strain with rings around a loading post, various strain magnitudes can be applied to individual samples simultaneously. Circular loading posts were used to apply uniaxial straining. The system could be expanded to apply biaxial loading protocols to mimic the native loading condition. To apply biaxial straining, square loading posts and scaffolds are required. Pilot studies investigated the effect of biaxial straining consisting of 2% dynamic strain in one direction and 4% in the perpendicular direction. No preferred collagen orientation was observed and the mechanical properties were similar in both directions. Further studies should investigate whether biaxial strain protocols with larger differences in strain magnitudes will lead to anisotropic structural and mechanical properties.

### Methods to quantify collagen architecture

In this work, specific attention was paid to certain aspects of the collagen architecture, namely the amount of collagen, the collagen cross-link density, and the orientation of the fibers. To quantify the effect of strain on collagen amount and cross-links, both parameters were measured at gene expression and protein levels. The effects on the level of gene expression corresponded to protein data, indicating that gene expression data can be used as early markers to predict tissue formation.

The total collagen amount is a net result of collagen synthesis and degradation. To discriminate between these processes, specific markers in the culture medium were measured. This represented an on-line non-destructive measurement of collagen synthesis and degradation activities.

To quantify collagen fiber orientation, a novel technique was developed, based on 3D vital imaging using two-photon microscopy combined with image analysis (Rubbens *et al.*, 2009a). Previously used visualization techniques include elastic scattering spectroscopy (Kostyuk and Brown, 2004), microscopic elliptical polarimetry (Tower and Tranquillo, 2001b), and small light scattering (Engelmayer *et al.*, 2006). However, these measurement techniques only monitor global collagen orientation, and do not provide spatial three-dimensional information throughout the sample. More detailed techniques to obtain information on the collagen organization include confocal reflection laser scanning microscopy (Brightman *et al.*, 2000; Voytik-Harbin *et al.*, 2001) and autofluorescence and second harmonic generation (SHG) using multi-photon microscopy (Campagnola *et al.*, 2002; Konig and Riemann, 2003; Zipfel *et al.*, 2003). The latter is considered to be a very effective technique to visualize collagen (Schenke-Layland, 2008). However, the feasibility of SHG depends on the tissue properties and SHG requires high laser power, which increases the risk of damage to the tissue. To overcome these problems a vital collagen specific fluorescent probe (CNA-35) was used to visualize the collagen fibers using two-photon microscopy. This probe enabled the visualization of very young, thin collagen fibers with more contrast compared to SHG (Boerboom *et al.*, 2007a). The advantage of using two-photon microscopy is that the collagen organization can be imaged non-invasively and no tissue processing such as fixation is required. A disadvantage of this method is that the imaging depth is limited to the penetration depth of the laser and the probe.

The two-photon images generated in the present study contain complex collagen networks, making it unfeasible to extract and analyze single fibers. Therefore, similar to other studies (Elbischger *et al.*, 2004; Karlon *et al.*, 1998; Karlon *et al.*, 1999), the orientation analysis was based on the spatial context of the images using methods developed in differential geometry, based on an Eigen-analysis of the second order Hessian matrix. The principal curvatures, calculated at multiple scales, are used in adaptive de-noising of datasets and have been shown to be robust measures for the local fiber shape and orientation (Ter Haar Romeny, 2003).

Besides collagen amount, cross-links, and orientation, the collagen architecture includes other aspects, such as collagen type, fiber thickness, length and morphology. It is important in cardiovascular tissue engineering that the appropriate types of collagen are formed by the cells. Native cardiovascular tissues mainly contain collagen type I

and III, of which collagen type I is the major constituent. mRNA analyses showed that myofibroblasts expressed both collagen type I and III, of which type I was mostly expressed (figure 3.3). Future research should focus on these types of collagen at a protein level, for example using immunohistochemistry or western blotting. Then, the temporal and relative contribution of the different types of collagen to the mechanical properties of the engineered tissues can be investigated. To quantify collagen fiber characteristics such as thickness, length, and morphology, the quantification method for collagen orientation could be expanded to extract these features from two-photon images of the collagen fibers.

## 7.4 Future challenges

Figure 7.2 shows the aspects that were studied in this thesis. The effects of well-defined loading protocols (static, dynamic, and intermittent conditioning) were investigated in relation to collagen architecture (collagen amount, cross-links, and orientation) and mechanical properties (modulus and ultimate tensile stress). After analyzing and interpreting the results some fundamental questions and challenges remain before it will be possible to create functional engineered cardiovascular tissues with controlled structure and mechanical properties. The challenges mainly include:

- 1) elucidating the underlying mechano-regulatory mechanisms of collagen architecture
- 2) tuning of tissue composition and organization towards native-like tissue
- 3) targeting functional mechanical properties.

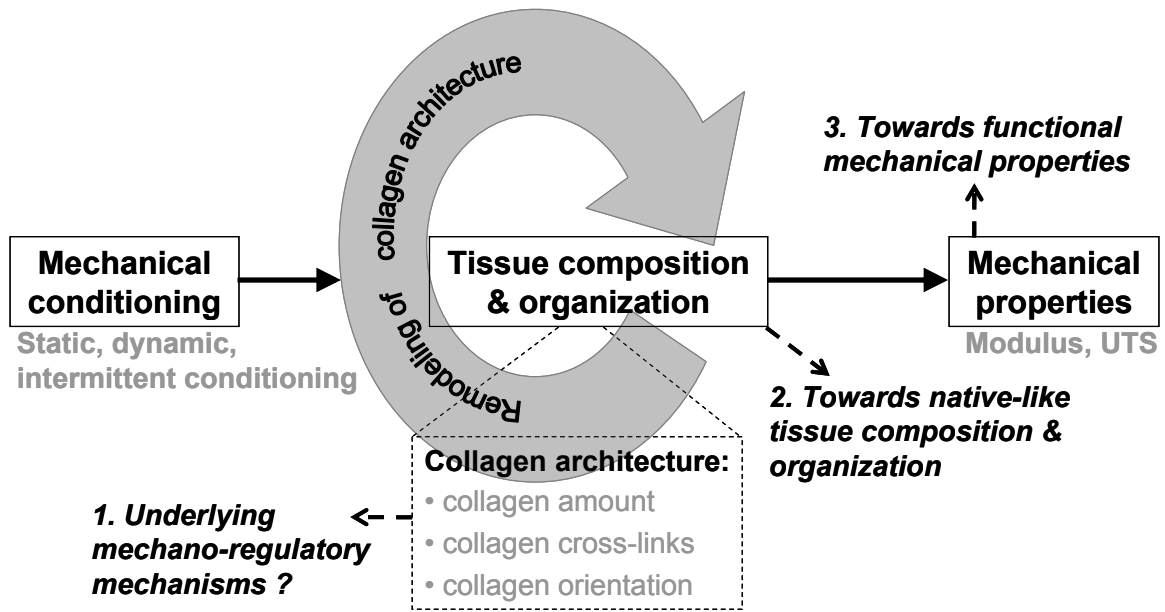


Figure 7.2: Summary of current achievements and future challenges. The investigated parameters presented in this thesis are shown in grey. To obtain functional engineered tissues with controlled architecture and mechanical properties, the following challenges remain: 1) elucidating the underlying mechano-regulatory mechanisms of collagen architecture, 2) tuning of tissue composition and organization towards native-like tissue, and 3) targeting functional mechanical properties.

### How do cells organize the collagen architecture?

A hypothesis of how cells organize their collagen matrix is depicted in figure 7.3. It is assumed that cells produce collagen in a random fashion. When a certain amount of collagen is present, cells are able to exert forces on these collagen fibers such that bridges of the collagen fibers are formed between them. Thereafter, the collagen architecture matures further by increasing the number of cross-links.

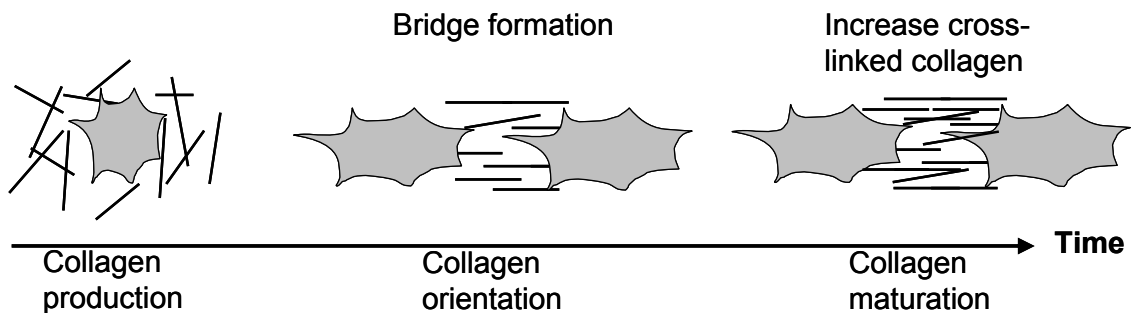


Figure 7.3: Hypothesis on the formation of collagen architecture including random collagen production followed by collagen orientation and maturation.

The developed viable collagen-specific probe opens numerous opportunities for research in the field of collagen formation and remodeling. Using two-photon microscopy, very detailed images of the cells and collagen fibers can be obtained. From these images, early collagen formation and bridge formation of collagen between cells were observed (figure 7.4).

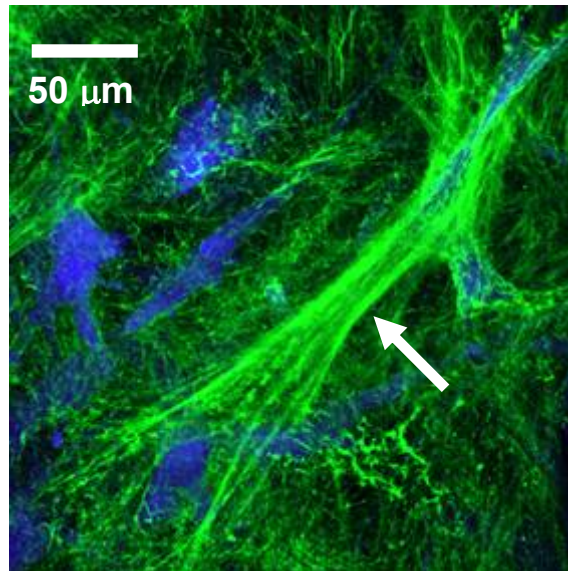


Figure 7.4: Two-photon image showing the myofibroblast cells (blue) and collagen fiber bridge formation (green) between the cells, indicated by the arrow.

To elucidate the mechanisms underlying the formation of these bridges, the probe can be used to image collagen formation in real-time (Boerboom *et al.*, 2007a). The precise role of the cells can be studied by systematically blocking cell-matrix interactions or by inhibiting cytoskeletal and contractile properties, via integrin-blockers and actin-depolymerising agents such as cytochalasin D.

As shown in chapter 3, markers in the culture medium can be measured to estimate the activity of collagen synthesis and degradation (figure 3.5). Visualization of these processes will enhance the understanding of how cells change the orientation of the fibers in response to changing mechanical conditions. Ongoing studies focus on the development of a probe that stains collagen in the presence of active matrix metalloproteinases. An experiment can be performed in which the cells are first strained in one direction, followed by straining in an orthogonal direction. It is hypothesized that the orientation of the cells and collagen fibers will follow this change in straining direction. Real-time visualization of collagen orientation will elucidate how cells synthesize and degrade the collagen structure. To specifically investigate the effect of changing the straining direction by 90°, other factors that could influence collagen orientation, such as contact guidance by the scaffold material, should be quantified. For this purpose, cells in a fibrin gel without a scaffold can be used as model system. The drawback of using fibrin is that it is weaker than PGA and, by implication, less resistant to straining. Moreover, it degrades within several days. The

use of higher fibrin concentrations or fibrin degradation inhibitors can be used to increase the strength of the gel.

In addition to experimental models, numerical studies can be used to understand the effect of mechanical loading and to test the hypotheses regarding collagen remodeling. Previous researchers in the host laboratory numerically studied strain-induced collagen remodeling by discriminating between collagen synthesis and degradation and collagen reorientation (Boerboom *et al.*, 2003; Driessen *et al.*, 2003). Using these computational models, the collagen architecture in the aortic valve and arterial wall were predicted (Driessen *et al.*, 2005). Data from the proposed experimental work are needed to confirm and optimize these models to predict the evolution of collagen architecture and mechanical properties in engineered cardiovascular tissues.

### **Towards native-like tissue composition and organization**

As shown in chapter 4, the engineered tissues contained lower amounts of collagen and cross-links when compared to adult human aortic valves. It can be questioned whether the values extracted from adult human tissue may be required as benchmarks for engineered tissues. Tissue-engineered heart valves and blood vessels may not need to approach adult native tissue to function adequately. A comparison between engineered tissues and pediatric valves and vessels may be more valid. However, such donor tissues are highly limited in their availability.

By contrast to the engineered tissues, mature native cardiovascular tissues exhibit an organized three-layered structure. It has already been demonstrated that ovine tissue-engineered heart valves, implanted at the pulmonary position in juvenile sheep, developed from a homogeneous tissue to the established three-layered structure in 20 weeks under the influence of an active *in vivo* remodeling process (Hoerstrup *et al.*, 2000). We therefore speculate that ultimate tissue remodeling of engineered valves and blood vessels to a three-layered structure will also take place *in vivo*.

To study the effects of mechanical conditioning on tissue properties, the collagen architecture was the primary focus of attention. In native heart valves and blood vessels, elastin is another critical structural and regulatory matrix protein, responsible for tissue flexibility and resilience. Indeed disturbances in the elastin homeostasis in heart valves and arteries are believed to represent an underlying cause of valve replacement failure (Schoof *et al.*, 2006) and the formation of aneurysms (Anidjar *et al.*, 1990). Therefore, elastin formation has been acknowledged as a missing component for a complete biomechanical function of tissue-engineered cardiovascular replacements (Patel *et al.*, 2006). Mechanical conditioning tends to increase elastin synthesis by vascular smooth muscle cells, although the effects are sensitive to straining magnitude and mode (Isenberg and Tranquillo, 2003; Sutcliffe and Davidson, 1990). It should be investigated whether mechanical conditioning leads to an organized elastin network in engineered cardiovascular tissues or whether biochemical cues are also required.

### **Towards functional mechanical properties**

In this thesis, the collagen architecture was related to global tissue mechanical properties, such as ultimate tensile stress and modulus. These parameters provide information on the strength and stiffness of the engineered tissues, in particular at strains that are higher than the physiological strains occurring in valves and vessels. In heart valves, for example, the circumferential strain *in vivo* are of the order of 10% during diastole (Lo and Vesely, 1995; Thubrikar *et al.*, 1980), while the tissues in this thesis were tested in the linear region (in the range of 15-30% strain) of the stress-strain curves. For more appropriate testing and translation of the test results, it would therefore be necessary to also focus on the stiffness and flexibility of the engineered tissues in the *in vivo* strain region (Mirnajafi *et al.*, 2006). For heart valves, this would provide insight into the opening and closing behavior of the valve during the cardiac cycle. Preferably, these functional mechanical parameters should be monitored and controlled during culture in a bioreactor, where mechanical stimuli are well-controlled (Kortsmmit *et al.*, 2009b; Kortsmmit *et al.*, 2009a). To obtain benchmarks for these parameters, mechanical properties of native human tissue should be determined.

## **7.5 Relevance for cardiovascular tissue engineering**

The methods and results of this work are of importance and have impact on tissue engineering strategies. Relevance of these results for mechanical conditioning as a tool in cardiovascular tissue engineering is summarized by the following findings:

- Compared to constrained tissue culture, continuous dynamic strain does not increase the amount of collagen in the tissue.
- Dynamic strain improves the quality of the tissue expressed by enhanced cross-link densities and collagen fiber alignment.
- Intermittent dynamic strain accelerates the production of collagen, cross-links, and collagen fiber alignment.

Based on these findings, the following aspects regarding the conditioning protocol of engineered heart valves and blood vessels should be taken into consideration. The magnitude of strain should be chosen with caution. Native heart valves experience 10% stretch during diastole under normal physiological conditions (Lo and Vesely, 1995; Thubrikar *et al.*, 1980). These physiological amounts of strain are not optimal for conditioning of engineered cardiovascular tissues as the continuous application of these strains reduces the net production of collagen and therefore leads to suboptimal mechanical properties. One approach to overcome this is to slowly increase the dynamic strain magnitude. By changing the magnitude of the stimulus over time the adaptation response of cells might be disrupted (Syedain *et al.*, 2008), thus increasing the effectiveness of the stimulus.

An alternative strategy involves the use of straining mode-dependent effects. Application of intermittent strain can be used to balance collagen production during static conditioning and enhancement of cross-links and alignment during dynamic

conditioning. It is recommended to apply a sequential protocol, according to the hypothesis as shown in figure 7.3. In different phases of the development of the collagen architecture, different modes of conditioning might be required. First static conditioning is needed to enhance collagen production, followed by (intermittent) dynamic conditioning in a later phase to induce cross-links and collagen alignment. The experimental techniques presented in this thesis can be used to optimize these protocols for engineered heart valves and blood vessels. Within this respect, it is important to consider the total tissue architecture, including amount of collagen, cross-link concentration, and fiber orientation, as a focus for creating engineered tissues with sufficient load-bearing capacities.





# References

- Aikawa E., Whittaker P., Farber M., Mendelson K., Padera R.F., Aikawa M., and Schoen F.J. (2006). Human semilunar cardiac valve remodeling by activated cells from fetus to adult: implications for postnatal adaptation, pathology, and tissue engineering. *Circulation*, **113**(10) 1344-1352.
- Anderson R.N. and Smith B.L. (2005). Deaths: leading causes for 2002. *Natl Vital Stat Rep*, **53**(17) 1-89.
- Anidjar S., Salzman J.L., Gentric D., Lagneau P., Camilleri J.P., and Michel J.B. (1990). Elastase-induced experimental aneurysms in rats. *Circulation*, **82**(3) 973-981.
- Aper T., Schmidt A., Duchrow M., and Bruch H.P. (2007). Autologous blood vessels engineered from peripheral blood sample. *Eur J Vasc Endovasc Surg*, **33**(1) 33-39.
- Asanuma K., Magid R., Johnson C., Nerem R.M., and Galis Z.S. (2003). Uniaxial strain upregulates matrix-degrading enzymes produced by human vascular smooth muscle cells. *Am J Physiol Heart Circ Physiol*, **284**(5) H1778-H1784.
- Avery N.C. and Bailey A.J. (2005). Enzymic and non-enzymic cross-linking mechanisms in relation to turnover of collagen: relevance to aging and exercise. *Scand J Med Sci Sports*, **15**(4) 231-240.
- Balachandran K., Konduri S., Sucusky P., Jo H., and Yoganathan A.P. (2006). An ex vivo study of the biological properties of porcine aortic valves in response to circumferential cyclic stretch. *Ann Biomed Eng*, **34**(11) 1655-1665.
- Balguid A., Mol A., Marion M.H.v., Bank R.A., Bouten C.V., and Baaijens F.P. (2008). Tailoring Fiber Diameter in Electrospun Poly (e-Caprolactone) Scaffolds for Optimal Cellular Infiltration in Cardiovascular Tissue Engineering. *Tissue Eng Part A*, **15**(2) 437-444.
- Balguid A., Rubbens M.P., Mol A., Bank R.A., Bogers A.J.J.C., van Kats J.P., de Mol B.A.J.M., Baaijens F.P.T., and Bouten C.V.C. (2007). The role of collagen cross-links in biomechanical behavior of human aortic heart valve leaflets-relevance for tissue engineering. *Tissue Eng*, **13**(7) 1501-1511.
- Bank R.A., Beekman B., Verzijl N., de Roos J.A., Sakkee A.N., and TeKoppele J.M. (1997). Sensitive fluorimetric quantitation of pyridinium and pentosidine crosslinks in biological samples in a single high-performance liquid chromatographic run. *J Chromatogr B Biomed Sci Appl*, **703**(1-2) 37-44.
- Bank R.A., Jansen E.J., Beekman B., and te Koppele J.M. (1996). Amino acid analysis by reverse-phase high-performance liquid chromatography: improved derivatization and detection conditions with 9-fluorenylmethyl chloroformate. *Anal Biochem*, **240**(2) 167-176.
- Banse X., Sims T.J., and Bailey A.J. (2002). Mechanical properties of adult vertebral cancellous bone: correlation with collagen intermolecular cross-links. *J Bone Miner Res*, **17**(9) 1621-1628.
- Barkhausen T., van Griensven M., Zeichen J., and Bosch U. (2003). Modulation of cell functions of human tendon fibroblasts by different repetitive cyclic mechanical stress patterns. *Exp Toxicol Pathol*, **55**(2-3) 153-158.

- Bashey R.I., Torii S., and Angrist A. (1967). Age-related collagen and elastin content of human heart valves. *J Gerontol*, **22**(2) 203-208.
- Beekman B., Verzijl N., Bank R.A., von der M.K., and TeKoppele J.M. (1997). Synthesis of collagen by bovine chondrocytes cultured in alginate; posttranslational modifications and cell-matrix interaction. *Exp Cell Res*, **237**(1) 135-141.
- Berry C.C., Cacou C., Lee D.A., Bader D.L., and Shelton J.C. (2003). Dermal fibroblasts respond to mechanical conditioning in a strain profile dependent manner. *Biorheology*, **40**(1-3) 337-345.
- Bishop J.E. and Lindahl G. (1999). Regulation of cardiovascular collagen synthesis by mechanical load. *Cardiovasc Res*, **42**(1) 27-44.
- Boerboom R.A., Driessen N.J., Bouten C.V., Huyghe J.M., and Baaijens F.P. (2003). Finite element model of mechanically induced collagen fiber synthesis and degradation in the aortic valve. *Ann Biomed Eng*, **31**(9) 1040-1053.
- Boerboom R.A., Krahn K.N., Megens R.T., van Zandvoort M.A., Merckx M., and Bouten C.V. (2007a). High resolution imaging of collagen organisation and synthesis using a versatile collagen specific probe. *J Struct Biol*, **159**(3) 392-399.
- Boerboom R.A., Rubbens M.P., Driessen N.J., Bank R.A., Bouten C.V., and Baaijens F.P. (2007b). Mechano-control of tissue properties in engineered cardiovascular constructs, Chapter 4: Continuous versus intermittent loading of engineered cardiovascular constructs. *PhD thesis Eindhoven University of Technology*.
- Boerboom R.A., Rubbens M.P., Driessen N.J., Bouten C.V., and Baaijens F.P. (2008). Effect of strain magnitude on the tissue properties of engineered cardiovascular constructs. *Ann Biomed Eng*, **36**(2) 244-253.
- Bordenave L., Fernandez P., Remy-Zolghadri M., Villars S., Daculsi R., and Midy D. (2005). In vitro endothelialized ePTFE prostheses: clinical update 20 years after the first realization. *Clin Hemorheol Microcirc*, **33**(3) 227-234.
- Brightman A.O., Rajwa B.P., Sturgis J.E., McCallister M.E., Robinson J.P., and Voytik-Harbin S.L. (2000). Time-lapse confocal reflection microscopy of collagen fibrillogenesis and extracellular matrix assembly in vitro. *Biopolymers*, **54**(3) 222-234.
- Brown M.L., Schaff H.V., Lahr B.D., Mullany C.J., Sundt T.M., Dearani J.A., McGregor C.G., and Orszulak T.A. (2008). Aortic valve replacement in patients aged 50 to 70 years: improved outcome with mechanical versus biologic prostheses. *J Thorac Cardiovasc Surg*, **135**(4) 878-884.
- Brown T.D. (2000). Techniques for mechanical stimulation of cells in vitro: a review. *J Biomech*, **33**(1) 3-14.
- Butt R.P. and Bishop J.E. (1997). Mechanical load enhances the stimulatory effect of serum growth factors on cardiac fibroblast procollagen synthesis. *J Mol Cell Cardiol*, **29**(4) 1141-1151.
- Campagnola P.J., Millard A.C., Terasaki M., Hoppe P.E., Malone C.J., and Mohler W.A. (2002). Three-dimensional high-resolution second-harmonic generation imaging of endogenous structural proteins in biological tissues. *Biophys J*, **82**(1 Pt 1) 493-508.

- Canver C.C. (1995). Conduit options in coronary artery bypass surgery. *Chest*, **108**(4) 1150-1155.
- Cesarone C.F., Bolognesi C., and Santi L. (1979). Improved microfluorometric DNA determination in biological material using 33258 Hoechst. *Anal Biochem*, **100**(1) 188-197.
- Cho S.W., Jeon O., Lim J.E., Gwak S.J., Kim S.S., Choi C.Y., Kim D.I., and Kim B.S. (2006). Preliminary experience with tissue engineering of a venous vascular patch by using bone marrow-derived cells and a hybrid biodegradable polymer scaffold. *J Vasc Surg*, **44**(6) 1329-1340.
- Cho S.W., Park H.J., Ryu J.H., Kim S.H., Kim Y.H., Choi C.Y., Lee M.J., Kim J.S., Jang I.S., Kim D.I., and Kim B.S. (2005). Vascular patches tissue-engineered with autologous bone marrow-derived cells and decellularized tissue matrices. *Biomaterials*, **26**(14) 1915-1924.
- Chowdhury T.T., Bader D.L., Shelton J.C., and Lee D.A. (2003). Temporal regulation of chondrocyte metabolism in agarose constructs subjected to dynamic compression. *Arch Biochem Biophys*, **417**(1) 105-111.
- Christie G.W. and Barratt-Boyes B.G. (1995). Age-dependent changes in the radial stretch of human aortic valve leaflets determined by biaxial testing. *Ann Thorac Surg*, **60**(2 Suppl) S156-S158.
- Clark R.E. (1973). Stress-strain characteristics of fresh and frozen human aortic and mitral leaflets and chordae tendineae. Implications for clinical use. *J Thorac Cardiovasc Surg*, **66**(2) 202-208.
- Costa K.D., Lee E.J., and Holmes J.W. (2003). Creating alignment and anisotropy in engineered heart tissue: role of boundary conditions in a model three-dimensional culture system. *Tissue Eng*, **9**(4) 567-577.
- Cox M.A., Driessen N.J., Bouten C.V., and Baaijens F.P. (2006). Mechanical characterization of anisotropic planar biological soft tissues using large indentation: a computational feasibility study. *J Biomech Eng*, **128**(3) 428-436.
- Cummings C.L., Gawlitta D., Nerem R.M., and Stegemann J.P. (2004). Properties of engineered vascular constructs made from collagen, fibrin, and collagen-fibrin mixtures. *Biomaterials*, **25**(17) 3699-3706.
- Dahl S.L., Rucker R.B., and Niklason L.E. (2005). Effects of copper and cross-linking on the extracellular matrix of tissue-engineered arteries. *Cell Transplant*, **14**(10) 861-868.
- Daniels F., Ter Haar Romeny B.M., Rubbens M.P., and van Assen H. (2006). Quantification of collagen orientation in 3D engineered tissue. *Proc Intern Conf on Biomedical Engineering BioMed 2006*, 344-348.
- Dartsch P.C. and Hammerle H. (1986). Orientation response of arterial smooth muscle cells to mechanical stimulation. *Eur J Cell Biol*, **41**(2) 339-346.
- Dayan D., Hiss Y., Hirshberg A., Bubis J.J., and Wolman M. (1989). Are the polarization colors of picrosirius red-stained collagen determined only by the diameter of the fibers? *Histochemistry*, **93**(1) 27-29.
- de Lange F.J., Moorman A.F., Anderson R.H., Manner J., Soufan A.T., Gier-de Vries C., Schneider M.D., Webb S., van den Hoff M.J., and Christoffels V.M. (2004). Lineage and morphogenetic analysis of the cardiac valves. *Circ Res*, **95**(6) 645-654.

- Doehring T.C., Kahelin M., and Vesely I. (2005). Mesostructures of the aortic valve. *J Heart Valve Dis*, **14**(5) 679-686.
- Driessen N.J., Boerboom R.A., Huyghe J.M., Bouten C.V., and Baaijens F.P. (2003). Computational analyses of mechanically induced collagen fiber remodeling in the aortic heart valve. *J Biomech Eng*, **125**(4) 549-557.
- Driessen N.J., Bouten C.V., and Baaijens F.P. (2005). Improved prediction of the collagen fiber architecture in the aortic heart valve. *J Biomech Eng*, **127**(2) 329-336.
- Eastwood M., Mudera V.C., McGrouther D.A., and Brown R.A. (1998). Effect of precise mechanical loading on fibroblast populated collagen lattices: morphological changes. *Cell Motil Cytoskeleton*, **40**(1) 13-21.
- Elbischger P.J., Bischof H., Regitnig P., and Holzapfel G.A. (2004). Automatic analysis of collagen fiber orientation in the outermost layer of human arteries. *Pattern Anal Applic*, **7**(-) 269-284.
- Elbjeirami W.M., Yonter E.O., Starcher B.C., and West J.L. (2003). Enhancing mechanical properties of tissue-engineered constructs via lysyl oxidase crosslinking activity. *J Biomed Mater Res A*, **66**(3) 513-521.
- Engelmayr G.C., Jr., Rabkin E., Sutherland F.W., Schoen F.J., Mayer J.E., Jr., and Sacks M.S. (2005). The independent role of cyclic flexure in the early in vitro development of an engineered heart valve tissue. *Biomaterials*, **26**(2) 175-187.
- Engelmayr G.C.J., Papworth G.D., Watkins S.C., Mayer J.E.J., and Sacks M.S. (2006). Guidance of engineered tissue collagen orientation by large-scale scaffold microstructures. *J Biomech*, **39**(10) 1819-1831.
- Farndale R.W., Buttle D.J., and Barrett A.J. (1986). Improved quantitation and discrimination of sulphated glycosaminoglycans by use of dimethylmethylene blue. *Biochim Biophys Acta*, **883**(2) 173-177.
- Flanagan T.C., Cornelissen C., Koch S., Tschoeke B., Sachweh J.S., Schmitz-Rode T., and Jockenhoevel S. (2007). The in vitro development of autologous fibrin-based tissue-engineered heart valves through optimised dynamic conditioning. *Biomaterials*, **28**(23) 3388-3397.
- Flanagan T.C., Sachweh J., Frese J., Schnoering H., Gronloh N., Koch S., Tolba R., Schmitz-Rode T., and Jockenhoevel S. (2009). In Vivo Remodelling and Structural Characterisation of Fibrin-Based Tissue-Engineered Heart Valves in the Adult Sheep Model. *Tissue Eng Part A*, in press.
- Frank C., McDonald D., Wilson J., Eyre D., and Shrive N. (1995). Rabbit medial collateral ligament scar weakness is associated with decreased collagen pyridinoline crosslink density. *J Orthop Res*, **13**(2) 157-165.
- Glass-Brudzinski J., Perizzolo D., and Brunette D.M. (2002). Effects of substratum surface topography on the organization of cells and collagen fibers in collagen gel cultures. *J Biomed Mater Res*, **61**(4) 608-618.
- Grande-Allen K.J., Calabro A., Gupta V., Wight T.N., Hascall V.C., and Vesely I. (2004). Glycosaminoglycans and proteoglycans in normal mitral valve leaflets and chordae: association with regions of tensile and compressive loading. *Glycobiology*, **14**(7) 621-633.

- Grenier G., Remy-Zolghadri M., Larouche D., Gauvin R., Baker K., Bergeron F., Dupuis D., Langelier E., Rancourt D., Auger F.A., and Germain L. (2005). Tissue reorganization in response to mechanical load increases functionality. *Tissue Eng*, **11**(1-2) 90-100.
- Grunkemeier G.L. and Rahimtoola S.H. (1990). Artificial heart valves. *Annu Rev Med*, **41**(-) 251-263.
- Hamilton D.W., Maul T.M., and Vorp D.A. (2004). Characterization of the response of bone marrow-derived progenitor cells to cyclic strain: implications for vascular tissue-engineering applications. *Tissue Eng*, **10**(3-4) 361-369.
- Hammermeister K., Sethi G.K., Henderson W.G., Grover F.L., Oprian C., and Rahimtoola S.H. (2000). Outcomes 15 years after valve replacement with a mechanical versus a bioprosthetic valve: final report of the Veterans Affairs randomized trial. *J Am Coll Cardiol*, **36**(4) 1152-1158.
- Haut R.C., Lancaster R.L., and DeCamp C.E. (1992). Mechanical properties of the canine patellar tendon: some correlations with age and the content of collagen. *J Biomech*, **25**(2) 163-173.
- Hoerstrup S.P., Cummings M., I, Lachat M., Schoen F.J., Jenni R., Leschka S., Neuenschwander S., Schmidt D., Mol A., Gunter C., Gossi M., Genoni M., and Zund G. (2006). Functional growth in tissue-engineered living, vascular grafts: follow-up at 100 weeks in a large animal model. *Circulation*, **114**(1 Suppl) I159-I166.
- Hoerstrup S.P., Kadner A., Breymann C., Maurus C.F., Guenter C.I., Sodian R., Visjager J.F., Zund G., and Turina M.I. (2002a). Living, autologous pulmonary artery conduits tissue engineered from human umbilical cord cells. *Ann Thorac Surg*, **74**(1) 46-52.
- Hoerstrup S.P., Sodian R., Daebritz S., Wang J., Bacha E.A., Martin D.P., Moran A.M., Guleserian K.J., Sperling J.S., Kaushal S., Vacanti J.P., Schoen F.J., and Mayer J.E., Jr. (2000). Functional living trileaflet heart valves grown in vitro. *Circulation*, **102**(19 Suppl 3) III44-III49.
- Hoerstrup S.P., Zund G., Cheng S., Melnitchouk S., Kadner A., Sodian R., Kolb S.A., and Turina M. (2002b). A new approach to completely autologous cardiovascular tissue in humans. *ASAIO J*, **48**(3) 234-238.
- Hoffman J.I. and Kaplan S. (2002). The incidence of congenital heart disease. *J Am Coll Cardiol*, **39**(12) 1890-1900.
- Hopkins R.A. (2005). Tissue engineering of heart valves: decellularized valve scaffolds. *Circulation*, **111**(21) 2712-2714.
- Iba T. and Sumpio B.E. (1991). Morphological response of human endothelial cells subjected to cyclic strain in vitro. *Microvasc Res*, **42**(3) 245-254.
- Isenberg B.C. and Tranquillo R.T. (2003). Long-term cyclic distention enhances the mechanical properties of collagen-based media-equivalents. *Ann Biomed Eng*, **31**(8) 937-949.
- Jamieson W.R. (1993). Modern cardiac valve devices--bioprostheses and mechanical prostheses: state of the art. *J Card Surg*, **8**(1) 89-98.
- Jeong S.I., Kwon J.H., Lim J.I., Cho S.W., Jung Y., Sung W.J., Kim S.H., Kim Y.H., Lee Y.M., Kim B.S., Choi C.Y., and Kim S.J. (2005). Mechano-active tissue engineering of vascular smooth muscle using pulsatile perfusion bioreactors and elastic PLCL scaffolds. *Biomaterials*, **26**(12) 1405-1411.

- Jockenhoevel S., Zund G., Hoerstrup S.P., Chalabi K., Sachweh J.S., Demircan L., Messmer B.J., and Turina M. (2001). Fibrin gel -- advantages of a new scaffold in cardiovascular tissue engineering. *Eur J Cardiothorac Surg*, **19**(4) 424-430.
- Kadler K.E., Holmes D.F., Trotter J.A., and Chapman J.A. (1996). Collagen fibril formation. *Biochem J*, **316**(1) 1-11.
- Karlon W.J., Covell J.W., McCulloch A.D., Hunter J.J., and Omens J.H. (1998). Automated measurement of myofiber disarray in transgenic mice with ventricular expression of ras. *Anat Rec*, **252**(4) 612-625.
- Karlon W.J., Hsu P.P., Li S., Chien S., McCulloch A.D., and Omens J.H. (1999). Measurement of orientation and distribution of cellular alignment and cytoskeletal organization. *Ann Biomed Eng*, **27**(6) 712-720.
- Kim B.S. and Mooney D.J. (2000). Scaffolds for engineering smooth muscle under cyclic mechanical strain conditions. *J Biomech Eng*, **122**(3) 210-215.
- Kim S.S., Lim S.H., Hong Y.S., Cho S.W., Ryu J.H., Chang B.C., Choi C.Y., and Kim B.S. (2006). Tissue engineering of heart valves in vivo using bone marrow-derived cells. *Artif Organs*, **30**(7) 554-557.
- Kolpakov V., Rekhter M.D., Gordon D., Wang W.H., and Kulik T.J. (1995). Effect of mechanical forces on growth and matrix protein synthesis in the in vitro pulmonary artery. Analysis of the role of individual cell types. *Circ Res*, **77**(4) 823-831.
- Konduri S., Xing Y., Warnock J.N., He Z., and Yoganathan A.P. (2005). Normal physiological conditions maintain the biological characteristics of porcine aortic heart valves: an ex vivo organ culture study. *Ann Biomed Eng*, **33**(9) 1158-1166.
- Konig K. and Riemann I. (2003). High-resolution multiphoton tomography of human skin with subcellular spatial resolution and picosecond time resolution. *J Biomed Opt*, **8**(3) 432-439.
- Kortsmit J., Driessen N.J., Rutten M.C., and Baaijens F.P. (2009a). Real time, non-invasive assessment of leaflet deformation in heart valve tissue engineering. *Ann Biomed Eng*, **37**(3) 532-541.
- Kortsmit J., Rutten M., Wijlaars M., and Baaijens F. (2009b). Deformation controlled load application in heart valve tissue-engineering. *Tissue Eng Part C Methods*, in press.
- Kostyuk O. and Brown R.A. (2004). Novel spectroscopic technique for in situ monitoring of collagen fibril alignment in gels. *Biophys J*, **87**(1) 648-655.
- Krahn K.N., Bouten C.V.C., van Tuijl S., van Zandvoort M.A.M.J., and Merckx M. (2006). Fluorescently labeled collagen binding proteins allow specific visualization of collagen in tissues and live cell culture. *Anal Biochem*, **350**(2) 177-185.
- Ku C.H., Johnson P.H., Batten P., Sarathchandra P., Chambers R.C., Taylor P.M., Yacoub M.H., and Chester A.H. (2006). Collagen synthesis by mesenchymal stem cells and aortic valve interstitial cells in response to mechanical stretch. *Cardiovasc Res*, **71**(3) 548-556.
- Kunzelman K.S., Cochran R.P., Murphree S.S., Ring W.S., Verrier E.D., and Eberhart R.C. (1993). Differential collagen distribution in the mitral valve and its influence on biomechanical behaviour. *J Heart Valve Dis*, **2**(2) 236-244.

- Langer R. and Vacanti J.P. (1993). Tissue engineering. *Science*, **260**(5110) 920-926.
- Lee A.A., Delhaas T., Waldman L.K., MacKenna D.A., Villarreal F.J., and McCulloch A.D. (1996). An equibiaxial strain system for cultured cells. *Am J Physiol*, **271**(4 Pt 1) C1400-C1408.
- Lindeman J.H.N., Hanemaaijer R., Mulder A., Dijkstra P.D.S., Szuhai K., Bromme D., Verheijen J.H., and Hogendoorn P.C.W. (2004). Cathepsin K is the principal protease in giant cell tumor of bone. *Am J Pathol*, **165**(2) 593-600.
- Lis Y., Burleigh M.C., Parker D.J., Child A.H., Hogg J., and Davies M.J. (1987). Biochemical characterization of individual normal, floppy and rheumatic human mitral valves. *Biochem J*, **244**(3) 597-603.
- Liu J.Y., Swartz D.D., Peng H.F., Gugino S.F., Russell J.A., and Andreadis S.T. (2007). Functional tissue-engineered blood vessels from bone marrow progenitor cells. *Cardiovasc Res*, **75**(3) 618-628.
- Lo D. and Vesely I. (1995). Biaxial strain analysis of the porcine aortic valve. *Ann Thorac Surg*, **60**(2 Suppl) S374-S378.
- Lund O. and Bland M. (2006). Risk-corrected impact of mechanical versus bioprosthetic valves on long-term mortality after aortic valve replacement. *J Thorac Cardiovasc Surg*, **132**(1) 20-26.
- MacKenna D., Summerour S.R., and Villarreal F.J. (2000). Role of mechanical factors in modulating cardiac fibroblast function and extracellular matrix synthesis. *Cardiovasc Res*, **46**(2) 257-263.
- Matsumura G., Hibino N., Ikada Y., Kurosawa H., and Shin'oka T. (2003). Successful application of tissue engineered vascular autografts: clinical experience. *Biomaterials*, **24**(13) 2303-2308.
- Mayer J.E.J. (1995). Uses of homograft conduits for right ventricle to pulmonary artery connections in the neonatal period. *Semin Thorac Cardiovasc Surg*, **7**(3) 130-132.
- McDonald P.C., Wilson J.E., McNeill S., Gao M., Spinelli J.J., Rosenberg F., Wiebe H., and McManus B.M. (2002). The challenge of defining normality for human mitral and aortic valves: geometrical and compositional analysis. *Cardiovasc Pathol*, **11**(4) 193-209.
- Merryman W.D., Youn I., Lukoff H.D., Krueger P.M., Guilak F., Hopkins R.A., and Sacks M.S. (2006). Correlation between heart valve interstitial cell stiffness and transvalvular pressure: implications for collagen biosynthesis. *Am J Physiol Heart Circ Physiol*, **290**(1) H224-H231.
- Messier R.H., Jr., Bass B.L., Aly H.M., Jones J.L., Domkowski P.W., Wallace R.B., and Hopkins R.A. (1994). Dual structural and functional phenotypes of the porcine aortic valve interstitial population: characteristics of the leaflet myofibroblast. *J Surg Res*, **57**(1) 1-21.
- Mikos A.G., Herring S.W., Ochareon P., Elisseeff J., Lu H.H., Kandel R., Schoen F.J., Toner M., Mooney D., Atala A., Van Dyke M.E., Kaplan D., and Vunjak-Novakovic G. (2006). Engineering complex tissues. *Tissue Eng*, **12**(12) 3307-3339.
- Mirnajafi A., Raymer J.M., McClure L.R., and Sacks M.S. (2006). The flexural rigidity of the aortic valve leaflet in the commissural region. *J Biomech*, **39**(16) 2966-2973.



- Mol A., Bouten C.V., Zund G., Gunter C.I., Visjager J.F., Turina M.I., Baaijens F.P., and Hoerstrup S.P. (2003). The relevance of large strains in functional tissue engineering of heart valves. *Thorac Cardiovasc Surg*, **51**(2) 78-83.
- Mol A., Driessen N.J., Rutten M.C., Hoerstrup S.P., Bouten C.V., and Baaijens F.P. (2005a). Tissue engineering of human heart valve leaflets: a novel bioreactor for a strain-based conditioning approach. *Ann Biomed Eng*, **33**(12) 1778-1788.
- Mol A. and Hoerstrup S.P. (2004). Heart valve tissue engineering -- where do we stand? *Int J Cardiol*, **95**(1) S57-S58.
- Mol A., Rutten M.C., Driessen N.J., Bouten C.V., Zund G., Baaijens F.P., and Hoerstrup S.P. (2006). Autologous human tissue-engineered heart valves: prospects for systemic application. *Circulation*, **114**(1 Suppl) I152-I158.
- Mol A., van Lieshout M.I., Dam-de Veen C.G., Neuenschwander S., Hoerstrup S.P., Baaijens F.P., and Bouten C.V. (2005b). Fibrin as a cell carrier in cardiovascular tissue engineering applications. *Biomaterials*, **26**(16) 3113-3121.
- Neidert M.R. and Tranquillo R.T. (2006). Tissue-engineered valves with commissural alignment. *Tissue Eng*, **12**(4) 891-903.
- Neidlinger-Wilke C., Grood E.S., Brand R.A., and Claes L. (2001). Cell alignment is induced by cyclic changes in cell length: studies of cells grown in cyclically stretched substrates. *J Orthop Res*, **19**(2) 286-293.
- Neuman R.E. and Logan M.A. (1950). The determination of collagen and elastin in tissues. *J Biol Chem*, **186**(2) 549-556.
- Nieponice A., Maul T.M., Cumer J.M., Soletti L., and Vorp D.A. (2007). Mechanical stimulation induces morphological and phenotypic changes in bone marrow-derived progenitor cells within a three-dimensional fibrin matrix. *J Biomed Mater Res A*, **81**(3) 523-530.
- Niessen W.J., López A.M., Van Enk W.J., van Roermund P.M., Ter Haar Romeny B.M., and Viergever M.A. (1997). In vivo analysis of trabecular bone architecture. *Lecture Notes In Computer Science*, **1230**(-) 435-440.
- Niklason L.E., Gao J., Abbott W.M., Hirschi K.K., Houser S., Marini R., and Langer R. (1999). Functional arteries grown in vitro. *Science*, **284**(5413) 489-493.
- O'Callaghan C.J. and Williams B. (2002). The regulation of human vascular smooth muscle extracellular matrix protein production by alpha- and beta-adrenoceptor stimulation. *J Hypertens*, **20**(2) 287-294.
- Ottani V., Raspanti M., and Ruggeri A. (2001). Collagen structure and functional implications. *Micron*, **32**(3) 251-260.
- Patel A., Fine B., Sandig M., and Mequanint K. (2006). Elastin biosynthesis: The missing link in tissue-engineered blood vessels. *Cardiovasc Res*, **71**(1) 40-49.
- Pickering J.G. and Boughner D.R. (1991). Quantitative assessment of the age of fibrotic lesions using polarized light microscopy and digital image analysis. *Am J Pathol*, **138**(5) 1225-1231.

- Puvimanasinghe J.P., Steyerberg E.W., Takkenberg J.J., Eijkemans M.J., van Herwerden L.A., Bogers A.J., and Habbema J.D. (2001). Prognosis after aortic valve replacement with a bioprosthesis: predictions based on meta-analysis and microsimulation. *Circulation*, **103**(11) 1535-1541.
- Rabau M.Y. and Dayan D. (1994). Polarization microscopy of picrosirius red stained sections: a useful method for qualitative evaluation of intestinal wall collagen. *Histol Histopathol*, **9**(3) 525-528.
- Rabkin E. and Schoen F.J. (2002). Cardiovascular tissue engineering. *Cardiovasc Pathol*, **11**(6) 305-317.
- Rabkin-Aikawa E., Farber M., Aikawa M., and Schoen F.J. (2004). Dynamic and reversible changes of interstitial cell phenotype during remodeling of cardiac valves. *J Heart Valve Dis*, **13**(5) 841-847.
- Raja S.G., Haider Z., Ahmad M., and Zaman H. (2004). Saphenous vein grafts: to use or not to use? *Heart Lung Circ*, **13**(4) 403-409.
- Robins S.P., Duncan A., Wilson N., and Evans B.J. (1996). Standardization of pyridinium crosslinks, pyridinoline and deoxypyridinoline, for use as biochemical markers of collagen degradation. *Clin Chem*, **42**(10) 1621-1626.
- Robling A.G., Hinant F.M., Burr D.B., and Turner C.H. (2002). Improved bone structure and strength after long-term mechanical loading is greatest if loading is separated into short bouts. *J Bone Miner Res*, **17**(8) 1545-1554.
- Rosamond W., Flegal K., Furie K., Go A., Greenlund K., Haase N., Hailpern S.M., Ho M., Howard V., Kissela B., Kittner S., Lloyd-Jones D., McDermott M., Meigs J., Moy C., Nichol G., O'Donnell C., Roger V., Sorlie P., Steinberger J., Thom T., Wilson M., and Hong Y. (2008). Heart disease and stroke statistics--2008 update: a report from the American Heart Association Statistics Committee and Stroke Statistics Subcommittee. *Circulation*, **117**(4) e25-146.
- Rosamond W., Flegal K., and Friday G. (2007). et al. Heart disease and stroke statistics--2007 update: a report from the American Heart Association Statistics Committee and Stroke Statistics Subcommittee. *Circulation*, **115**(5) e69-171.
- Rubbens M.P., Driessen-Mol A., Boerboom R.A., Koppert M.M., van Assen H.C., TerHaar Romeny B.M., Baaijens F.P., and Bouten C.V. (2009a). Quantification of the temporal evolution of collagen orientation in mechanically conditioned engineered cardiovascular tissues. *Ann Biomed Eng*, **37**(7) 1263-1272.
- Rubbens M.P., Mol A., Boerboom R.A., Bank R.A., Baaijens F.P., and Bouten C.V. (2009b). Intermittent Straining Accelerates the Development of Tissue Properties in Engineered Heart Valve Tissue. *Tissue Eng Part A*, **15**(5) 999-1008.
- Rubbens M.P., Mol A., van Marion M.H., Hanemaaijer R., Bank R.A., Baaijens F.P., and Bouten C.V. (2009c). Straining mode-dependent collagen remodeling in engineered cardiovascular tissue. *Tissue Eng Part A*, **15**(4) 841-849.
- Sabik J.F., III, Lytle B.W., Blackstone E.H., Houghtaling P.L., and Cosgrove D.M. (2005). Comparison of saphenous vein and internal thoracic artery graft patency by coronary system. *Ann Thorac Surg*, **79**(2) 544-551.

- Sabik J.F., Blackstone E.H., Gillinov A.M., Smedira N.G., and Lytle B.W. (2006). Occurrence and risk factors for reintervention after coronary artery bypass grafting. *Circulation*, **114**(1 Suppl) I454-I460.
- Sauren A.A., Kuijpers W., van Steenhoven A.A., and Veldpaus F.E. (1980). Aortic valve histology and its relation with mechanics-preliminary report. *J Biomech*, **13**(2) 97-104.
- Sawhney R.K. and Howard J. (2002). Slow local movements of collagen fibers by fibroblasts drive the rapid global self-organization of collagen gels. *J Cell Biol*, **157**(6) 1083-1091.
- Schenke-Layland K. (2008). Non-invasive multiphoton imaging of extracellular matrix structures. *J Biophotonics*, **1**(6) 451-462.
- Schenke-Layland K., Riemann I., Opitz F., Konig K., Halbhuber K.J., and Stock U.A. (2004). Comparative study of cellular and extracellular matrix composition of native and tissue engineered heart valves. *Matrix Biol*, **23**(2) 113-125.
- Schnell A.M., Hoerstrup S.P., Zund G., Kolb S., Sodian R., Visjager J.F., Grunfelder J., Suter A., and Turina M. (2001). Optimal cell source for cardiovascular tissue engineering: venous vs. aortic human myofibroblasts. *Thorac Cardiovasc Surg*, **49**(4) 221-225.
- Schoen F.J. (1997). Aortic valve structure-function correlations: role of elastic fibers no longer a stretch of the imagination. *J Heart Valve Dis*, **6**(1) 1-6.
- Schoen F.J. and Levy R.J. (1999). Founder's Award, 25th Annual Meeting of the Society for Biomaterials, perspectives. Providence, RI, April 28-May 2, 1999. Tissue heart valves: current challenges and future research perspectives. *J Biomed Mater Res*, **47**(4) 439-465.
- Schoof P.H., Takkenberg J.J., van Suylen R.J., Zondervan P.E., Hazekamp M.G., Dion R.A., and Bogers A.J. (2006). Degeneration of the pulmonary autograft: an explant study. *J Thorac Cardiovasc Surg*, **132**(6) 1426-1432.
- Scott J.E. and Parry D.A. (1992). Control of collagen fibril diameters in tissues. *Int J Biol Macromol*, **14**(5) 292-293.
- Seliktar D., Black R.A., Vito R.P., and Nerem R.M. (2000). Dynamic mechanical conditioning of collagen-gel blood vessel constructs induces remodeling in vitro. *Ann Biomed Eng*, **28**(4) 351-362.
- Seliktar D., Nerem R.M., and Galis Z.S. (2001). The role of matrix metalloproteinase-2 in the remodeling of cell-seeded vascular constructs subjected to cyclic strain. *Ann Biomed Eng*, **29**(11) 923-934.
- Seliktar D., Nerem R.M., and Galis Z.S. (2003). Mechanical strain-stimulated remodeling of tissue-engineered blood vessel constructs. *Tissue Eng*, **9**(4) 657-666.
- Senthilnathan V., Treasure T., Grunkemeier G., and Starr A. (1999). Heart valves: which is the best choice? *Cardiovasc Surg*, **7**(4) 393-397.
- Shin'oka T., Imai Y., and Ikada Y. (2001). Transplantation of a tissue-engineered pulmonary artery. *N Engl J Med*, **344**(7) 532-533.

- Shinoka T., Breuer C.K., Tanel R.E., Zund G., Miura T., Ma P.X., Langer R., Vacanti J.P., and Mayer J.E., Jr. (1995). Tissue engineering heart valves: valve leaflet replacement study in a lamb model. *Ann Thorac Surg*, **60**(6 Suppl) S513-S516.
- Shinoka T., Ma P.X., Shum-Tim D., Breuer C.K., Cusick R.A., Zund G., Langer R., Vacanti J.P., and Mayer J.E., Jr. (1996). Tissue-engineered heart valves. Autologous valve leaflet replacement study in a lamb model. *Circulation*, **94**(9 Suppl) II164-II168.
- Shinoka T., Shum-Tim D., Ma P.X., Tanel R.E., Isogai N., Langer R., Vacanti J.P., and Mayer J.E., Jr. (1998). Creation of viable pulmonary artery autografts through tissue engineering. *J Thorac Cardiovasc Surg*, **115**(3) 536-545.
- Snowden J.M. (1982). The stabilization of in vivo assembled collagen fibrils by proteoglycans/glycosaminoglycans. *Biochim Biophys Acta*, **703**(1) 21-25.
- Sodian R., Hoerstrup S.P., Sperling J.S., Daebritz S., Martin D.P., Moran A.M., Kim B.S., Schoen F.J., Vacanti J.P., and Mayer J.E., Jr. (2000a). Early in vivo experience with tissue-engineered trileaflet heart valves. *Circulation*, **102**(19 Suppl 3) III22-III29.
- Sodian R., Hoerstrup S.P., Sperling J.S., Daebritz S.H., Martin D.P., Schoen F.J., Vacanti J.P., and Mayer J.E., Jr. (2000b). Tissue engineering of heart valves: in vitro experiences. *Ann Thorac Surg*, **70**(1) 140-144.
- Sodian R., Sperling J.S., Martin D.P., Stock U., Mayer J.E., Jr., and Vacanti J.P. (1999). Tissue engineering of a trileaflet heart valve-early in vitro experiences with a combined polymer. *Tissue Eng*, **5**(5) 489-494.
- Stadelmann W.K., Digenis A.G., and Tobin G.R. (1998). Physiology and healing dynamics of chronic cutaneous wounds. *Am J Surg*, **176**(2A Suppl) 26S-38S.
- Stanley A.G., Patel H., Knight A.L., and Williams B. (2000). Mechanical strain-induced human vascular matrix synthesis: the role of angiotensin II. *J Renin Angiotensin Aldosterone Syst*, **1**(1) 32-35.
- Stegemann J.P. and Nerem R.M. (2003). Phenotype modulation in vascular tissue engineering using biochemical and mechanical stimulation. *Ann Biomed Eng*, **31**(4) 391-402.
- Steinhoff G., Stock U., Karim N., Mertsching H., Timke A., Meliss R.R., Pethig K., Haverich A., and Bader A. (2000). Tissue engineering of pulmonary heart valves on allogenic acellular matrix conduits: in vivo restoration of valve tissue. *Circulation*, **102**(19 Suppl 3) III50-III55.
- Stekelenburg M., Rutten M.C., Snoeckx L.H., and Baaijens F.P. (2009). Dynamic Straining Combined with Fibrin Gel Cell Seeding Improves Strength of Tissue-Engineered Small-Diameter Vascular Grafts. *Tissue Eng Part A*, **15**(5) 1081-1089.
- Stradins P., Lacis R., Ozolanta I., Purina B., Ose V., Feldmane L., and Kasyanov V. (2004). Comparison of biomechanical and structural properties between human aortic and pulmonary valve. *Eur J Cardiothorac Surg*, **26**(3) 634-639.
- Sutcliffe M.C. and Davidson J.M. (1990). Effect of static stretching on elastin production by porcine aortic smooth muscle cells. *Matrix*, **10**(3) 148-153.

- Sutherland F.W., Perry T.E., Yu Y., Sherwood M.C., Rabkin E., Masuda Y., Garcia G.A., McLellan D.L., Engelmayr G.C., Jr., Sacks M.S., Schoen F.J., and Mayer J.E., Jr. (2005). From stem cells to viable autologous semilunar heart valve. *Circulation*, **111**(21) 2783-2791.
- Swartz D.D., Russell J.A., and Andreadis S.T. (2005). Engineering of fibrin-based functional and implantable small-diameter blood vessels. *Am J Physiol Heart Circ Physiol*, **288**(3) H1451-H1460.
- Syedain Z.H., Weinberg J.S., and Tranquillo R.T. (2008). Cyclic distension of fibrin-based tissue constructs: evidence of adaptation during growth of engineered connective tissue. *Proc Natl Acad Sci U S A*, **105**(18) 6537-6542.
- Taylor P.M., Batten P., Brand N.J., Thomas P.S., and Yacoub M.H. (2003). The cardiac valve interstitial cell. *Int J Biochem Cell Biol*, **35**(2) 113-118.
- Ter Haar Romeny B.M. (2003). Front-end vision and multi-scale image analysis. *Series on Computational Imaging and Vision*, Springer Verlag.
- Thomopoulos S., Fomovsky G.M., and Holmes J.W. (2005). The development of structural and mechanical anisotropy in fibroblast populated collagen gels. *J Biomech Eng*, **127**(5) 742-750.
- Thubrikar M., Piepgrass W.C., Bosher L.P., and Nolan S.P. (1980). The elastic modulus of canine aortic valve leaflets in vivo and in vitro. *Circ Res*, **47**(5) 792-800.
- Tower T.T. and Tranquillo R.T. (2001a). Alignment maps of tissues: I. Microscopic elliptical polarimetry. *Biophys J*, **81**(5) 2954-2963.
- Tower T.T. and Tranquillo R.T. (2001b). Alignment maps of tissues: II. Fast harmonic analysis for imaging. *Biophys J*, **81**(5) 2964-2971.
- van der Slot A.J., Zuurmond A.M., Bardoel A.F., Wijmenga C., Pruijs H.E., Sillence D.O., Brinckmann J., Abraham D.J., Black C.M., Verzijl N., DeGroot J., Hanemaaijer R., TeKoppele J.M., Huizinga T.W., and Bank R.A. (2003). Identification of PLOD2 as telopeptide lysyl hydroxylase, an important enzyme in fibrosis. *J Biol Chem*, **278**(42) 40967-40972.
- Vara D.S., Salacinski H.J., Kannan R.Y., Bordenave L., Hamilton G., and Seifalian A.M. (2005). Cardiovascular tissue engineering: state of the art. *Pathol Biol (Paris)*, **53**(10) 599-612.
- Vesely I. (1998). The role of elastin in aortic valve mechanics. *J Biomech*, **31**(2) 115-123.
- Voytik-Harbin S.L., Rajwa B., and Robinson J.P. (2001). Three-dimensional imaging of extracellular matrix and extracellular matrix-cell interactions. *Methods Cell Biol*, **63**(-) 583-597.
- Wang J.H., Goldschmidt-Clermont P., Wille J., and Yin F.C. (2001). Specificity of endothelial cell reorientation in response to cyclic mechanical stretching. *J Biomech*, **34**(12) 1563-1572.
- Wang J.H.C., Jia F., Gilbert T.W., and Woo S.L.Y. (2003). Cell orientation determines the alignment of cell-produced collagenous matrix. *J Biomech*, **36**(1) 97-102.
- Watanabe M., Shin'oka T., Tohyama S., Hibino N., Konuma T., Matsumura G., Kosaka Y., Ishida T., Imai Y., Yamakawa M., Ikada Y., and Morita S. (2001). Tissue-engineered vascular autograft: inferior vena cava replacement in a dog model. *Tissue Eng*, **7**(4) 429-439.

- Webb A.R., Yang J., and Ameer G.A. (2004). Biodegradable polyester elastomers in tissue engineering. *Expert Opin Biol Ther*, **4**(6) 801-812.
- Weickert J. (1999). Coherence-enhancing diffusion filtering. *Int J Comp Vision*, **31**(-) 111-127.
- Weston M.W. and Yoganathan A.P. (2001). Biosynthetic activity in heart valve leaflets in response to in vitro flow environments. *Ann Biomed Eng*, **29**(9) 752-763.
- Winter L.C., Walboomers X.F., Bumgardner J.D., and Jansen J.A. (2003). Intermittent versus continuous stretching effects on osteoblast-like cells in vitro. *J Biomed Mater Res A*, **67**(4) 1269-1275.
- Wu J., Rajwa B., Filmer D.L., Hoffmann C.M., Yuan B., Chiang C., Sturgis J., and Robinson J.P. (2003a). Automated quantification and reconstruction of collagen matrix from 3D confocal datasets. *J Microsc*, **210**(Pt 2) 158-165.
- Wu J., Rajwa B., Filmer D.L., Hoffmann C.M., Yuan B., Chiang C.S., Sturgis J., and Robinson J.P. (2003b). Analysis of orientations of collagen fibers by novel fiber-tracking software. *Microsc Microanal*, **9**(6) 574-580.
- Xing Y., He Z., Warnock J.N., Hilbert S.L., and Yoganathan A.P. (2004a). Effects of constant static pressure on the biological properties of porcine aortic valve leaflets. *Ann Biomed Eng*, **32**(4) 555-562.
- Xing Y., Warnock J.N., He Z., Hilbert S.L., and Yoganathan A.P. (2004b). Cyclic pressure affects the biological properties of porcine aortic valve leaflets in a magnitude and frequency dependent manner. *Ann Biomed Eng*, **32**(11) 1461-1470.
- Yacoub M.H., Kilner P.J., Birks E.J., and Misfeld M. (1999). The aortic outflow and root: a tale of dynamism and crosstalk. *Ann Thorac Surg*, **68**(3 Suppl) S37-S43.
- Yacoub M.H. and Takkenberg J.J. (2005). Will heart valve tissue engineering change the world? *Nat Clin Pract Cardiovasc Med*, **2**(2) 60-61.
- Yang G., Crawford R.C., and Wang J.H. (2004). Proliferation and collagen production of human patellar tendon fibroblasts in response to cyclic uniaxial stretching in serum-free conditions. *J Biomech*, **37**(10) 1543-1550.
- Yang J.H., Briggs W.H., Libby P., and Lee R.T. (1998). Small mechanical strains selectively suppress matrix metalloproteinase-1 expression by human vascular smooth muscle cells. *J Biol Chem*, **273**(11) 6550-6555.
- Zar J.H. (1999). Biostatistical analysis, Prentice-Hall, Inc. 4th edition. 592-594.
- Zipfel W.R., Williams R.M., Christie R., Nikitin A.Y., Hyman B.T., and Webb W.W. (2003). Live tissue intrinsic emission microscopy using multiphoton-excited native fluorescence and second harmonic generation. *Proc Natl Acad Sci U S A*, **100**(12) 7075-7080.



# Samenvatting

De huidige prothesen die gebruikt worden voor de vervanging van hartkleppen bestaan uit niet-levende materialen, waardoor ze niet in staat zijn mee te groeien met de patiënt. Hierdoor zijn verscheidende heroperaties noodzakelijk om de hartklep te vervangen door een groter exemplaar. Tevens is er een grote behoefte aan levende bloedvatprothesen die de beperkingen van bestaande bloedvatvervangingen verhelpen. Cardiovasculaire tissue engineering richt zich op de productie van levende hartkleppen en bloedvaten die in staat zijn mee te groeien, zich aan te passen en te remodelleren. Kort samengevat worden de cellen van een patiënt op een biologisch afbreekbare mal, ofwel een scaffold, gezaaid. Deze gezaaide scaffold wordt vervolgens in een bioreactor geplaatst, waar mechanische en biochemische conditioneringsprotocollen worden gebruikt om de ontwikkeling van weefsel te stimuleren. Na enkele weken in een bioreactor is de oorspronkelijke mal verdwenen en vervangen door weefsel dat geproduceerd is door de cellen van de patiënt zelf. De gevormde weefsels kunnen dan geïmplant worden om de niet-functionerende weefsels in de patiënt te vervangen.

Om goed te kunnen functioneren moeten deze getissue-engineerde weefsels structuren bevatten die sterk genoeg zijn om de (veranderingen in) drukken te weerstaan die in het lichaam optreden. De mechanische sterkte van hartkleppen en bloedvaten wordt grotendeels bepaald door een sterk georganiseerd netwerk van collageenvezels. De collageenarchitectuur is gerelateerd aan de belastingsconditie van het weefsel. Mechanische conditionering wordt daarom ook beschouwd als een belangrijke strategie om getissue-engineerde weefsels te maken met de gewenste structuur en mechanische eigenschappen.

In dit proefschrift is het effect onderzocht van mechanische belasting op de collageenarchitectuur in getissue-engineerde weefsels. Drie belangrijke aspecten van de collageenarchitectuur zijn gekwantificeerd: de hoeveelheid collageen, de collageen cross-linkconcentratie en de oriëntatie van de collageenvezels. Om deze effecten systematisch te onderzoeken is gebruik gemaakt van een modelsysteem, gebaseerd op protocollen voor tissue engineering van hartkleppen en bloedvaten. Het modelweefsel bestaat uit rechthoekige strips van een biologisch afbreekbaar polymeer die gezaaid worden met humane vasculaire cellen. Het voordeel van dit modelsysteem is dat er minder cellen nodig zijn en meerdere tests tegelijkertijd uitgevoerd kunnen worden. Bovendien wordt de belasting op een gecontroleerde manier opgelegd. Statische belasting wordt opgelegd door de uiteinden van deze strips vast te zetten. Met behulp van een geoptimaliseerd reksysteem zijn de strips tevens aan dynamische (4%, 1Hz, gedurende 10 dagen en 4 weken) of intermitterend (3 uur aan/uit, 4%, 1Hz, gedurende 2, 3 en 4 weken) belastingsprotocollen onderworpen.

Het temporele effect van statische en dynamische belasting gedurende 10 dagen is bepaald op basis van genexpressie- en eiwitanalyses. Beide conditioneringsprotocollen verhogen de collageenhoeveelheid en cross-linkconcentraties in de tijd op zowel genexpressie- als op eiwitniveau. Dynamische belasting resulteert in lagere



collageenwaarden, maar in hogere cross-linkconcentraties in vergelijking met statische belasting.

Om tevens het effect van belasting op de mechanische eigenschappen van de weefsels te onderzoeken, zijn de weefsels 4 weken gekweekt. Na 4 weken is de initiële scaffold afgebroken en wordt de mechanische integriteit van het weefsel volledig bepaald door het nieuw gevormde weefsel. Dynamische belasting resulteert in vergelijkbare collageenhoeveelheden en in hogere cross-linkconcentraties vergeleken met statische belasting. Deze verhoging in cross-links correleert met verbeterde mechanische eigenschappen van het weefsel. Hiermee wordt aangetoond dat bij een gelijke collageenhoeveelheid in het weefsel de kwaliteit van het weefsel verbeterd kan worden met behulp van dynamische belasting door een verhoging van de cross-linkconcentratie.

Een nieuwe niet-destructieve techniek, gebaseerd op 3D visualisatie met behulp van twee-photon microscopie, gecombineerd met beeldanalyse, is ontwikkeld om de collageenvezeloriëntaties te kwantificeren. Deze analyses tonen aan dat de collageenvezels zich door mechanisch conditioneren in de belastingsrichting gaan richten. Intermittent belasting resulteert het snelst in het meest georiënteerde netwerk van de collageenvezels. Tevens leidt intermitterend belasting sneller tot een verhoogde collageenhoeveelheid, cross-linkconcentratie en mechanische eigenschappen dan statische belasting. Hierdoor kunnen sterkere weefsels binnen een kortere kweekperiode gemaakt worden

Samenvattend laten deze studies zien dat, in vergelijking met statische belasting, dynamische belasting de hoeveelheid collageen niet verhoogt, maar de cross-linkconcentratie en mate van vezeloriëntatie in de belastingsrichting wel. Intermittent belasting verhoogt en versnelt de collageenproductie, cross-linkconcentratie en vezelvorming in de richting van de belasting. Intermittent belasting kan dus gebruikt worden om de productie van weefsels met een goed georganiseerde collageenarchitectuur te versnellen. Deze bevindingen zijn zeer relevant voor cardiovasculaire tissue engineering waar een sterke en goed georganiseerde structuur noodzakelijk is voor het goed functioneren van getissue-engineerde hartkleppen en bloedvaten in het menselijk lichaam.

# Dankwoord

Promoveren doe je niet alleen. Graag wil ik iedereen bedanken die heeft bijgedragen aan mijn proefschrift. Allereerst mijn promotor Frank Baaijens. Bedankt voor de mogelijkheden en vrijheden die je me hebt geboden tijdens mijn promotie. Carlijn, ik heb met veel plezier in jouw Vici-programma gewerkt. Vooral jouw talent voor het aanscherpen van mijn tekst heeft mij veel geholpen. Anita, ik ben heel erg blij dat jij bereid bent geweest mij mede te begeleiden. Jouw gestructureerde manier van werken waardeer ik zeer en ik heb altijd van onze discussies genoten. Ralf, ik vond het prettig om met jou samen te werken, jouw werk heeft een belangrijke basis gevormd voor dit proefschrift. Zelfs toen je al lang een andere baan had, was je nog bereid om mee te denken met mijn onderzoek.

Ook alle andere collega's van vloer 4 wil ik bedanken voor de goede samenwerking. Vooral met de collageen- en hartkleppen/bloedvaten-mensen heb ik veel samengewerkt en gelachen. Ik kijk al weer uit naar het volgende collageenetentje! Anita (Wainita), dank voor de vele analyses die je zeer nauwkeurig hebt uitgewerkt. Marcel, erg fijn dat ik altijd bij je terecht kon met vragen over de twee-foton microscoop. Rob, bedankt voor je hulp bij de experimentele opstellingen.

Op kamer WH 4.11 heb ik altijd heel prettig kunnen werken. De kameretentjes waren erg gezellig! Martijn, Anita, Leonie (en ook even Rolf) van de QTIS/e-kamer, erg fijn om jullie als kamergenoten te hebben. Angelique, Debbie, Karlien, Julienne en Lisette, onze meidenavonden vind ik super en gelukkig staat de volgende ook al weer gepland.

Ook wil ik een aantal mensen van buiten de vakgroep bedanken voor hun bijdrage. Ruud Bank, Roeland Hanemaaijer en Jessica Snabel van TNO Leiden, hartelijk dank voor jullie waardevolle discussies en analyses. Bart ter Haar Romeny, ik wil je bedanken voor de mogelijkheid die je geboden hebt om samen met jouw groep aan een methode voor oriëntatieanalyse te werken. Dear Dan Bader, thank you for reading and correcting my thesis. Your comments have considerably strengthened my thesis. Dear Swiss colleagues, I really appreciated our fruitful discussions in the mountains. I learned a lot of you (besides skiing ☺).

Tijdens mijn promotie heb ik ook een aantal stagiaires en afstudeerders mogen begeleiden: Chris, Lieke, Florie, Marc en Mieke. Hans, Florie en Marc, heel veel dank voor de ontwikkeling van de software voor de oriëntatieanalyses. Mieke, hoofdstuk 3 is door jouw inzet een mooi hoofdstuk geworden.

Verder wil ik mijn vrienden (o.a. uit Hulst, van mijn studie/promotie bij BMT en van het sporten) bedanken voor de nodige ontspanning en gezelligheid. Koninginnedag in Amsterdam, Oud&Nieuw in Eindhoven en carnaval in Den Bosch/Hulst zijn voor mij dankzij jullie altijd leuke feestjes. Voor de mountainbikers/kegelaars onder ons, ik kijk erg uit naar ons volgende Ardennenweekend. BMT-meiden, wordt het niet weer eens tijd voor een terrasjes-fietstocht? Sonja's, wat is het toch leuk een Sonja te zijn! Anne, erg bedankt voor het ontwerpen van mijn kaft.

## *Dankwoord*

Wilma en Leonie, fijn dat jullie mijn paranimfen willen zijn en mij bijstaan tijdens de verdediging. Helaas kunnen we onze goedgeoefende buiging niet laten zien want dat past in Eindhoven niet in het protocol.

Ik wil al mijn familieleden bedanken voor hun belangstelling tijdens de afgelopen periode. Erg fijn dat jullie zo geïnteresseerd waren in mijn laatste vorderingen. Stefan en Leonie, fijn dat jullie mijn broer en zus zijn. Pa, Ma, bedankt voor al jullie steun en vertrouwen. Door jullie ben ik geworden wie ik ben. Lieve Alexander, al vele jaren kan ik alles met je delen. Je staat altijd voor me klaar. Ik kijk uit naar de vele jaren die nog gaan komen, laten we er een mooie reis van maken!

Mirjam Rubbens  
Eindhoven, juli 2009

# Curriculum vitae

Mirjam Rubbens is geboren op 12 augustus 1980 in Spijkenisse. In 1998 behaalde zij haar VWO diploma aan het Janseniuscholengemeenschap in Hulst. Aansluitend studeerde zij Biomedische Technologie aan de Technische Universiteit Eindhoven. Als onderdeel van deze studie heeft zij stage gelopen aan de Politecnico di Milano (Italië). Hier onderzocht zij de invloed van een shunt op de vloeistofdynamica rond het hart met behulp van een experimentele opstelling. Haar afstudeerwerk in de vakgroep Cardiovasculaire Biomechanica van de Technische Universiteit Eindhoven richtte zich op het modelleren van de vezeloriëntatie in het hart. In 2004 startte zij met haar promotieonderzoek binnen de vakgroep Soft Tissue Biomechanics & Engineering aan de faculteit Biomedische Technologie van de Technische Universiteit Eindhoven, resulterend in dit proefschrift. Sinds 2007 combineert zij haar onderzoek met het management van QTIS/e, een spin-off bedrijf van de Technische Universiteit Eindhoven dat zich richt op de commercialisatie van het tissue engineering onderzoek.

